Investigating the Roles of F-BAR proteins CIP4 and FBP17 in Cortical Development and Neuronal Migration

By

Lauren A. English

A dissertation submitted in partial fulfillment of

the requirements for the degree of

Doctor of Philosophy

(Neuroscience)

at the

UNIVERSITY OF WISCONSIN-MADISON

2025

Date of final oral examination: 07/07/2025

The dissertation is approved by the following members of the Final Oral Committee:

Erik Dent, Professor, Neuroscience

Timothy Gomez, Professor, Neuroscience

Anita Bhattacharyya, Associate Professor, Cell and Regenerative Biology

Mrinalini Hoon, Associate Professor, Department of Ophthalmology and Visual Sciences

Jeffery Hardin, Raymond E. Keller and Wayland Noland Distinguished Professor, Integrative Biology

Table of Contents

Acknowledgments

There are so many people and programs that helped me get here today. I would first like to thank my advisor Dr. Erik Dent. Erik, thank you for listening to my complaining and ramblings about why nothing ever works. Thank you for the scientific, writing, and life advice. I feel that training in your lab has made me a better scientist and taught me how to be more critical of data and statistics. Lastly, thank you Erik for creating the lab environment that you do, I'm not sure how you do it, but the people that the Dent lab attracts are wonderful and have made grad school all the better.

To the Dent lab, past and present; thank you for being you. Russ, you have been an incredible mentor and friend, thank you for showing me how to do literally everything. Lizzi, thank you for just being in lab third year. I think we both needed each other just to show up. I am so glad to have gone through this journey together. Hannah, Jillian, Tara, and Madison, thank you for rounding out the “Ladies of WIMR 5”, this group has brought me so much support and joy. To my undergrads Connor, Emily, Emma, and Gabby, thank you for all the hard work you put into my projects. I could not have sectioned, imaged and analyzed as may brains as I did without you.

I would also like to thank the NTP student community. Thank you to my thesis committee—Drs. Anita Bhattacharyya, Mrinalini Hoon, Tim Gomez, and Jeff Hardin—for all their advice and guidance. I would also like to thank the SciMed community and its leader Dr. Michelle Parmenter. Michelle, you have been a wonderful and friendly face throughout grad school. I would also like to thank the Research Animal Resource and Compliance

staff, specifically the vivarium staff. Thank you to the Neuroscience department admin, and the WIMR 5 community.

Outside of UW I have family and friends to thank. Marissa and Dave, thank you for your years of friendship, here's to many more to come. Suite Tau + Evan, thank you for your support in getting me to grad school. Mom, Dad, Grant, and Julia I know I was a weird kid, thank you for encouraging me to be me. Thank you for summers at ecology camp, trips to the science and industry museum, and pushing me to follow my passions in science. I don't know if I would be defending my PhD in neuroscience without your support. And a special thank you to Drs. Elizabeth Glater and Chuck Taylor, you two saw the scientist in my before I did. Thank you for pushing me to be here.

The last and most important person to thank is my fiancé, Collin Dott. Collin, thank you for thinking science is cool and asking about what I do. You have been my rock for the last five years. I know I could have done this without you, but it's been so much better with you by my side. Thank you for listening to all my practice talks and reading over many abstracts and papers. Thank you for listening to me vent about grad school, talk about experiments, or just scream. You and Walleye have my whole heart, thank you both for everything you do.

Abstract

Neuronal migration is a critical process in the development of the embryonic cerebral cortex, ensuring that neurons reach their proper locations to form functional circuits. Excitatory neurons migrate radially from the ventricular zone to the cortical plate through several migratory zones, changing their morphology as they progress. Migrating neurons start out in a bipolar morphology, switch to a multipolar morphology, and then must switch back to a bipolar morphology. These transitions require tightly regulated cytoskeletal remodeling and plasma membrane dynamics. Failure to coordinate these processes can result in severe cortical malformations, such as lissencephaly and periventricular heterotopia. Rho GTPases and actin-associated proteins have been implicated in regulating the morphological changes required for migration, however, the molecular coordination between membrane and cytoskeletal dynamics remains poorly understood. Members of the F-BAR protein family are emerging as key candidates in this coordination, due to their unique ability to sense and induce membrane curvature and interact with actin regulatory proteins. This dissertation investigates the roles of two F-BAR proteins, CIP4 and FBP17, in radial neuronal migration. We show that both CIP4 and FBP17 drive migration by coordinating neurite dynamics in radial migrating neurons. These results suggest that CIP4 and FBP17 function in distinct yet complementary ways to regulate the morphological transitions necessary for successful migration. Furthermore, this work supports a broader model in which F-BAR proteins act as integrators of membrane shape and cytoskeletal architecture during neuronal development. Together, these findings expand our understanding of the

molecular control of neuronal migration and position F-BAR proteins as critical mediators of membrane–cytoskeletal coordination in the developing brain.

Chapter 1:

Introduction to Cell Dynamics During Radial Migration

Radial neuronal migration in the neocortex

The development of the human brain relies on the correct migration of newborn neurons to their final destination (Herculano-Houzel 2012). This chapter will focus on the neocortex, the brain's outermost region, and its development. Specifically, this chapter will explore how key regulators of cell membrane dynamics contribute to this radial migration (Lodato and Arlotta 2015). The neocortex is a distinct mammalian brain structure responsible for coordinating higher-order cognition, sensory perception, and integration, as well as premotor planning and control. Thus, the development of the neocortex must happen in a precise temporal and spatial pattern for proper function (Lodato and Arlotta 2015). The neocortex is made up of both excitatory and inhibitory neurons that work together to create functional circuitry. Born in different places, excitatory and inhibitory neurons must migrate through the developing cortex to their final destinations in the cortical plate (Kriegstein and Noctor 2004, Turrero Garcia and Harwell 2017). Disruptions in the precise timing and phase of migration can result in a range of cortical malformations and dysfunctions. There disruptions are collectively referred to as cortical migration disorders.

Cortical migration disorders can lead to a spectrum of developmental and cognitive defects (Buchsbaum and Cappello 2019). Common examples of cortical migration disorders include lissencephaly type I, periventricular heterotopia, and subcortical band heterotopia, also known as double cortex. These three migration disorders produce distinct changes in brain structures due to neurons failing to migrate properly (Buchsbaum and Cappello 2019) **(Fig. 1)**. Lissencephaly type I, also referred to as smooth brain, arises from mutations in genes associated with microtubule dynamics and transport, actin regulation,

and centrosome dynamics during mitosis (Buchsbaum and Cappello 2019). These disruptions in cytoskeletal function cause migrating cortical neurons to halt migration early, resulting in a four-layer cortex and flattened gyri (Dobyns and Truwit 1995, des Portes, Pinard et al. 1998). Lissencephaly often presents with a subcortical band heterotopia, a band of grey matter under the cortex, due to additional mutations in genes regulating microtubule stability (Buchsbaum and Cappello 2019). Patients diagnosed with lissencephaly without subcortical band heterotopia suffer from impaired cognitive ability and epilepsy, in addition to disruptions in fine motor control and muscle tone (Bahi-Buisson and Guerrini 2013).

Periventricular heterotopia is a second migration disorder that is also caused by mutations in cytoskeletal-associated genes (Romero, Bahi-Buisson et al. 2018, Buchsbaum and Cappello 2019). Periventricular heterotopia causes bundles or nodes of disorganized neurons to clump together on the surface of the ventricles. These heterotopic nodes are formed due to newborn neurons failing to migrate out of the ventricular zone. Many of the gene mutations involved in periventricular heterotopia cause malfunctions in actin dynamics, cell-cell adhesions, and trafficking (Romero, Bahi-Buisson et al. 2018, Buchsbaum and Cappello 2019). Periventricular heterotopia has varying effects on patients, ranging from some seizure activity to more severe epilepsy, developmental delays, and microencephaly (Lu and Sheen 2005, Romero, Bahi-Buisson et al. 2018).

The effects of migration disorders on patient outcomes vary, with the most severe cases resulting in extreme developmental delays, cognitive impairment, and severe epilepsy. Many migration disorders are also comorbid with progenitor proliferation disorders like macro and microencephaly, as well as organizational disorders such as cobblestone

lissencephaly and polymicrogyria (Romero, Bahi-Buisson et al. 2018, Buchsbaum and Cappello 2019). The need for further research into these devastating developmental disorders is paramount. However, to better understand how these disorders arise we must first uncover how typical neuronal development occurs. This chapter will focus on the development of excitatory neurons that migrate radially in the cortex of typically developing brains.

Excitatory neurons are born in the dorsal region of the lateral ventricles and migrate radially upward to the cortical plate. There are two forms of migration used by newborn excitatory neurons in the developing cortex, somal translocation and glial-guided radial migration (Nadarajah, Brunstrom et al. 2001). Early born neurons (neurons born on or before embryonic day 13.5 (E13.5)) use somal translocation to migrate by extending a long leading process towards to marginal zone (Nadarajah, Brunstrom et al. 2001, Nadarajah and Parnavelas 2002). This leading process responds to both attractive and repulsive cues secreted by Cajal-Retzius cells in the marginal zone (Franco, Martinez-Garay et al. 2011, Jossin and Cooper 2011, Gil-Sanz, Franco et al. 2013) **(Fig. 2)**. The extension towards attractive cues and retraction away from repulsive cues is mediated by Rho GTPase-regulated actin polymerization and reorganization (Ridley 2001). In response to an attractive cue, the neuron next undergoes nucleokinesis, utilizing microtubules to move its nucleus and cell body towards its leading process at a constant pace (Nadarajah, Brunstrom et al. 2001, Nadarajah and Parnavelas 2002).

Later-born neurons (neurons born after E13.5) use radial glial cells as a guide when migrating, as described in **Figure 2** (Nadarajah, Brunstrom et al. 2001, Noctor, Martinez-

Cerdeno et al. 2004). Their migration can be divided into five phases **(Fig. 2a-e)**. Phase one begins after the asymmetrical division of a radial glial cell. In phase two the newborn neuron resides in the ventricular zone exhibiting a bipolar shape that allows it to climb the radial glial cell into the subventricular zone **(Fig. 2a & b)**. As young bipolar neurons exit the subventricular zone, they transition to a multipolar morphology in the lower intermediate zone. This is the beginning of phase three, where neurons assume a multipolar morphology **(Fig. 2c)**. In phase four, neurons return to a bipolar morphology upon entering the upper intermediate zone **(Fig. 2d)**. The progression from phase one to phase three takes around 26-48 hours(Kriegstein and Noctor 2004). For the fifth and final phase, neurons extend a leading process towards the marginal zone and complete migration to the cortical plate **(Fig. 2e)** (Kriegstein and Noctor 2004, Noctor, Martinez-Cerdeno et al. 2004). During the final phase of migration, the migrating neuron must reach a specific, predetermined final location in the cortical plate (Kriegstein and Noctor 2004, Buchsbaum and Cappello 2019). Later born neurons, when traveling to their destination in the cortical plate must navigate through earlier-born neurons that have already completed migration **(Fig. 2f)**. This migration pattern leads to the "inside out" formation of the cerebral cortex **(Fig. 2g)** (Molyneaux, Arlotta et al. 2007, Sekine, Honda et al. 2011)**.**

The cytoskeleton in radial neuronal migration

During migration, neurons undergo membrane remodeling and morphological changes driven by the cytoskeleton. The actin and microtubule cytoskeletons must be properly regulated during migration, with the actin cytoskeleton involved in filopodia and lamellipodia formation during radial migration (Machesky 2008). Many groups have studied

regulators of actin to better understand how actin dynamics are controlled during radial migration. Rho GTPases are one of the main regulators of actin dynamics in migrating neurons. Two specific Rho GTPases, Ras-related C3 botulinum toxin substrate 1 (Rac1) and Cell division cycle protein 42 (Cdc42), have been heavily implicated in actin polymerization during neurodevelopment for their roles in lamellipodia and filopodia formation, respectively (Mattila and Lappalainen 2008, Krause and Gautreau 2014).

Filopodia are required for neurite initiation, and multiple regulators of filopodial outgrowth have been implicated as key players in radial migration (Dent, Kwiatkowski et al. 2007, Heng, Chariot et al. 2010). The process of filopodial outgrowth is regulated by Rho-GTPases, cytoskeletal associated proteins and actin nucleators. The Rho GTPase Cdc42 has a direct pathway in which it promotes the actin assembly needed for filopodial outgrowth (Mattila and Lappalainen 2008). Briefly, actin polymerization needed for filopodial formation is regulated by phosphatidylinositol 4,5-biphosphate (PIP_2) activation of Cdc42, which binds to neural Wiskott-Aldrich syndrome protein (N-WASP), recruiting actin related protein 2/3 (Arp2/3) to activate actin polymerization (Mattila and Lappalainen 2008) **(Fig. 3)**.

Many groups have investigated the effects of inhibiting or negatively affecting the Cdc42/actin assembly pathway on filopodial outgrowth and neuronal migration. Starting at the beginning of the pathway, one group inhibited the activation of PIP2, and expressed both constitutively active and dominant negative Cdc42. Their experiments showed decreased migration to the cortical plate in all three cases (Konno, Yoshimura et al. 2005). Additionally, recent work has shown that Cdc42 regulates the morphology of migrating neurons through activation by its guanine nucleotide exchange factor (GEF), Tuba. Knockdown of Tuba

decreased migration at E18.5 and inhibited neurite outgrowth (Urrutia, Bodaleo et al. 2021). These studies show that inhibition of PIP2 and mutations to Cdc42, which mediate filopodial outgrowth, inhibit migration, suggesting that's Cdc42 plays an important role in neurite outgrowth of migrating neurons

Rac1 activity is also essential for lamellipodial actin networks during neuronal migration (Krause and Gautreau 2014). Rac1 mediated actin branching and lamellipodial formation follows a distinct pathway. Initially PI3K phosphorylates PIP2, generating PIP3. PIP3 activates Rac1, leading to WAVE1 activation of Arp2/3, which is required for the actin polymerization that forms lamellipodia (Tahirovic, Hellal et al. 2010, Krause and Gautreau 2014, Tariq and Luikart 2021) **(Fig. 3)**. Lamellipodia have long been shown to be the driving force behind cell migration (Krause and Gautreau 2014, Innocenti 2018). Specifically, in neuronal migration lamellipodia have been hypothesized to aid in guidance sensing and environmental probing in primates (Cortay, Delaunay et al. 2020).

Rac1's role in migration has been more extensively studied, compared to Cdc42. Point mutations in Rac1 have been shown to cause decreases in migration (Kawauchi, Chihama et al. 2003, Konno, Yoshimura et al. 2005). Expression of a dominate negative Rac1 (Rac1-N17) halts migration in the intermediate zone, however, these neurons develop normally despite their incorrect positioning (Kawauchi, Chihama et al. 2003). Expression of a constitutively active Rac1 (Rac1-V12) also decreases migration, presumably because the migrating neurons fail to develop a functional leading process (Konno, Yoshimura et al. 2005). A weaker constitutively active Rac1 mutation (Rac1-L61) also decreases migration, although to a lesser extent than Rac-V12.

While Cdc42 and Rac1 are well-established regulators of actin dynamics during neuronal migration, they have not been directly linked to specific cortical migration disorders. In contrast, mutations in other actin-associated proteins have been shown to cause migration disorders and cortical malformations. One such protein is filamin A (FLNA), which has been strongly implicated in periventricular heterotopia (PH) (Fox, Lamperti et al. 1998, Guerrini and Parrini 2010, Moon and Wynshaw-Boris 2013). FLNA is part of a family of actin-binding proteins that cross link actin filaments into three-dimensional networks (Feng and Walsh 2004), a function essential for maintaining cytoskeletal integrity during cell migration.

Mechanistically, mutations in FLNA disrupt actin cross-linking, resulting in neurons that fail to migrate to the cortical plate. Instead, these neurons accumulate near the ventricular zone, forming ectopic nodules characteristic of PH (Romero, Bahi-Buisson et al. 2018, Buchsbaum and Cappello 2019) **(Fig. 1)**. To understand the role of FNLA in migration groups have studied FLNA expression and functionality in mice. FLNA expression was found to be elevated during peak periods of neuronal migration and declines after birth (Fox, Lamperti et al. 1998). Regarding migration, knockdown of FLNA via RNA interference impairs migration, leading to an accumulation of multipolar neurons in the intermediate zone (Nagano, Morikubo et al. 2004). These findings suggest that FLNA facilitates actin remodeling necessary for process retraction and remodeling during migration. Without proper actin network stability, neurons may be unable to generate the protrusions required for effective migration.

Lissencephaly type I is also caused by mutations in cytoskeletal-associated genes that affect not actin filaments but microtubules. The LIS1 gene regulates cytoplasmic dynein, a microtubule-based motor protein (DeSantis, Cianfrocco et al. 2017). LIS1 regulates dynein localization, microtubule stability, and centrosome dynamics during somal translocation (Faulkner, Dujardin et al. 2000, Tsai, Bremner et al. 2007, DeSantis, Cianfrocco et al. 2017). Overexpressed LIS1 removes dynein from microtubule plus ends, negatively affecting transport and microtubule stability (Faulkner, Dujardin et al. 2000). This loss of proper microtubule and centrosome stability could lead to dysregulation of somal translocation causing the migration deficits seen in lissencephaly type I.

These studies have shown that the ability to regulate cytoskeletal dynamics during development is crucial for proper radial migration. The actin networks and microtubule extension at the leading process require not only the coordination of the cytoskeleton but also communication with the plasma membrane. Indeed, the extension of the leading process requires plasma membrane flexibility (Noctor, Martinez-Cerdeno et al. 2004, Krause and Gautreau 2014). There is currently a lack of understanding of how the cytoskeleton and plasma membrane coordinate during migration. To answer these questions groups have turned to **B**in **A**mphisphysin- **R**vs (BAR) domain proteins, a family of proteins known for their roles in membrane remodeling and cytoskeletal regulation (Aspenstrom 2009, Fricke, Gohl et al. 2010, Liu, Xiong et al. 2015).

F-BAR proteins in cell membrane dynamics

Members of the BAR superfamily of proteins are well known for their roles in cellular membrane alteration and remodeling. BAR proteins, named for their characteristic BAR domain, play essential roles in endocytosis and membrane curvature (Ahmed, Bu et al. 2010, Fricke, Gohl et al. 2010, Liu, Xiong et al. 2015, Su, Zhuang et al. 2020). The F-BAR subfamily of BAR proteins is a group of multi-domain proteins involved in sensing and altering membrane curvature, as well as interacting with the cytoskeleton (Aspenstrom 2009, Su, Zhuang et al. 2020). F-BAR proteins are categorized by their FES-CIP4 homology (F-BAR) domain (Liu, Xiong et al. 2015). The banana-shaped F-BAR domain dimerizes, allowing for interaction with the membrane by binding to negatively charged phospholipids along its concave surface (Shimada, Niwa et al. 2007, Frost, Perera et al. 2008). During endocytosis, F-BAR proteins elongate endocytosing membrane via head-to-tail polymerization of their F-BAR domains. Each F-BAR dimer senses a specific shape of curvature, with the curvature of the endocytosing membrane determining which F-BAR dimers bind (Shimada, Niwa et al. 2007, Frost, Perera et al. 2008). In addition to the N-terminal F-BAR domain, some F-BAR proteins also contain a C-terminal SH3 domain, which associates with actin-associated proteins such as dynamin, Dia1, Dia2, DAAM1, and WASP (Liu, Xiong et al. 2015). The combination of the F-BAR and SH3 domains implicates these proteins in playing a key role in the formation of tubulating, endocytosing membrane, and cytoskeletal coordination in neuronal migration.

Within the F-BAR family, there are 9 subfamilies, each grouped by their common domains. The **C**dc42 **i**nteracting **p**rotein **4** (CIP4) subfamily is a distinct group characterized

by their homology related 1 (HR1) or Rho effector motif class 1 (REM-1) domain (Reid, Furuyashiki et al. 1996). This domain binds active Rho-GTPases, namely Cdc42. However, evidence suggests RhoGAP, Rac1, and Rnd2 may be additional binding partners (Aspenstrom 1997, Wakita, Kakimoto et al. 2011, Saengsawang, Taylor et al. 2013). CIP4 is the eponymous member of the family, followed by **f**ormin **b**inding **p**rotein **17** (FBP17) and **t**ransducer **o**f **C**dc42 dependent **a**ctin assembly protein **1** (TOCA1) (Liu, Xiong et al. 2015). Functionally, the CIP4 subfamily has roles in endocytosis, filopodial extension, invadopodia formation, and cancer metastasis in non-neuronal cells (Kamioka, Fukuhara et al. 2004, Itoh, Erdmann et al. 2005, Shimada, Niwa et al. 2007, Fricke, Gohl et al. 2010, Suman, Mishra et al. 2018, Hu, Zhu et al. 2022). However, evidence from our lab and others suggest they have additional roles in neurons (Saengsawang, Mitok et al. 2012, Saengsawang, Taylor et al. 2013, Taylor, Taylor et al. 2019, Blake, Fox et al. 2024).

In 1997 Pontus Aspenstrom initially discovered CIP4 using a yeast two-hybrid screen to discover binding partners of Cdc42 (Aspenstrom 1997). CIP4 was found to localize to the periphery of cells and colocalize with constitutively active Cdc42 (Aspenstrom 1997). Further examination of CIP4 determined it had a similar SH3 domain to the already known protein FBP17 (Chan, Bedford et al. 1996). FBP17 has been studied for its role in multiple forms of endocytosis. FBP17 functions in clathrin-mediated endocytosis by recruiting WASP and dynamin to the endocytosing vesicle, as well as colocalizing with Rab5a (Tsujita, Suetsugu et al. 2006, Shimada, Niwa et al. 2007). The tubular invaginations resulting from FBP17 overexpression in COS7 cells have been shown to have the membrane curvature present in dynamin-dependent endocytosis (Itoh, Erdmann et al. 2005, Layden, Saengsawang et al.

2008). Other studies have demonstrated that FBP17 recruits SHIP2 and lamellipodin in fast-endophilin-mediated endocytosis (Tsujita, Suetsugu et al. 2006, Chan Wah Hak, Khan et al. 2018). The third member of CIP4 subfamily is TOCA1. TOCA1 was discovered in bovine brain extracts by a group searching for regulators of Cdc42-driven actin polymerization (Ho, Rohatgi et al. 2004). Loss of TOCA1 in *Xenopus* brain extracts decreased actin assembly by both Cdc42 and PIP_2, indicating that TOCA1 is necessary for Cdc42 and PIP2-induced actin polymerization(Ho, Rohatgi et al. 2004). TOCA1 also binds to N-WASP to promote filopodial formation (Bu, Chou et al. 2009). Due to their roles in filopodia formation, some groups have begun to examine the roles of F-BAR proteins in coordinating the plasma membrane and cytoskeleton during neurite development (Kakimoto, Katoh et al. 2006, Saengsawang, Mitok et al. 2012, Saengsawang, Taylor et al. 2013, Taylor, Taylor et al. 2019, Blake, Fox et al. 2024).

F-BAR proteins in neurite outgrowth and neuronal migration

CIP4 has emerged as a key regulator of neuronal morphology, particularly in the context of neurite initiation and outgrowth**.** In dissociated primary cortical neurons, CIP4 localizes to the cell periphery and promotes the formation of lamellipodial protrusions or veils**.** These lamellipodial protrusions inhibit neurite outgrowth, suggesting that CIP4 plays a negative role in neurite initiation (Saengsawang, Mitok et al. 2012). Furthermore, primary cortical neurons from CIP4 knockout mice exhibit earlier neurite initiation and develop longer neurites compared to wild-type controls, reinforcing the idea that CIP4 serves as a negative regulator of neurite formation (Saengsawang, Mitok et al. 2012). To understand the mechanism of CIP4 in neurite inhibition, co-transfection of primary cortical neurons with dominant negative Rac1 and CIP4 was carried out. These neurons showed decreased CIP4

localization at the peripheral membrane, while CIP4 was dispersed in puncta throughout the cytoplasm (Saengsawang, Mitok et al. 2012). This work suggests that active Rac1 may positively regulate CIP4 localization in neurons. These results position CIP4 as an inhibitory modulator of neurite outgrowth, functioning at the intersection of membrane remodeling and actin dynamics.

FBP17 has also been implicated in neuronal development, particularly in neurite outgrowth and filopodial dynamics (Fujita, Katoh et al. 2002, Taylor, Taylor et al. 2019, English, Taylor et al. 2024). When overexpressed in neurons, FBP17 enhances filopodial extension and induces premature neurite outgrowth, a phenotype that contrasts with the inhibitory effects of CIP4 (Taylor, Taylor et al. 2019). Mechanistically, FBP17 has been shown to interact with Rnd2, a small Rho GTPase known to regulate neuronal morphology (Fujita, Katoh et al. 2002, Kakimoto, Katoh et al. 2004). FBP17 and GTP-loaded Rnd2 were shown to bind to each other via FBP17's HR1 domain in dot-blot analysis (Fujita, Katoh et al. 2002, Kakimoto, Katoh et al. 2004). Additionally, FBP17 and Rnd2 co-localize to the membrane in PC12 cells, suggesting FBP17 may recruit to Rnd2 to coordinate actin dynamics at the membrane (Fujita, Katoh et al. 2002). Besides its effects on neurite structure, FBP17 expression also leads to the formation of membrane tubules and an increase in filopodia, indicating it is actively involved in shaping the neuronal membrane and supporting neurite outgrowth[55]. Our lab has hypothesized that tubule formation during endocytosis results in additional protruding membrane that can become a filopodial protrusion **(Fig. 4)**. Under this hypothesis, the increase in membrane tubulation by FBP17 expression leads in increased filopodial extension and neurite outgrowth.

These findings highlight FBP17 as a positive regulator of neuronal process formation. By promoting filopodia and interacting with small GTPases like Rnd2, FBP17 likely facilitates the initial steps of neurite extension. Its distinct activity relative to CIP4 suggests a complementary or opposing role within the CIP4 subfamily, emphasizing the finely tuned balance of membrane-cytoskeletal regulation required for proper neuronal differentiation.

The third member of the CIP4 subfamily, TOCA1, also plays a crucial role in neurite outgrowth, axon branching, and filopodial tip extension. Initial studies demonstrated that TOCA1 expression in mouse neuroblastoma cells induces neurite outgrowth and activates the N-WASP/WIP complex in *Xenopus* egg extracts (Ho, Rohatgi et al. 2004). A recent paper showed that TOCA1 functions in neuronal filopodial dynamics. TOCA1 localized to the tips of filopodia before tip extension, suggesting that it may play a role in the initiation or stabilization of filopodia growth (Blake, Fox et al. 2024). Furthermore, this study showed that TOCA1 interacts with Ena, a member of the Ena/VASP complex, which is known to promote actin elongation in filopodia (Blake, Fox et al. 2024). The TOCA1-Ena/VASP interaction and TOCA1's activation N-WASP/WIP suggests a potential mechanism by which TOCA1 facilitates actin polymerization to drive filopodia extension (Ho, Rohatgi et al. 2004). While not all of these studies were conducted in neurons, the data suggests an important role for TOCA1 in neuronal filopodia extension. Collectively, these findings indicate that TOCA1, like other members of the CIP4 subfamily, serves as a critical link between membrane dynamics and the cytoskeleton, regulating neurite outgrowth and structural plasticity in neurons.

Although F-BAR proteins have not been extensively studied in the context of neuronal migration, a growing body of evidence supports their involvement in neuronal morphology

and process formation. *In vitro* studies have demonstrated that several F-BAR family members, including those in the CIP4 subfamily, play key roles in filopodia formation and neurite outgrowth, with TOCA1 and FBP17 consistently implicated as positive regulators of these processes (Fujita, Katoh et al. 2002, Taylor, Taylor et al. 2019). While *in vivo* research is still limited, a few studies have begun to explore the roles of F-BAR proteins in neuronal development. Notably, srGAP2 and GAS7, two other F-BAR-containing proteins, have been shown to regulate aspects of neuronal migration, highlighting the potential for broader roles of this protein family beyond neurite extension (Guerrier, Coutinho-Budd et al. 2009, Zhang, Zheng et al. 2016, English, Taylor et al. 2024) . Furthermore, our recent 2024 preprint provides evidence that CIP4 and FBP17 may directly influence neuronal process outgrowth during radial neuronal migration, suggesting these proteins could serve as critical links between membrane remodeling, cytoskeletal regulation, and migratory behavior (English, Taylor et al. 2024). These findings underscore the need for further investigation into F-BAR proteins during brain development, particularly *in vivo*, where their dynamic coordination of membrane and cytoskeletal remodeling may prove essential for proper neuronal positioning and cortical organization.

The following two chapters will explore how CIP4 and FBP17 contribute to radial neuronal migration in the developing cortex. Chapter two will demonstrate that the expression levels of CIP4 and FBP17 must be precisely regulated during migration. Overexpression or knockdown of either protein disrupts migration. CIP4 regulates neurite outgrowth during migration while FBP17 may promote neurite extension during later stages or migration. Chapter three builds on these findings by characterizing the spatial and

temporal expression patterns of CIP4 and FBP17 using *in situ* hybridization techniques and a novel CIP4-HA mouse model. These studies reveal spatially and temporally distinct expression profiles of CIP4 and FBP17. Data from both chapters suggest that CIP4 and FBP17 act in a spatially and temporally regulated manner to mediate process remodeling during radial migration, providing new insights into how membrane associated proteins shape cortical development.

Figures

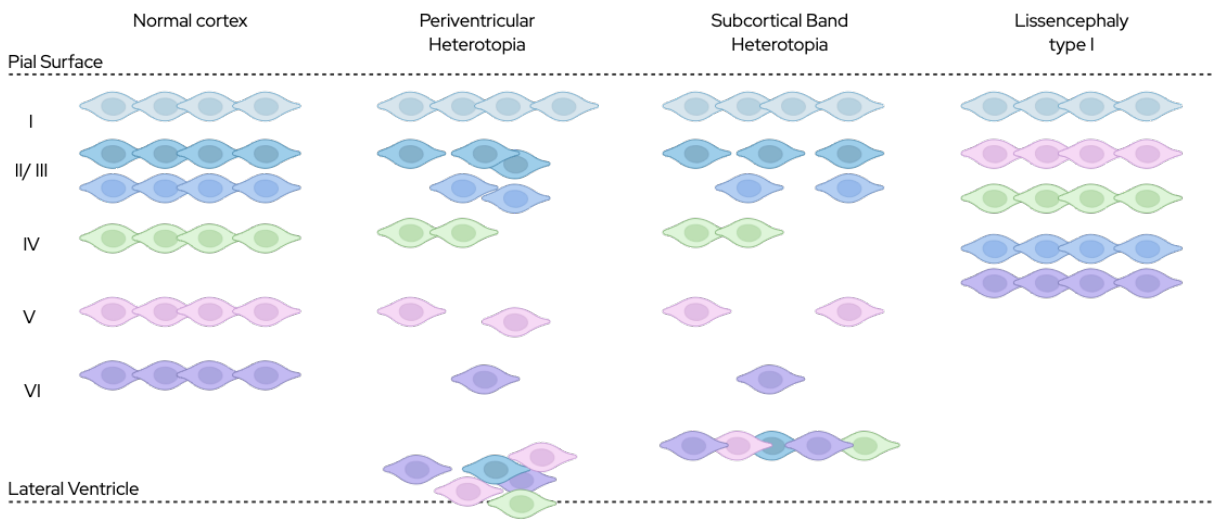

Figure1. Cortical Migration disorders

Diagrams of the migration defects in adult normal, periventricular heterotopia, subcortical band heterotopia, and lissencephaly type 1 corticies . Normal cortex shows six layers (layer I: light blue, layer II/III: darks blues, layer IV: light green, layer V: pink, layer VI: dark purple. Periventricular heterotopia cortices show unmigrated neurons in a nodule at the ventricle. Subcortical band heterotopia cortex shows a band of unmigrated neurons under the cortex proper. Lissencephaly type 1 cortices have four layers of neurons that fail to migrate through earlier born neurons (Romero, Bahi-Buisson et al. 2018, Buchsbaum and Cappello 2019). Created in BioRender. English, L. (2025) https://BioRender.com/hsl058e

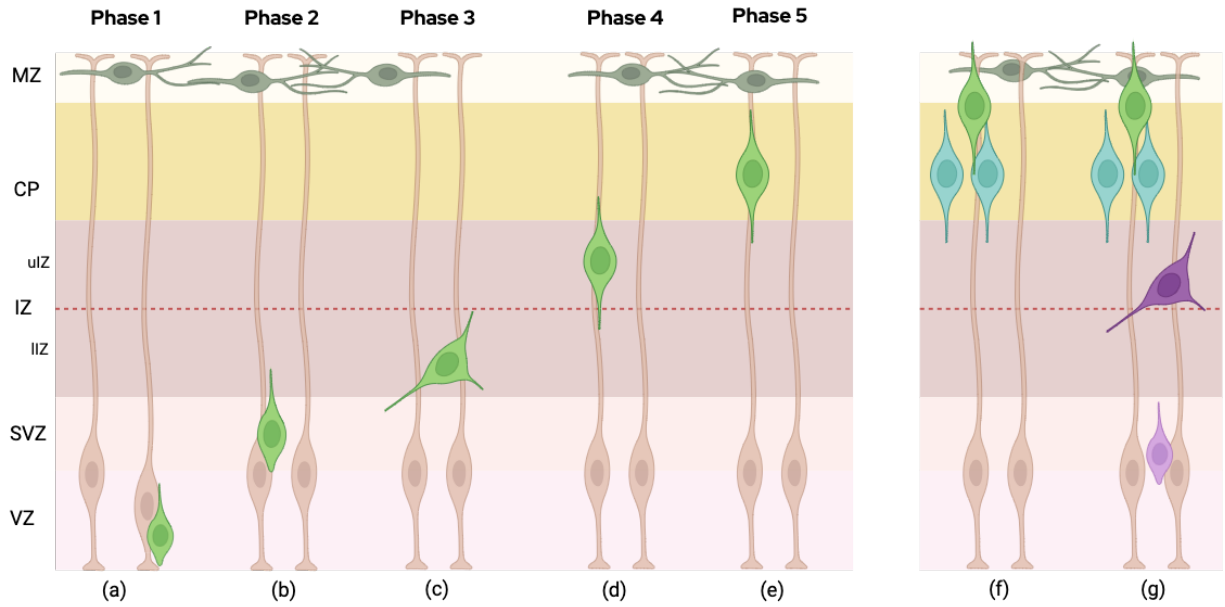

Figure 2. Phases of radial migration in the developing neocortex.

(a) Phase 1, a radial glial cell divides asymmetrically into another radial glial cell and newborn neuron (green). **(b)** Phase 2, the newborn neuron migrates through the subventricular zone in a bipolar morphology. **(c)** Phase 3, the migrating neuron switches to a multipolar morphology in the lower intermediate zone. **(d)** Phase 4, the neuron continues migration switching back to a bipolar morphology as it enters the upper intermediate zone. **(e)** Phase 5, the neuron completes migration to the cortical plate. **(f)** Neurons finishing migration in the cortical plate (green) must migrate through earlier born neurons (blue), stopping before reaching the Cajal-Retzius cells in the marginal zone (dark green). **(g)** As neurons are completing migration (green) newborn neurons begin (light purple) and continue (dark purple) the migratory process. VZ= ventricular zone, SVZ= Subventricular zone, IZ= Intermediate zone, lIZ= Lower intermediate zone, uIZ= Upper intermediate zone, CP= Cortical plate, MZ= Marginal zone. Adapted from (Kriegstein and Noctor 2004). Created in BioRender. English, L. (2025) https://BioRender.com/hsl058e

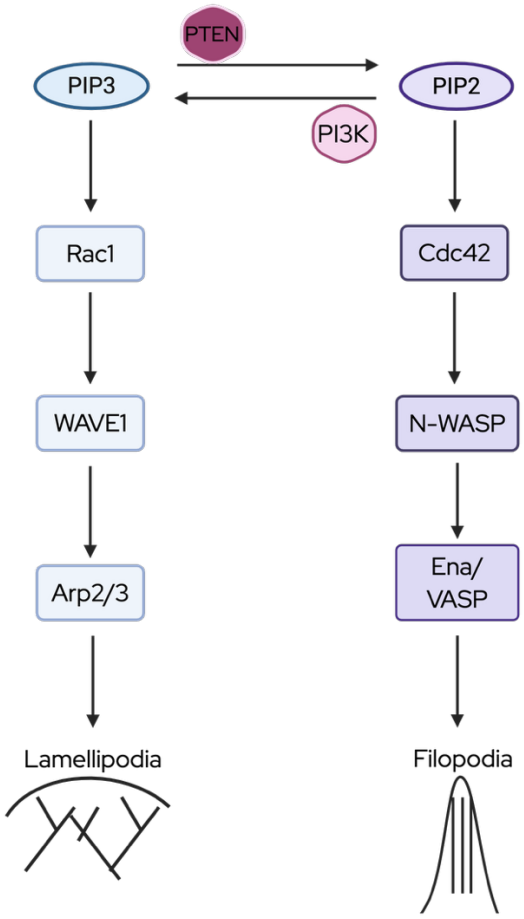

Figure 3. Rac1 and Cdc42 mediated pathways of actin assembly for lamellipodia and filopodia formation.

Rac1 pathway (left): PI3K (pink hexagon) phosphorylates PIP2 to PIP3 (blue oval) leading to Rac1 (blue rectangle) activation of WAVE1 (blue rectangle) which recruits Arp2/3 (blue rectangle) leading to actin branching for lamellipoda formation (Tahirovic, Hellal et al. 2010, Saengsawang, Taylor et al. 2013, Krause and Gautreau 2014, Tariq and Luikart 2021). Cdc42 pathway (right): PTEN (dark pink hexagon) dephosphorylates PIP3 to PIP2 (purple oval) leading to Cdc42 (purple rectangle) activation of N-WASP (purple rectangle) which recruits Ena/VASP (purple rectangle) to activate actin polymerization for filopodia formation (Mattila and Lappalainen 2008, Saengsawang, Taylor et al. 2013, Tariq and Luikart 2021). Created in BioRender. English, L. (2025) https://BioRender.com/mnancqg

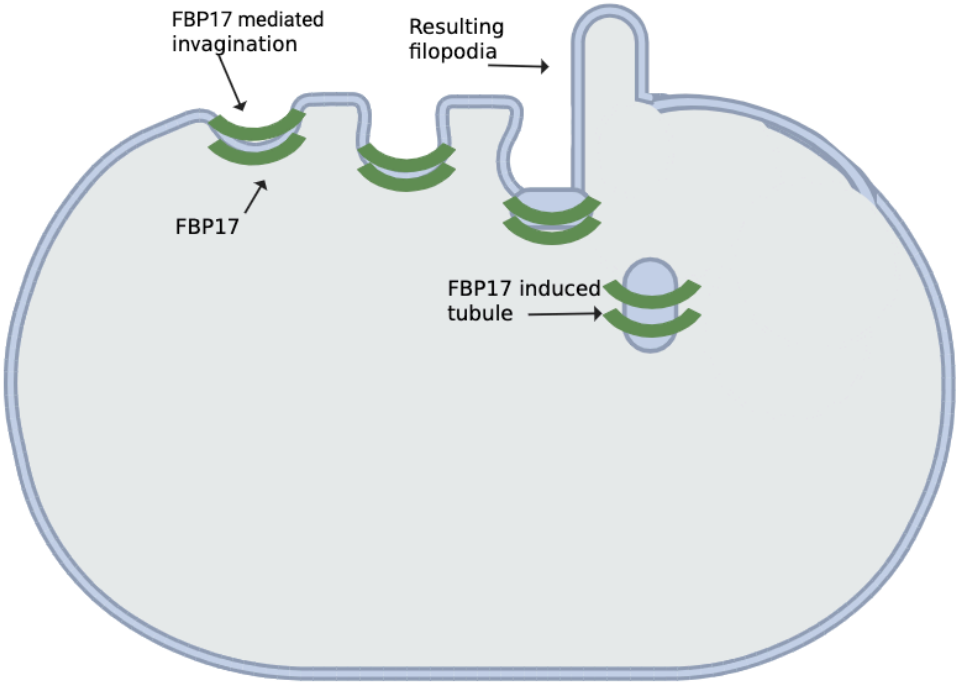

Figure 4. FBP17 mediated membrane invagination and resulting filopodia.

FBP17 (green) localizes to endocytic pits aiding in membrane deformation. The resulting invagination leaves a filopodia-like protrusion, while FBP17 itself localizes to the endocytosed membrane tubule. Created in BioRender. English, L. (2025) https://BioRender.com/xzxrvg1

References

Ahmed, S., Bu, W., Lee, R. T., Maurer-Stroh, S., & Goh, W. I. (2010). F-BAR domain proteins: Families and function. *Communicative & integrative biology*, *3*(2), 116-121. http://www.ncbi.nlm.nih.gov/pubmed/20585502

Aspenstrom, P. (1997). A Cdc42 target protein with homology to the non-kinase domain of FER has a potential role in regulating the actin cytoskeleton. *Curr Biol*, *7*(7), 479-487. http://www.ncbi.nlm.nih.gov/entrez/query.fcgi?cmd=Retrieve&db=PubMed&dopt=Citation&list_uids=9210375

Aspenstrom, P. (2009). Roles of F-BAR/PCH proteins in the regulation of membrane dynamics and actin reorganization. *Int Rev Cell Mol Biol*, *272*, 1-31. https://doi.org/S1937-6448(08)01601-8

Bahi-Buisson, N., & Guerrini, R. (2013). Diffuse malformations of cortical development. *Handb Clin Neurol*, *111*, 653-665. https://doi.org/10.1016/B978-0-444-52891-9.00068-3

Blake, T. C. A., Fox, H. M., Urbancic, V., Ravishankar, R., Wolowczyk, A., Allgeyer, E. S., Mason, J., Danuser, G., & Gallop, J. L. (2024). Filopodial protrusion driven by density-dependent Ena-TOCA-1 interactions. *J Cell Sci*, *137*(6). https://doi.org/10.1242/jcs.261057

Bu, W., Chou, A. M., Lim, K. B., Sudhaharan, T., & Ahmed, S. (2009). The Toca-1-N-WASP complex links filopodial formation to endocytosis. *J Biol Chem*, *284*(17), 11622-11636. https://doi.org/10.1074/jbc.M805940200

Buchsbaum, I. Y., & Cappello, S. (2019). Neuronal migration in the CNS during development and disease: insights from in vivo and in vitro models. *Development*, *146*(1). https://doi.org/10.1242/dev.163766

Chan, D. C., Bedford, M. T., & Leder, P. (1996). Formin binding proteins bear WWP/WW domains that bind proline-rich peptides and functionally resemble SH3 domains. *EMBO J*, *15*(5), 1045-1054. https://www.ncbi.nlm.nih.gov/pubmed/8605874

Chan Wah Hak, L., Khan, S., Di Meglio, I., Law, A. L., Lucken-Ardjomande Hasler, S., Quintaneiro, L. M., Ferreira, A. P. A., Krause, M., McMahon, H. T., & Boucrot, E. (2018). FBP17 and CIP4 recruit SHIP2 and lamellipodin to prime the plasma membrane for fast endophilin-mediated endocytosis. *Nat Cell Biol*, *20*(9), 1023-1031. https://doi.org/10.1038/s41556-018-0146-8

Cortay, V., Delaunay, D., Patti, D., Gautier, E., Doerflinger, N., Giroud, P., Knoblauch, K., Huissoud, C., Kennedy, H., & Dehay, C. (2020). Radial Migration Dynamics Is Modulated in a

Laminar and Area-Specific Manner During Primate Corticogenesis. *Front Cell Dev Biol*, *8*, 588814. https://doi.org/10.3389/fcell.2020.588814

Dent, E. W., Kwiatkowski, A. V., Mebane, L. M., Philippar, U., Barzik, M., Rubinson, D. A., Gupton, S., Van Veen, J. E., Furman, C., Zhang, J., Alberts, A. S., Mori, S., & Gertler, F. B. (2007). Filopodia are required for cortical neurite initiation. *Nat Cell Biol*, *9*(12), 1347-1359. http://www.ncbi.nlm.nih.gov/entrez/query.fcgi?cmd=Retrieve&db=PubMed&dopt=Citation&list_uids=18026093

des Portes, V., Pinard, J. M., Billuart, P., Vinet, M. C., Koulakoff, A., Carrie, A., Gelot, A., Dupuis, E., Motte, J., Berwald-Netter, Y., Catala, M., Kahn, A., Beldjord, C., & Chelly, J. (1998). A novel CNS gene required for neuronal migration and involved in X-linked subcortical laminar heterotopia and lissencephaly syndrome. *Cell*, *92*(1), 51-61. https://doi.org/10.1016/s0092-8674(00)80898-3

DeSantis, M. E., Cianfrocco, M. A., Htet, Z. M., Tran, P. T., Reck-Peterson, S. L., & Leschziner, A. E. (2017). Lis1 Has Two Opposing Modes of Regulating Cytoplasmic Dynein. *Cell*, *170*(6), 1197-1208 e1112. https://doi.org/10.1016/j.cell.2017.08.037

Dobyns, W. B., & Truwit, C. L. (1995). Lissencephaly and other malformations of cortical development: 1995 update. *Neuropediatrics*, *26*(3), 132-147. https://doi.org/10.1055/s-2007-979744

English, L. A., Taylor, R. J., Cameron, C. J., Broker, E. A., & Dent, E. W. (2024). F-BAR proteins CIP4 and FBP17 function in cortical neuron radial migration and process outgrowth. *bioRxiv*. https://doi.org/10.1101/2024.10.25.620310

Faulkner, N. E., Dujardin, D. L., Tai, C. Y., Vaughan, K. T., O'Connell, C. B., Wang, Y., & Vallee, R. B. (2000). A role for the lissencephaly gene LIS1 in mitosis and cytoplasmic dynein function. *Nat Cell Biol*, *2*(11), 784-791. https://doi.org/10.1038/35041020

Feng, Y., & Walsh, C. A. (2004). The many faces of filamin: a versatile molecular scaffold for cell motility and signalling. *Nat Cell Biol*, *6*(11), 1034-1038. https://doi.org/10.1038/ncb1104-1034

Fox, J. W., Lamperti, E. D., Eksioglu, Y. Z., Hong, S. E., Feng, Y., Graham, D. A., Scheffer, I. E., Dobyns, W. B., Hirsch, B. A., Radtke, R. A., Berkovic, S. F., Huttenlocher, P. R., & Walsh, C. A. (1998). Mutations in filamin 1 prevent migration of cerebral cortical neurons in human periventricular heterotopia. *Neuron*, *21*(6), 1315-1325. http://www.ncbi.nlm.nih.gov/entrez/query.fcgi?cmd=Retrieve&db=PubMed&dopt=Citation&list_uids=9883725

Franco, S. J., Martinez-Garay, I., Gil-Sanz, C., Harkins-Perry, S. R., & Muller, U. (2011). Reelin regulates cadherin function via Dab1/Rap1 to control neuronal migration and lamination in the neocortex. *Neuron*, *69*(3), 482-497. https://doi.org/10.1016/j.neuron.2011.01.003

Fricke, R., Gohl, C., & Bogdan, S. (2010). The F-BAR protein family Actin' on the membrane. *Communicative & integrative biology*, *3*(2), 89-94. http://www.ncbi.nlm.nih.gov/pubmed/20585497

Frost, A., Perera, R., Roux, A., Spasov, K., Destaing, O., Egelman, E. H., De Camilli, P., & Unger, V. M. (2008). Structural basis of membrane invagination by F-BAR domains [Research Support, N.I.H., Extramural
Research Support, Non-U.S. Gov't]. *Cell*, *132*(5), 807-817. https://doi.org/10.1016/j.cell.2007.12.041

Fujita, H., Katoh, H., Ishikawa, Y., Mori, K., & Negishi, M. (2002). Rapostlin is a novel effector of Rnd2 GTPase inducing neurite branching [Research Support, Non-U.S. Gov't]. *J Biol Chem*, *277*(47), 45428-45434. https://doi.org/10.1074/jbc.M208090200

Gil-Sanz, C., Franco, S. J., Martinez-Garay, I., Espinosa, A., Harkins-Perry, S., & Muller, U. (2013). Cajal-Retzius cells instruct neuronal migration by coincidence signaling between secreted and contact-dependent guidance cues. *Neuron*, *79*(3), 461-477. https://doi.org/10.1016/j.neuron.2013.06.040

Guerrier, S., Coutinho-Budd, J., Sassa, T., Gresset, A., Jordan, N. V., Chen, K., Jin, W. L., Frost, A., & Polleux, F. (2009). The F-BAR domain of srGAP2 induces membrane protrusions required for neuronal migration and morphogenesis. *Cell*, *138*(5), 990-1004. https://doi.org/10.1016/j.cell.2009.06.047

Guerrini, R., & Parrini, E. (2010). Neuronal migration disorders. *Neurobiol Dis*, *38*(2), 154-166. https://doi.org/10.1016/j.nbd.2009.02.008

Heng, J. I., Chariot, A., & Nguyen, L. (2010). Molecular layers underlying cytoskeletal remodelling during cortical development. *Trends Neurosci*, *33*(1), 38-47. https://doi.org/10.1016/j.tins.2009.09.003

Herculano-Houzel, S. (2012). The remarkable, yet not extraordinary, human brain as a scaled-up primate brain and its associated cost. *Proc Natl Acad Sci U S A*, *109 Suppl 1*(Suppl 1), 10661-10668. https://doi.org/10.1073/pnas.1201895109

Ho, H. Y., Rohatgi, R., Lebensohn, A. M., Le, M., Li, J., Gygi, S. P., & Kirschner, M. W. (2004). Toca-1 mediates Cdc42-dependent actin nucleation by activating the N-WASP-WIP complex. *Cell*, *118*(2), 203-216. https://doi.org/10.1016/j.cell.2004.06.027

Hu, Z., Zhu, J., Ma, Y., Long, T., Gao, L., Zhong, Y., Wang, X., & Li, Z. (2022). CIP4 targeted to recruit GTP-Cdc42 involving in invadopodia formation via NF-kappaB signaling pathway promotes invasion and metastasis of CRC. *Mol Ther Oncolytics*, *24*, 873-886. https://doi.org/10.1016/j.omto.2022.02.023

Innocenti, M. (2018). New insights into the formation and the function of lamellipodia and ruffles in mesenchymal cell migration. *Cell Adh Migr*, *12*(5), 401-416. https://doi.org/10.1080/19336918.2018.1448352

Itoh, T., Erdmann, K. S., Roux, A., Habermann, B., Werner, H., & De Camilli, P. (2005). Dynamin and the actin cytoskeleton cooperatively regulate plasma membrane invagination by BAR and F-BAR proteins. *Dev Cell*, *9*(6), 791-804. http://www.ncbi.nlm.nih.gov/entrez/query.fcgi?cmd=Retrieve&db=PubMed&dopt=Citation&list_uids=16326391

Jossin, Y., & Cooper, J. A. (2011). Reelin, Rap1 and N-cadherin orient the migration of multipolar neurons in the developing neocortex. *Nat Neurosci*, *14*(6), 697-703. https://doi.org/10.1038/nn.2816

Kakimoto, T., Katoh, H., & Negishi, M. (2004). Identification of splicing variants of Rapostlin, a novel RND2 effector that interacts with neural Wiskott-Aldrich syndrome protein and induces neurite branching [Research Support, Non-U.S. Gov't]. *J Biol Chem*, *279*(14), 14104-14110. https://doi.org/10.1074/jbc.M312763200

Kakimoto, T., Katoh, H., & Negishi, M. (2006). Regulation of neuronal morphology by Toca-1, an F-BAR/EFC protein that induces plasma membrane invagination. *J Biol Chem*, *281*(39), 29042-29053. http://www.ncbi.nlm.nih.gov/entrez/query.fcgi?cmd=Retrieve&db=PubMed&dopt=Citation&list_uids=16885158

Kamioka, Y., Fukuhara, S., Sawa, H., Nagashima, K., Masuda, M., Matsuda, M., & Mochizuki, N. (2004). A novel dynamin-associating molecule, formin-binding protein 17, induces tubular membrane invaginations and participates in endocytosis [Research Support, Non-U.S. Gov't]. *J Biol Chem*, *279*(38), 40091-40099. https://doi.org/10.1074/jbc.M404899200

Kawauchi, T., Chihama, K., Nabeshima, Y., & Hoshino, M. (2003). The in vivo roles of STEF/Tiam1, Rac1 and JNK in cortical neuronal migration. *EMBO J*, *22*(16), 4190-4201. https://doi.org/10.1093/emboj/cdg413

Konno, D., Yoshimura, S., Hori, K., Maruoka, H., & Sobue, K. (2005). Involvement of the phosphatidylinositol 3-kinase/rac1 and cdc42 pathways in radial migration of cortical neurons. *J Biol Chem*, *280*(6), 5082-5088. https://doi.org/10.1074/jbc.M408251200

Krause, M., & Gautreau, A. (2014). Steering cell migration: lamellipodium dynamics and the regulation of directional persistence. *Nat Rev Mol Cell Biol*, *15*(9), 577-590. https://doi.org/10.1038/nrm3861

Kriegstein, A. R., & Noctor, S. C. (2004). Patterns of neuronal migration in the embryonic cortex. *Trends Neurosci*, *27*(7), 392-399. https://doi.org/10.1016/j.tins.2004.05.001

Layden, B. T., Saengsawang, W., Donati, R. J., Yang, S., Mulhearn, D. C., Johnson, M. E., & Rasenick, M. M. (2008). Structural model of a complex between the heterotrimeric G protein, Gsalpha, and tubulin [Research Support, N.I.H., Extramural]. *Biochim Biophys Acta*, *1783*(6), 964-973. https://doi.org/10.1016/j.bbamcr.2008.02.017

Liu, S., Xiong, X., Zhao, X., Yang, X., & Wang, H. (2015). F-BAR family proteins, emerging regulators for cell membrane dynamic changes-from structure to human diseases. *J Hematol Oncol*, *8*, 47. https://doi.org/10.1186/s13045-015-0144-2

Lodato, S., & Arlotta, P. (2015). Generating neuronal diversity in the mammalian cerebral cortex. *Annu Rev Cell Dev Biol*, *31*, 699-720. https://doi.org/10.1146/annurev-cellbio-100814-125353

Lu, J., & Sheen, V. (2005). Periventricular heterotopia. *Epilepsy Behav*, *7*(2), 143-149. https://doi.org/10.1016/j.yebeh.2005.05.001

Machesky, L. M. (2008). Lamellipodia and filopodia in metastasis and invasion. *FEBS Lett*, *582*(14), 2102-2111. https://doi.org/10.1016/j.febslet.2008.03.039

Mattila, P. K., & Lappalainen, P. (2008). Filopodia: molecular architecture and cellular functions. *Nat Rev Mol Cell Biol*, *9*(6), 446-454. https://doi.org/10.1038/nrm2406

Molyneaux, B. J., Arlotta, P., Menezes, J. R., & Macklis, J. D. (2007). Neuronal subtype specification in the cerebral cortex. *Nat Rev Neurosci*, *8*(6), 427-437. https://doi.org/10.1038/nrn2151

Moon, H. M., & Wynshaw-Boris, A. (2013). Cytoskeleton in action: lissencephaly, a neuronal migration disorder. *Wiley Interdiscip Rev Dev Biol*, *2*(2), 229-245. https://doi.org/10.1002/wdev.67

Nadarajah, B., Brunstrom, J. E., Grutzendler, J., Wong, R. O., & Pearlman, A. L. (2001). Two modes of radial migration in early development of the cerebral cortex. *Nat Neurosci*, *4*(2), 143-150. https://doi.org/10.1038/83967

Nadarajah, B., & Parnavelas, J. G. (2002). Modes of neuronal migration in the developing cerebral cortex. *Nat Rev Neurosci*, *3*(6), 423-432. https://doi.org/10.1038/nrn845

Nagano, T., Morikubo, S., & Sato, M. (2004). Filamin A and FILIP (Filamin A-Interacting Protein) regulate cell polarity and motility in neocortical subventricular and intermediate zones during radial migration. *J Neurosci*, *24*(43), 9648-9657. https://doi.org/10.1523/JNEUROSCI.2363-04.2004

Noctor, S. C., Martinez-Cerdeno, V., Ivic, L., & Kriegstein, A. R. (2004). Cortical neurons arise in symmetric and asymmetric division zones and migrate through specific phases. *Nat Neurosci*, *7*(2), 136-144. https://doi.org/10.1038/nn1172

Reid, T., Furuyashiki, T., Ishizaki, T., Watanabe, G., Watanabe, N., Fujisawa, K., Morii, N., Madaule, P., & Narumiya, S. (1996). Rhotekin, a new putative target for Rho bearing homology to a serine/threonine kinase, PKN, and rhophilin in the rho-binding domain. *J Biol Chem*, *271*(23), 13556-13560. https://doi.org/10.1074/jbc.271.23.13556

Ridley, A. J. (2001). Rho GTPases and cell migration. *J Cell Sci*, *114*(Pt 15), 2713-2722. https://doi.org/10.1242/jcs.114.15.2713

Romero, D. M., Bahi-Buisson, N., & Francis, F. (2018). Genetics and mechanisms leading to human cortical malformations. *Semin Cell Dev Biol*, *76*, 33-75. https://doi.org/10.1016/j.semcdb.2017.09.031

Saengsawang, W., Mitok, K., Viesselmann, C., Pietila, L., Lumbard, D. C., Corey, S. J., & Dent, E. W. (2012). The F-BAR protein CIP4 inhibits neurite formation by producing lamellipodial protrusions [Research Support, N.I.H., Extramural Research Support, Non-U.S. Gov't]. *Curr Biol*, *22*(6), 494-501. https://doi.org/10.1016/j.cub.2012.01.038

Saengsawang, W., Taylor, K. L., Lumbard, D. C., Mitok, K., Price, A., Pietila, L., Gomez, T. M., & Dent, E. W. (2013). CIP4 coordinates with phospholipids and actin-associated proteins to localize to the protruding edge and produce actin ribs and veils. *J Cell Sci*, *126*(Pt 11), 2411-2423. https://doi.org/10.1242/jcs.117473

Sekine, K., Honda, T., Kawauchi, T., Kubo, K., & Nakajima, K. (2011). The outermost region of the developing cortical plate is crucial for both the switch of the radial migration mode and

the Dab1-dependent "inside-out" lamination in the neocortex. *J Neurosci*, *31*(25), 9426-9439. https://doi.org/10.1523/JNEUROSCI.0650-11.2011

Shimada, A., Niwa, H., Tsujita, K., Suetsugu, S., Nitta, K., Hanawa-Suetsugu, K., Akasaka, R., Nishino, Y., Toyama, M., Chen, L., Liu, Z. J., Wang, B. C., Yamamoto, M., Terada, T., Miyazawa, A., Tanaka, A., Sugano, S., Shirouzu, M., Nagayama, K., . . . Yokoyama, S. (2007). Curved EFC/F-BAR-domain dimers are joined end to end into a filament for membrane invagination in endocytosis [Research Support, Non-U.S. Gov't Research Support, U.S. Gov't, Non-P.H.S.]. *Cell*, *129*(4), 761-772. https://doi.org/10.1016/j.cell.2007.03.040

Su, M., Zhuang, Y., Miao, X., Zeng, Y., Gao, W., Zhao, W., & Wu, M. (2020). Comparative Study of Curvature Sensing Mediated by F-BAR and an Intrinsically Disordered Region of FBP17. *iScience*, *23*(11), 101712. https://doi.org/10.1016/j.isci.2020.101712

Suman, P., Mishra, S., & Chander, H. (2018). High expression of FBP17 in invasive breast cancer cells promotes invadopodia formation. *Med Oncol*, *35*(5), 71. https://doi.org/10.1007/s12032-018-1132-5

Tahirovic, S., Hellal, F., Neukirchen, D., Hindges, R., Garvalov, B. K., Flynn, K. C., Stradal, T. E., Chrostek-Grashoff, A., Brakebusch, C., & Bradke, F. (2010). Rac1 regulates neuronal polarization through the WAVE complex. *J Neurosci*, *30*(20), 6930-6943. https://doi.org/10.1523/JNEUROSCI.5395-09.2010

Tariq, K., & Luikart, B. W. (2021). Striking a balance: PIP(2) and PIP(3) signaling in neuronal health and disease. *Explor Neuroprotective Ther*, *1*, 86-100. https://doi.org/10.37349/ent.2021.00008

Taylor, K. L., Taylor, R. J., Richters, K. E., Huynh, B., Carrington, J., McDermott, M. E., Wilson, R. L., & Dent, E. W. (2019). Opposing functions of F-BAR proteins in neuronal membrane protrusion, tubule formation, and neurite outgrowth. *Life Sci Alliance*, *2*(3), e201800288. https://doi.org/10.26508/lsa.201800288

Tsai, J. W., Bremner, K. H., & Vallee, R. B. (2007). Dual subcellular roles for LIS1 and dynein in radial neuronal migration in live brain tissue [In Vitro Research Support, N.I.H., Extramural Research Support, Non-U.S. Gov't]. *Nat Neurosci*, *10*(8), 970-979. https://doi.org/10.1038/nn1934

Tsujita, K., Suetsugu, S., Sasaki, N., Furutani, M., Oikawa, T., & Takenawa, T. (2006). Coordination between the actin cytoskeleton and membrane deformation by a novel membrane tubulation domain of PCH proteins is involved in endocytosis [Research Support, Non-U.S. Gov't]. *J Cell Biol*, *172*(2), 269-279. https://doi.org/10.1083/jcb.200508091

Turrero Garcia, M., & Harwell, C. C. (2017). Radial glia in the ventral telencephalon. *FEBS Lett*, *591*(24), 3942-3959. https://doi.org/10.1002/1873-3468.12829

Urrutia, P. J., Bodaleo, F., Borquez, D. A., Homma, Y., Rozes-Salvador, V., Villablanca, C., Conde, C., Fukuda, M., & Gonzalez-Billault, C. (2021). Tuba Activates Cdc42 during Neuronal Polarization Downstream of the Small GTPase Rab8a. *J Neurosci*, *41*(8), 1636-1649. https://doi.org/10.1523/JNEUROSCI.0633-20.2020

Wakita, Y., Kakimoto, T., Katoh, H., & Negishi, M. (2011). The F-BAR protein Rapostlin regulates dendritic spine formation in hippocampal neurons [Research Support, Non-U.S. Gov't]. *J Biol Chem*, *286*(37), 32672-32683. https://doi.org/10.1074/jbc.M111.236265

Zhang, Z., Zheng, F., You, Y., Ma, Y., Lu, T., Yue, W., & Zhang, D. (2016). Growth arrest specific gene 7 is associated with schizophrenia and regulates neuronal migration and morphogenesis. *Mol Brain*, *9*(1), 54. https://doi.org/10.1186/s13041-016-0238-y

Chapter2:

F-BAR proteins CIP4 and FBP17 function in cortical neuron radial migration and process outgrowth

This chapter is under review as the following journal article:

English, L.A., Taylor R.J., Palmos J., Cameron C.J. Brooker E.A. TeVogt. E.M. Dent E.W. F-Bar proteins CIP4 and FBP17 function in cortical neuron migration radial migration and process outgrowth. 2025 (under review) *.

*L.A.E, and E.W.D. conceived the project with input from R.J.T. L.A.E., R.J.T., J.P., C.J.C, E.A.B., and E.M.T. executed the experiments. L.A.E and E.W.D wrote the manuscript with input from all authors. E.W.D supervised all aspects of the work.

ABSTRACT

Neurite initiation from newly born neurons is a critical step in neuronal differentiation and migration. Neuronal migration in the developing cortex is accompanied by dynamic extension and retraction of neurites as neurons progress through bipolar and multipolar states. However, there is a relative lack of understanding regarding how the dynamic extension and retraction of neurites is regulated during neuronal migration. In recent work we have shown that CIP4, a member of the F-BAR family of membrane bending proteins, inhibits cortical neurite formation in culture, while family member FBP17 induces premature neurite outgrowth. These results beg the question of how CIP4 and FBP17 function in radial neuron migration and differentiation *in vivo*, including the timing and manner of neurite extension and retraction. Indeed, the regulation of neurite outgrowth is essential for the transitions between bipolar and multipolar states during radial migration. To examine the effects of modulating expression of CIP4 and FBP17 *in vivo*, we used *in utero* electroporation, in combination with our published Double UP technique, to compare knockdown or overexpression cells with control cells within the same mouse tissue of either sex. We show that either knockdown or overexpression of CIP4 and FBP17 results in the marked disruption of radial neuron migration by modulating neuronal morphology and neurite outgrowth, consistent with our findings in culture. Our results demonstrate that the F-BAR proteins CIP4 and FBP17 are essential for proper radial migration in the developing cortex and thus play a key role in cortical development.

INTRODUCTION

The development of the mouse cerebral cortex requires precisely timed birth, migration, and maturation of millions of neurons. Pyramidal excitatory neurons are born in the ventricular zone, adjacent to the lateral ventricles **(Parnavelas 2000)**, then undergo a series of stereotyped morphological changes as they migrate radially from the ventricular zone to the cortical plate, taking their positions in a newly forming six-layer cortex **(Noctor, Martinez-Cerdeno et al. 2004)**. Newly born pyramidal neurons start out as spherical cells that extend short neurites termed leading and trailing processes. They begin their journey as a bipolar neuron in the ventricular zone, but in the subventricular zone they pause and develop a multipolar morphology. Subsequently, they retract these extraneous processes, at which point they resume radial migration as a bipolar neuron, until they reach their destination in the cortical plate, where they extend an axon toward the ventricular zone and a dendrite toward the pial surface **(Noctor, Martinez-Cerdeno et al. 2004)**.

Rho GTPases, and their associated GEFs and GAPs, are well known to play important roles in radial migration of cortical neurons **(Govek, Hatten et al. 2010, Azzarelli, Kerloch et al. 2014, Xu, Chen et al. 2019)**. Activated Rho GTPases, including Rac1, Cdc42 and RhoA, are recruited to the plasma membrane and interact with selected membrane-associated proteins **(Bement, Goryachev et al. 2024)**. One family of proteins that plays important roles in Rho GTPase signaling cascades are the F-BAR family of proteins. Although certain F-BAR proteins play key roles in cortical migration and neuronal development **(Guerrier, Coutinho-Budd et al. 2009, Charrier, Joshi et al. 2012)**, the roles of other F-BAR family members have been little studied, including the Cdc42 interacting protein 4 (CIP4) family of proteins.

The CIP4 family proteins are a subgroup of F-BAR proteins that are expressed in many tissues and act as polymeric, membrane binding complexes that interact with activated Rho GTPases and recruit actin associated proteins **(Aspenstrom 2009, Snider, Wan Mohamad Noor et al. 2021)**. The CIP4 subfamily is comprised of three members: CIP4, formin binding protein 17 (FBP17) and transducer of Cdc42-dependent actin assembly protein 1 (TOCA1) **(Aspenstrom 2009)**. These proteins typically sense and induce membrane curvature during endocytosis **(Itoh, Erdmann et al. 2005, Henne, Kent et al. 2007)**. However, we have shown that in dissociated cortical neurons CIP4 does not appear to function in membrane tubulation, but instead localizes to the protruding, peripheral plasma membrane **(Saengsawang, Mitok et al. 2012, Saengsawang, Taylor et al. 2013, Taylor, Taylor et al. 2019)**. Sustained overexpression of CIP4 inhibits neurite formation in dissociated cortical neurons, while newly plated neurons from CIP4 knockout mice initiate neurites prematurely **(Saengsawang, Mitok et al. 2012)**. CIP4 is expressed in the early embryonic cortex, with levels decreasing until birth, at which point it remains largely absent **(Saengsawang, Mitok et al. 2012)**. Curiously, FBP17 has an opposite effect in neurons compared to CIP4. FBP17 functions in endocytosis by localizing to discrete tubules in the cytoplasm and overexpression of FBP17 induces premature and excess neurite outgrowth **(Taylor, Taylor et al. 2019)**. Moreover, unlike CIP4, brain-wide FBP17 expression increases in late embryonic development and peaks in adulthood **(Wakita, Kakimoto et al. 2011)**. These findings suggest that CIP4 and FBP17 may have important and distinct roles in embryonic cortical neuron development.

To investigate the roles of CIP4 and FBP17 in radial migration we utilized *in utero* electroporation (IUE) to introduce plasmid DNA into newly born neurons along the lateral ventricles in the embryonic mouse cortex **(Saito and Nakatsuji 2001, Tabata and Nakajima 2001)**. Recently, we increased the rigor and reproducibility of IUE through a technique we describe as Double UP **(Taylor, Carrington et al. 2020)**. Double UP generates green cells containing no manipulation, and magenta cells that express a manipulation of interest (overexpression or knockdown) in the same electroporated region of cortex. This technique allows direct comparisons of control and manipulated neurons within the same section of cortex, as neurons dynamically migrate and change their morphology. Applying this technique, we show that CIP4 and FBP17 play critical, yet distinct roles in radial migration.

METHODS

DNA Constructs

Double UP mNeon to mScarlet is available through Addgene (#125134). pCAG-iCre was a gift from Wilson Wong (Addgene plasmid #89573). pSico PGK Puro was a gift from Tyler Jacks (Addgene plasmid #11586). The three shRNA sequences targeting mouse CIP4 are: (1) 5'- GTGTGTGGCTATCTACCATTT (2) 5'-GTCTGGAGCTGGCTAAGTA-3' and (3) 5'-GCCTAGATCAGGACATTAA -3'. The three shRNA sequences targeting mouse FBP17 are: (1) 5'-GCAAGCTCTGGCCATTCAT-3', (2) 5'- CCAGGAGCAATGGGAATACTA and (3) 5'-GTCGTAGAAGCCTATAAGT-3'. The shRNA sequence for the scramble construct is 5'-GGCGGAGATTTCTGACTGA-3'. Human CIP4 (short isoform- 545 aa, NM_004240.4) and human FBP17 (long isoform – 617 aa, NM_0.15033.3) were utilized for these experiments **(Taylor, Taylor et al. 2019)**. Human CIP4 short and FBP17 long isoforms that are C-terminally tagged with either EGFP or mScarlet are available from Addgene (#178363-178366). Deletions of essential domains were undertaken using uniport.org to define the bounds of those domains. CIP4ΔF-BAR was generated by deleting amino acids 2-264 from CIP4, CIP4ΔHR1 was generated by deleting amino acids 339-418, CIP4ΔSH3 was generated by deleting amino acids 484-545. FBP17ΔF-BAR was generated by deleting amino acids 2-264 from FBP17, FBP17ΔHR1 was generated by deleting amino acids 406-483, and FBP17ΔSH3 was generated by deleting amino acids 550-617. Further information and requests for resources and reagents should be directed to and will be fulfilled by the lead contact, Erik Dent (ewdent@wisc.edu).

Animal Models

All mouse procedures were approved by the University of Wisconsin Committee on Animal Care and were in accordance with NIH guidelines. Timed matings of Swiss Webster mice (Inotiv) were performed, with the morning of sperm plug visualization considered E0.5. IUE was performed at E14.5, with embryos perfused either two or four days later, as specified in the text. Both male and female embryos were used, with the sex of embryos not recorded. Pregnant females were housed individually. Prior to becoming pregnant, females were housed with 3-4 other females.

In Utero Electroporation (IUE)

For overexpression studies, 280ng of pCAG-iCre was mixed with 30µg of Double UP, Double UP CIP4, or Double UP FBP17. For knockdown studies, 280ng pCAG-iCre was mixed with 15µg Double UP and 30µg of either pSico-CIP4, pSico-FBP17, or pSico-scramble **(Taylor, Carrington et al. 2020)**. Plasmid DNA was then combined with Fast Green FCF to a final concentration of 0.05% and loaded into pulled capillary needles. The dam was anesthetized with isoflurane and a laparotomy was performed, exposing the embryos. The embryos were gently removed from the abdominal cavity. Capillary needles were inserted into the lateral ventricles of embryos, and approximately 0.25-0.5µL DNA/Fast Green FCF was injected using a PicoSpritzer II (Parker Instrumentation). Electrical current was passed across the head, in five pulses of 40 volts each lasting 100ms on and 900ms off, with a CUY21 Electroporator (Bex Co. LTD). After the last embryo was electroporated, the embryos were inserted back into the mother, and the laparotomy was sutured closed. Dams were

given 20 mg/kg Carprofen and 3.25 mg/kg extended-release buprenorphine S.C (Ethiqa). Dams were monitored for signs of pain every twelve hours for two days. Embryos were allowed to develop normally for 2-4 days, as indicated, until perfusion with saline, followed by 4% Paraformaldehyde (PFA). For postnatal collections, animals were anesthetized at 20-24 days with 120mg/kg sodium pentobarbital until a state of deep anesthesia is reached. Then animals were perfused with saline followed by 4% PFA.

Tissue Collection and Sectioning

For both IUE experiments, embryos were exposed via laparotomy after deep anesthesia of the pregnant dam with isoflurane. Embryos were removed from the uterus one by one and perfused by opening the chest cavity, making a small incision in the right atrium and inserting of a 25-gauge needle into the left ventricle. Through this needle, the animal was perfused with approximately 1mL of sterile saline and 3mL of 4% paraformaldehyde in PBS (PFA) at the rate of approximately 1.25mL per minute with a perfusion pump (Instech). Following perfusion, heads were removed and placed in 4% PFA at 4°C overnight. After the last embryo was perfused, the dam was euthanized via live decapitation.

After 16 hours in 4% PFA at 4°C, heads were transferred to PBS and brains were removed from skulls. The brains were placed in 6% low melt agarose and allowed to set on ice. After the agarose hardened, the brains or heads were sectioned on a Leica VT1000S vibratome at 100µm in phosphate-buffered saline (PBS). Sections from animals that underwent IUE were stored for less than one week in PBS before being stained with 4',6-diamidino-2-phenylindole (DAPI) and imaged. Sections were incubated in DAPI (2.4nM in

0.4% Triton/PBS) for 1 hour with gentle rotation at room temperature. Slices were washed in PBS and mounted onto slides with Aqua-Poly Mount (Polysciences). Slides were allowed to dry for at least one hour and then imaged within two days.

Imaging, Data Collection and Quantification

Imaging was performed on a Zeiss LSM 800 confocal microscope. For migration analysis, 12 optical sections were obtained, each 1µm apart. 2x2 tiles were collected with a 20x/0.8NA Plan Apochromat objective, with 2x averaging. For fixed morphology analysis 80-120 optical sections were obtained through the entirety of the 100µm section, each at 0.5µm. Although the entire section was imaged in the z-plane, less than 100µm was needed due to tissue compression. These images were also collected with a 20x/0.8NA Plan Apochromat objective, with 2x averaging. For IUE experiments, gain/laser power were altered between each image set to optimize image quality. Tiles were stitched together using the stitching tool in Zen 2.3 (Zeiss) software. Images of cortical neuron radial migration were analyzed and migration distances were calculated using the TRON software program **(Taylor, Carrington et al. 2020)**. Process number, length and angle of E14.5+2 and E14.5+4 neurons were calculated in Zen 2.3 (Zeiss) software. Neuronal polarity was calculated from process number data. All experimenters were blinded to condition.

Western Blot Analysis

For validation of shRNA constructs HEK293 cells were transfected with a post-cre recombined version of the pSico plasmid and either mouse CIP4-mScarlet or mouse FBP17-mScarlet using Lipofectamine 3000 (Invitrogen) following the manufacturers' protocol. After

48 hours, cells were washed once with cold PBS before being lysed using 300µL NP-40 Lysis Buffer (Invitrogen) with Complete Mini (Roche). Lysate was spun at 21,000*g* for 10 minutes, and supernatants were flash-frozen and stored at -80°C until use. Samples were thawed and loaded onto a 4–10% SDS-Page gel, then transferred to PVDF membrane (Millipore). Membranes were blocked in 5% milk in 0.1% TBS-T, incubated with primary antibody overnight at 4°C, and blotted with an HRP-conjugated secondary antibody for 1 hour at RT. Antibodies used were mouse anti-CIP4 (1:1000, BD Biosciences Cat#: 612556, RRID:AB_399847), Rabbit anti-FBP17 (1:500, Proteintech Cat#: 27056-1, RRID:AB_2880734), goat-anti-mouse HRP (1:10000, Jackson, Cat#: 115-035-166, RRID: AB_2338511), and goat-anti-rabbit HRP (1:5,000, Thermo Scientific Cat#: 31460, RRID:AB_228341). Protein bands were visualized using Pierce ECL Western blotting substrate (Thermo Scientific).

Quantification and Statistical Analysis

Radial migration distances, number of processes, length of longest process, and angle of longest process data were averaged for each color in each brain. Weighted, paired two-tailed t-tests were performed on averages from each brain. Mean migration and morphology data was weighted according to number of neurons and data variance within each brain **(Yu, Guindani et al. 2022, Li, Shelton et al. 2023)**. Neuronal polarity was analyzed by a two-way ANOVA with multiple comparisons. Complete data is available upon request. Weighted, paired t-tests were performed in Excel, and ANOVAs were performed in Prism 8 (GraphPad). Several graphs are presented as Superplots **(Lord, Velle et al. 2020, Goedhart 2021)**.

RESULTS

Overexpression of either CIP4 or FBP17 results in migration defects

Radial migration relies on a stereotyped series of extensions and retractions of minor processes during migration from the ventricular zone to the cortical plate **(Noctor, Martinez-Cerdeno et al. 2004)**. Sustained CIP4 or FBP17 overexpression markedly inhibits or promotes the formation and growth of neurites in cortical neurons *in vitro,* respectively **(Saengsawang, Mitok et al. 2012, Saengsawang, Taylor et al. 2013, Taylor, Taylor et al. 2019)**. Since CIP4 inhibits neurite formation and outgrowth, we hypothesized that it would result in a cell without any leading or trailing processes and thus be unable to migrate. Additionally, we hypothesized that sustained FBP17 overexpression *in vivo* would result in neurons with excess processes and likewise lead to a migration defect. To test these hypotheses, we utilized *in utero* electroporation (IUE) on embryonic day 14.5 (E14.5) brains in combination with the Double UP technique developed in the lab **(Taylor, Carrington et al. 2020)**. Double UP allowed us to generate both control (mNeon-green) and manipulated (mScarlet, shown in magenta) cells in the same brain, by utilizing limiting amounts of Cre to recombine plasmids in roughly half of the transfected cells **(Fig. 1a, b)**. This technique eliminates the need for section matching, decreasing variability between conditions and allows us to do a more rigorous assessment of changes in migration between control and experimental conditions **(Taylor, Carrington et al. 2020)**. Double UP also allows for the statistical comparison of matching mean migration distances in control and manipulated cells **(Fig. 1b)**. For these experiments we created two versions of the Double UP construct to

either overexpress mScarlet + unlabeled CIP4 (Double UP-CIP4) or mScarlet + unlabeled FBP17 (Double UP-FBP17) **(Fig. 1a, b)**, while control neurons expressed only mNeon.

We first confirmed our previous work **(Taylor, Carrington et al. 2020)** showing that expression of neither mNeon nor mScarlet fluorescent proteins alone differentially affect neuronal migration (Fig. 1c, d). Note that although the average distance migrated varied between experiments, both green and red cells within the same brain section generally migrated similar distances. Proceeding to our experimental conditions, we found that CIP4 overexpression in cortical neurons (magenta) from E14.5 to E18.5 (E14.5+4) resulted in a consistent, robust reduction of migration compared to green controls **(Fig. 1e, f)**. The majority of CIP4 overexpressing cells remained in the ventricular and subventricular zone **(Fig. 1e)**. FBP17 overexpression for four days (E14.5+4) showed a consistent, marked reduction in migration as well **(Fig. 1g, h)**. The mScarlet/FBP17 positive cells were primarily located in the intermediate zone compared to controls **(Fig. 1g)**. These results suggest that overexpression of either CIP4 or FBP17 markedly and consistently inhibits radial migration of cortical neurons.

Knockdown of CIP4 or FBP17 decreases migration in the intermediate zone at E14.5+4

Overexpression of either CIP4 or FBP17 resulted in dramatic migration defects. However, it is important to consider that overexpression of any protein may induce cellular defects from the inherent disruption of endogenous protein level. Therefore, we elected to examine whether decreasing expression of CIP4 and FBP17 would be similarly disruptive to radial migration. Utilizing an Empty Double UP vector, which induces the expression of only

mNeon or only mScarlet, in combination with a Cre-dependent shRNA vector, “pSico” **(Ventura, Meissner et al. 2004)**, we designed shRNAs to knockdown CIP4 and FBP17 *in utero*, while maintaining control (green) and knockdown (magenta) cells in the same slice. We utilized three different shRNAs for both CIP4 and FBP17 and tested their effectiveness in HEK293 cells overexpressing either mouse CIP4 (mCIP4) or mouse FBP17 (mFBP17). Quantification of western blots of HEK293 lysates showed significant knockdown of both expressed mCIP4 **(Fig. 2a, b)** and mFBP17 **(Fig. 2c d)**. We first tested a scrambled shRNA sequence as a control, electroporating Double UP combined with a scrambled shRNA into E14.5 embryos and allowing for four days of development (E18.5). This control experiment showed equivalent levels of migration between magenta and green cells **(Fig. 2e, f)**.

To determine how CIP4 knockdown affected radial migration we electroporated three separate shRNAs and measured their effects on migration. Although all three CIP4 shRNAs decreased expression of exogenous CIP4 in HEK293 cells **(Fig. 2a, b)**, we discovered that CIP4 knockdown with the stronger shRNAs 1 and 2 resulted in a robust and consistent reduction of migration **(Fig. 2g-j)**, while the weaker shRNA3 resulted in an inconsistent migration defect that was not statistically different than control cells **(Fig. 2k, l,)**. Cells expressing CIP4 shRNAs 1 and 2 consistently clustered in the intermediate zone below control cells. CIP4 shRNA3 showed inconsistent results with more cells spread throughout the intermediate zone and cortical plate **(Fig. 2g, i, k)**. These results suggest that two of three shRNAs to CIP4 were capable of markedly and consistently decreasing radial migration of cortical neurons.

We then tested whether our FBP17 shRNAs resulted in defects in radial migration. All three FBP17 shRNAs significantly decreased exogenous FBP17 expression in HEK293 cells **(Fig. 2c-d)**. However, only two of the three FBP17 shRNAs resulted in decreased radial migration **(Fig. 2m-p)**. FBP17 shRNA1 and 2 halted migration in the lower cortical plate and intermediate zone **(Fig. 2m, o)**, while FBP17 shRNA3 expressing cells migrated into the cortical plate but usually not as far as controls **(Fig. 2q)**. Like CIP4 shRNAs, the two shRNAs most effective at knocking down FBP17 in HEK293 cells were also effective at robustly and consistently inhibiting radial migration of cortical neurons. Together, these results suggest that either increasing or decreasing expression of either CIP4 or FBP17 consistently and markedly disrupts radial migration of cortical neurons in the developing brain.

Because these results suggest that levels of these two proteins need to be precisely titrated to allow proper radial migration, we did not attempt to rescue these migration defects with shRNA-resistant CIP4 or FBP17. All our overexpression constructs rely on a strong CAG promoter that does not allow titration of expression. Furthermore, because both proteins are changing expression from E14.5-E18.5 (CIP4 decreasing and FBP17 increasing) it would be difficult to titrate appropriate levels of proteins. Thus, we have relied on using several distinct shRNAs to show consistent defects in migration.

Overexpression of CIP4, but not FBP17, negatively affects migration by inhibiting process initiation at E14.5+2 days

We next examined an earlier timepoint after electroporation (E15.4+2) to glean insight into the mechanism underlying the disruption of radial migration induced by varying levels

of CIP4 and FBP17 expression. Migrating neurons assume a variety of morphologies during their migration from the ventricular zone to the cortical plate, transitioning between bipolar and multipolar shapes, corresponding to the zone of cortex they inhabit **(Noctor, Martinez-Cerdeno et al. 2004)**. Examination of neurons two days after electroporation allowed for the direct comparison of neuronal morphology between control and manipulated neurons within a similar region of cortex, because most cells had not yet migrated far from the ventricular zone. Again, to confirm that our findings were due to CIP4 or FBP17 overexpression, we utilized Empty Double UP, which induces the expression of only mNeon or only mScarlet after electroporation. Green and magenta cells showed no difference in migration two days after electroporation (E14.5+2) **(Fig. 3a, b)**. We also compared the morphology of cells expressing Double UP at E14.5+2. Green and magenta cells had similar morphologies, with no difference in the number or length of processes **(Fig. 3c-f)**. Additionally, we analyzed the polarity of migrating cells and found that most cells exhibited a multipolar morphology at E14.5+2 in both Double UP conditions **(Fig. 3g)**.

Surprisingly, CIP4 overexpression for two days (E14.5+2) still resulted in a significant inhibition of migration **(Fig. 3h, i)**. CIP4 overexpressing neurons also had significantly reduced complexity **(Fig. 3j, j', k)**, with very few processes **(Fig. 3l)**. Indeed, most neurons were spherical with few or no processes. This morphology *in* vivo is consistent with the circular morphology and lack of processes documented in CIP4 overexpressing neurons on a flat cell culture substrate **(Saengsawang, Mitok et al. 2012, Saengsawang, Taylor et al. 2013, Taylor, Taylor et al. 2019)**. Focusing only on cells that did produce processes, we found CIP4 expressing cells still had significantly shorter processes than control cells **(Fig.**

3m). When grouped by polarity, CIP4 overexpression induced a significantly higher number of nonpolar (process-less) cells and significantly fewer multipolar cells compared to controls **(Fig. 3n)**. Together, the effect of CIP4 overexpression on migration and morphology of radially migrating cortical neurons suggests that CIP4 delays or prevents process initiation, leading to a decrease in migration.

While CIP4 overexpression negatively affected migration at both two and four days after electroporation, FBP17 overexpression at two days after electroporation showed similar migration patterns to controls **(Fig. 3o, p)**. Moreover, FBP17 overexpressing cells did not differ significantly in their morphology compared to controls **(Fig. 3q, q', r)**, with a similar number of processes, length of longest process, and polarity compared to controls **(Fig. 3s-u)**. Since FBP17 overexpression at E14.5 +4 significantly affected migration, we completed additional analysis on the morphology of FBP17 cells at E14.5 +2 to understand further how FBP17 affects migration. We noticed some FBP17-expressing neurons seemed to be oriented perpendicular to the top of the cortical plate **(Fig. 3q' magenta triangle)** instead of at a 45 ° angle, like the controls. We measured the angle of the longest process of FBP17 and control cells, and between mNeon and mScarlet in the Double UP control condition. We did not find a significant difference between controls and FBP17 overexpressing cells or between control mNeon and mScarlet expressing cells **(Fig. S1a, b)**. These results indicate that FBP17 overexpression does not appear to affect morphology or migration after two days of post-electroporation expression.

One possibility for our strong effects of CIP4 overexpression after either two days **(Fig. 3h, i)** or four days **(Fig. 1e, f)** of expression is that CIP4 is killing the neurons, resulting in a

spherical cell, incapable of migrating or extending processes. We thought this an unlikely scenario given that we have expressed CIP4 in cultured cortical neurons for several days **(Saengsawang, Mitok et al. 2012, Saengsawang, Taylor et al. 2013)**. However, to determine if the cells were capable of remaining viable well after electroporation, we allowed several electroporated embryos to survive until postnatal day 21 (E14.5→P21). We discovered the CIP4 overexpressing cells were viable and present throughout the cortex **(Fig. S2a)**. However, they maintained a migration defect and had few processes, compared to green control neurons. Thus, overexpression of CIP4 in neurons that would normally downregulate the protein **(Saengsawang, Mitok et al. 2012)**, maintains neurons in a state where they only extend short processes and have defective migration.

Knockdown of CIP4, but not FBP17, negatively affects migration by promoting process initiation at E14.5+2 days

We next examined if we could detect a shRNA-mediated decrease in migration at the E14.5+2 timepoint. Consistent with the results at four days after electroporation **(Fig. 2e, f)**, the scrambled shRNA resulted in no difference between green and magenta neurons in either migration **(Fig. 4a, b)**, process number **(Fig. 4c-e)**, or polarity **(Fig. 4g)** two days post-electroporation. We did find a weak, but statistically significant difference in the process length between the control (green) and scrambled shRNA (magenta) neurons. This result may be due to scrambled shRNA having some effect on process outgrowth compared to the no shRNA control and process outgrowth may be a particularly sensitive measure.

Despite the shorter time for shRNA expression, CIP4 knockdown significantly inhibited migration **(Fig. 4h, i)**, suggesting radial migration is very sensitive to levels of CIP4 expression. Additionally, there was a pronounced effect of CIP4 knockdown on neuronal morphology **(Fig. 4j, j', k)**, resulting in more processes relative to adjacent, control cells **(Fig. 4l)**. Our data suggests there may be longer processes as well, but this cannot be determined with this approach due to the similar difference in process length detected in the control condition **(compare Fig. 4f and 4m)**. CIP4 knockdown also resulted in significantly more multipolar cells, and fewer bipolar cells compared to controls **(Fig. 4n)**. Additionally, we observed some CIP4 knockdown cells had long, thin processes that were oriented parallel to the top of the cortical plate **(Fig. 4j' pink arrows)**. Therefore, we analyzed the angle of the longest process to the top of the cortical plate as done previously. However, there was no significant difference between CIP4 knockdown and controls **(Fig. S3a, b)**. Consistent with previous CIP4 knockout data in culture **(Saengsawang, Mitok et al. 2012)**, we show that CIP4 knockdown resulted in precocious process outgrowth. Interestingly, CIP4 knockdown for an extended period (E14.5 →P24) resulted in an over-migration phenotype, where CIP4 knockdown neurons migrated beyond control neurons in the cortex **(Fig. S2b)**. This result suggests some quantity of CIP4 is important for stopping neuronal migration in the final stage of radial migration.

We also examined FBP17 knockdown at E14.5+2 and saw no significant effect on migration compared to controls **(Fig. 4o, p)**. Similarly, the morphology and migration angle of the FBP17 knockdown neurons was not different compared to controls **(Fig. 4q-u, Fig. S3c)**. These results suggest that FBP17 overexpression or knockdown has a more nuanced

effect on radial migration that is not detected by our morphology measurements at two days post-transfection. Thus, our FBP17 overexpression **(Fig. 1g-h)** and knockdown data **(Fig. 2m-p)** indicate that although there is a robust migration defect at four days post-electroporation, we could not detect any change in morphology or migration angle defect after FBP17 overexpression **(Fig. 3o-u, Fig. S1)** or knockdown **(Fig. 4o-u, Fig. S3c)** after only two days. Curious as to why this was the case, we analyzed the length of the leading process for both FBP17 overexpression and knockdown at E14.5+4. We discovered that overexpression or knockdown of FBP17 resulted in longer leading processes after four days **(Fig. S4a, b)**. Thus, four days of expression of FBP17 or FBP17 shRNA is required to produce migration and morphology defects, suggesting that FBP17 may be functioning later in radial migration than CIP4.

As mentioned above, we have not sought to rescue defects in migration with shRNA resistant CIP4 or FBP17 because of our lack of control of expression levels. However, we tried to rescue the defect in CIP4 knockdown with a weak, constitutively active Rac1 mutant (L61), since we have shown in cortical neurons that CIP4 is acting through Rac1, rather than Cdc42 **(Saengsawang, Mitok et al. 2012, Saengsawang, Taylor et al. 2013, Taylor, Taylor et al. 2019)**. However, unlike its ability to rescue a migration defect from Pyk2 overexpression, which inhibits Rac1 and increases neurite formation **(Fan, Lu et al. 2018)**, this mutant was incapable of rescuing the CIP4 shRNA migration defect **(Fig. S5c, d)**. This result suggests that CIP4 may be acting downstream of Rac1 and very precise levels of CIP4 are required for proper cortical neuron migration.

Domain deletions in CIP4 and FBP17 are less effective at inhibiting migration than full-length proteins

Previous work from our lab using exhaustive domain and linker swapping showed that each domain of CIP4 and FBP17 functions in distinct ways **(Taylor, Taylor et al. 2019)**. The F-BAR domain is required for dimerization and end-to-end binding, resulting in polymerization of CIP4 and FBP17 around membrane **(Shimada, Niwa et al. 2007, Frost, Perera et al. 2008)**. The HR1/REM domain of CIP4 is critical for binding to protruding plasma membrane, while the HR1/REM domain of FBP17 is likely in an autoinhibited state due to the SH3 domain binding to a polyproline region in the extended first linker region, which is absent in the CIP4 isoform present in cortical neurons **(Taylor, Taylor et al. 2019)**. The SH3 domain of CIP4 is important for plasma membrane dynamics, although deletion still results in a round phenotype, while the SH3 domain in FBP17 may be more important for autoinhibition by binding a poly-proline region in the extended first linker region of FBP17 **(Taylor, Taylor et al. 2019)**.

Considering the distinct functions of the three domains of CIP4 and FBP17, we were curious which domains are important for radial cortical migration. We created three constructs for each protein, one without the F-BAR domain (ΔF-BAR), one without the HR1/REM domain (ΔHR1), and one without the SH3 domain (ΔSH3) and compared them to the full length CIP4 or FBP17 **(Fig. 5)**. Not surprisingly, we found that each of the domain mutants was less effective at inhibiting migration than the CIP4 and FBP17 full-length proteins. Specifically, for CIP4 the ΔSH3 mutant resulted in the strongest migration phenotype (similar to full-length protein), followed by the ΔHR1 and ΔF-BAR mutants **(Fig.**

5a-h). All three mutants were significantly different than controls, suggesting each mutant had residual activity that resulted in migration defects. However, for FBP17 the ΔF-BAR and ΔHR1 mutants were not significantly different than control neurons, suggesting they play fundamental roles in the action of FBP17 on migration. Conversely, the ΔSH3 mutant was significantly different than controls, but to a lesser extent than the full-length protein, suggesting the SH3 domain is the most dispensable domain for both CIP4 and FBP17, whereas the F-BAR and HR1/REM domains are more intrinsic to the function of these proteins. These results are entirely consistent with our results from cultured cortical neurons (Taylor, Taylor et al. 2019).

DISCUSSION

Evidence presented here suggests that CIP4 and FBP17 have essential roles in brain development by modulating neurite formation and neuronal migration. Premature loss of CIP4 results in more and longer neurites, and prolonged overexpression of CIP4 inhibits neurites almost entirely, resulting in a robust migration deficit. Both loss of FBP17 and overexpression of FBP17 cause a migration defect at E14.5+4. However, we did not detect a significant difference in the morphology of cells transfected with FBP17 or FBP17 shRNA until four days of expression, consistent with a significant but weaker phenotype than CIP4. Thus, we hypothesize that precisely timed CIP4 downregulation is essential for the transition to the bipolar morphology that cortical neurons must develop to promote their migration out of the subventricular zone **(Fig. 6)**. FBP17 expression increases from low levels prenatally to higher levels postnatally (Wakita, Kakimoto et al. 2011), which is consistent with a weaker and later phenotype, after the transition from multipolar to bipolar morphology **(Fig. 6)**. These findings expand the opposing phenotypes of CIP4 and FBP17 from our previous cell culture work (Taylor, Taylor et al. 2019) to the radial migration of cortical neurons *in vivo*.

The first stage of radial migration occurs in the ventricular zone as the newborn neuron begins process initiation and transitions from a spherical to a bipolar morphology. This transition appears important for the subsequent migration of neurons up the radial glia cells toward the subventricular zone (Hatanaka and Murakami 2002, Noctor, Martinez-Cerdeno et al. 2004). We have shown that CIP4 overexpression inhibits newborn neurons from initiating processes, leading to an early halt in migration, with many cells incapable of migrating out of the subventricular zone **(Fig. 6)**. This phenotype is not due to the death of CIP4 overexpressing neurons because we

have examined CIP4 overexpression in postnatal animals (P21) and discovered that at least a portion of CIP4-overexpressing neurons manage to migrate out of the subventricular zone. Interestingly, prolonged CIP4 expression leads to three populations of cells, one that migrates relatively normally, one that migrates into the deep cortical layers, and one that never migrates out of the subventricular zone **(Fig. S2a)**. These data suggest that CIP4 must be downregulated for neurons to migrate out of the subventricular zone, and continued CIP4 expression results in spherical neurons that cannot migrate radially and eventually send out long processes in the developing cortex. However, our result in postnatal animals suggests that CIP4 is still present at some level during the final stage of migration because eliminating CIP4 through knockdown causes an over-migration phenotype **(Fig. S2b)**, suggesting CIP4 is also important for halting migration of neurons at the final stage of migration.

The second stage of migration occurs in the intermediate zone as neurons transition to a multipolar morphology. Subsequently, the final stage of migration occurs as the neurons exit the intermediate zone, where they transition back to a bipolar morphology and translocate through the cortical plate (Tabata and Nakajima 2001, Noctor, Martinez-Cerdeno et al. 2004, Namba, Kibe et al. 2014). While the purpose of neurons undergoing a multipolar phase is still unclear, failure to exit this phase of migration can result in lissencephaly, epilepsy and intellectual disability (Stouffer, Golden et al. 2016). When CIP4 is knocked down early in migration, neurons show a decrease in migration as early as E14.5+2 days, which persists to E14.5+4, with many CIP4 knockdown cells unable to translocate through the intermediate zone. Additionally, there is an increase in multipolar cells among CIP4 knockdown cells compared to controls at E14.5+2. We hypothesize that under endogenous conditions, CIP4 activity plays a vital role in regulating

neurite retraction. Thus, without CIP4 neurons cannot retract processes that are extended in the intermediate zone and continue their migration as bipolar neurons.

Our data suggest that the role FBP17 plays in neurite dynamics during radial migration may be delayed relative to CIP4. This idea is consistent with other studies that have shown that endogenous FBP17 expression begins to increase in the brain after E16.5 **(Wakita, Kakimoto et al. 2011)**. While it is interesting that early overexpression of FBP17 did not affect migration or morphology at E14.5 +2, the role of FBP17 in neurite dynamics may be more subtle, hence more challenging to detect *in vivo*. This hypothesis is corroborated by our data showing that knockdown of FBP17 does not affect migration until after E14.5+2. Consistent with our findings, FBP17 has been shown to play a role in neurite branching and dendritic spine development much later in development **(Fujita, Katoh et al. 2002, Wakita, Kakimoto et al. 2011)**.

An increasing number of proteins are found to be important for transitioning out of the multipolar stage, including Lis1 (Tsai, Chen et al. 2005), doublecortin (Bai, Ramos et al. 2003), filamin A (Nagano, Morikubo et al. 2004), lamellipodin (Pinheiro, Xie et al. 2011) and Nyap1 (Wang, Li et al. 2020). All these proteins are cytoskeletal-associated proteins, suggesting that remodeling of the cytoskeleton is essential for this morphological transition from multipolar to bipolar morphology upon exiting the intermediate zone during migration. While, two other F-BAR proteins, srGAP2 and GAS7 (Guerrier, Coutinho-Budd et al. 2009, Zhang, Zheng et al. 2016) have been implicated in neuronal migration, CIP4 and FBP17 would be the first F-BAR proteins shown to have a specific role in the multipolar to bipolar morphological transition.

The primary function of CIP4 and FBP17 is sensing and inducing membrane curvature (Tsujita, Suetsugu et al. 2006, Takano, Toyooka et al. 2008, Fricke, Gohl et al. 2009, Hartig, Ishikura et al. 2009, Saengsawang, Taylor et al. 2013, Stanishneva-Konovalova, Kelley et al. 2016) and the F-BAR domain (Shimada, Niwa et al. 2007, Frost, Perera et al. 2008) and a short poly-basic region following the F-BAR domain are both required for binding plasma membrane in primary cortical neurons (Taylor, Taylor et al. 2019). To assess if membrane binding is essential for migration we tested the effect on migration of CIP4ΔF-BAR and FBP17ΔF-BAR. We have previously shown that CIP4ΔF-BAR does not have a significant effect on morphology of cultured cortical neurons (Saengsawang, Mitok et al. 2012). Thus, we expected that CIP4ΔF-BAR and FBP17ΔF-BAR would not affect migration, because removal of the F-BAR domain would eliminate dimerization and membrane binding. To our surprise CIP4ΔF-BAR did indeed inhibit migration, but to lesser degree than full-length CIP4, while FBP17ΔF-BAR had no effect on migration. This effect may be due to CIP4ΔF-BAR binding and sequestering active Rac1, via the intact HR1/REM domain, away from the plasma membrane, since radial cortical neuron migration is very sensitive to Rac1 inhibition (Kawauchi, Chihama et al. 2003, Konno, Yoshimura et al. 2005, Taylor, Carrington et al. 2020). Whereas, FBP17ΔF-BAR is likely to bind active Cdc42 (Taylor, Taylor et al. 2019), which has less of an effect on migration than Rac1 (Konno, Yoshimura et al. 2005). Both CIP4ΔSH3 and FBP17ΔSH3 showed a significant effect on migration, indicating these mutants are acting most closely to the full-length protein, which suggests they are dispensable for radial migration. Together these results suggest that in radial migration of cortical neurons the order of domain importance is F-BAR>HR1>SH3 for both CIP4 and FBP17.

If during radial migration, CIP4 and FBP17 function with Rac1 and Cdc42, respectively, as we have shown they do in neurite generation in culture (Taylor, Taylor et al. 2019), then we would expect that knockdown of CIP4 and FBP17 could be rescued by constitutively active or wild-type versions of Rac1 and Cdc42, respectively. To begin to answer this question we attempted to rescue the migration phenotype resulting from CIP4 shRNA expression with a weakly constitutively active Rac1 mutant (L61). However, this mutant did not have any effect on migration in CIP4 knockdown neurons, suggesting that CIP4 may be acting downstream of Rac1 and even with overactive Rac1, lack of CIP4 still inhibits process retraction in the multipolar stage of migration.

We have shown here that titrated levels of CIP4 and, to a lesser degree, FBP17 are critical for proper radial migration and changing activity with constitutively active Rac1 mutant may be too blunt of an instrument for precisely regulating CIP4 and FBP17 activity. A more nuanced approach may be to regulate GTPase activity by decreasing Rac1/3 GEF activity by knocking down P-Rex1, or GTPase scaffolds such as POSH. Indeed, P-Rex1 **(Yoshizawa, Kawauchi et al. 2005, Dimidschstein, Passante et al. 2013, Li, Wang et al. 2019)** and POSH **(Yang, Sun et al. 2012)** have similar migration and morphological phenotypes as CIP4. Another possibility is that during radial migration, CIP4 and FBP17 interact with different GTPases, such as Rnd2 and Rnd3. In the developing cortex, Rnd2 and Rnd3 have similar phenotypes and expression patterns to CIP4 and FBP17, respectively **(Heng, Nguyen et al. 2008, Pacary, Heng et al. 2011)**. Thus, further work will be needed to define the cohort of proteins interacting with the CIP4 family of F-BAR proteins during cortical neuron radial migration in the developing cortex.

FIGURES

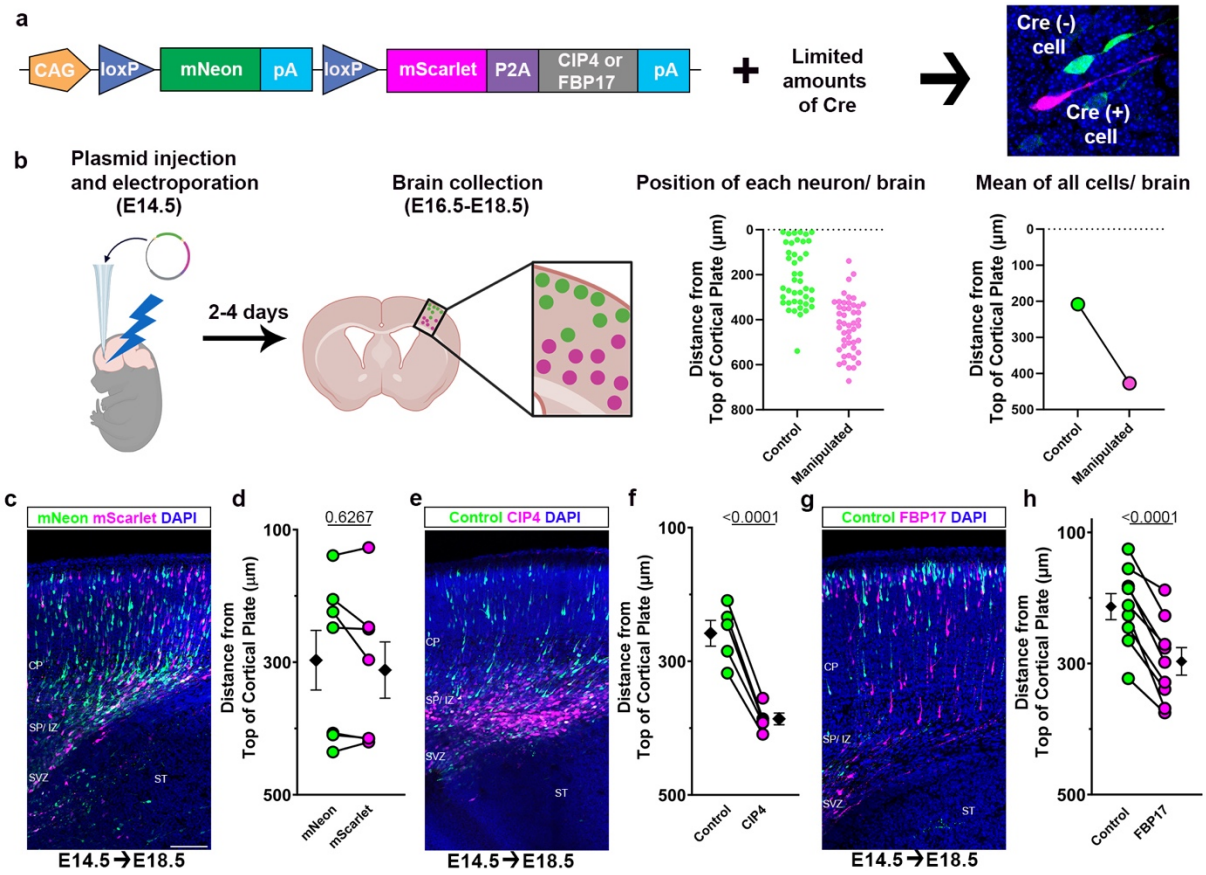

Figure 1. Overexpression of CIP4 or FBP17 decreases migration at E14.5+4 days.

(a) Representation of the Double UP overexpression plasmid construct used in these experiments. Neurons that are transfected with only the Double UP plasmid express mNeon-green (Cre(-) cell). When limited amounts of Cre are co-transfected into about half the neurons, these neurons express mScarlet (mNeon-green is excised) and unlabeled CIP4 or FBP17 (Cre(+) cell). (b) Schematic of experimental design and quantitation procedure. (c, e, g) Representative images of empty Double UP (c), Double UP + CIP4 (e), and Double UP + FBP17 (g) four days after electroporation at E14.5 (E14.5→E18.5). CP= cortical plate, SP/IZ=

subplate/intermediate zone, SVZ= subventricular zone, ST= striatum, V= lateral ventricle. Scale bar 100μm. (d, f, h) Dot plots of migration of green and magenta cells. Each dot represents the cumulative mean distance from the top of the cortical plate for all labeled neurons in a single coronal brain section. Connected dots indicate measurements were made in the same coronal section. Black diamonds and bars represent cumulative mean ± SEM. All p values are from a weighted, paired t-test (two-tailed). (d) 7 brains, mNeon: mean 295±45μm, 1316 cells, mScarlet: 310±42μm, 1055 cells. (f) 5 brains, Control: 258±19μm, 987 cells, CIP4: 386±9μm, 999 cells. (h) 9 brains, Control: 213±20μm, 2058 cells, FBP17: 297±21μm, 1724 cells. All values mean±SEM. (b) Created in BioRender. English, L. (2024) BioRender.com/u35d157

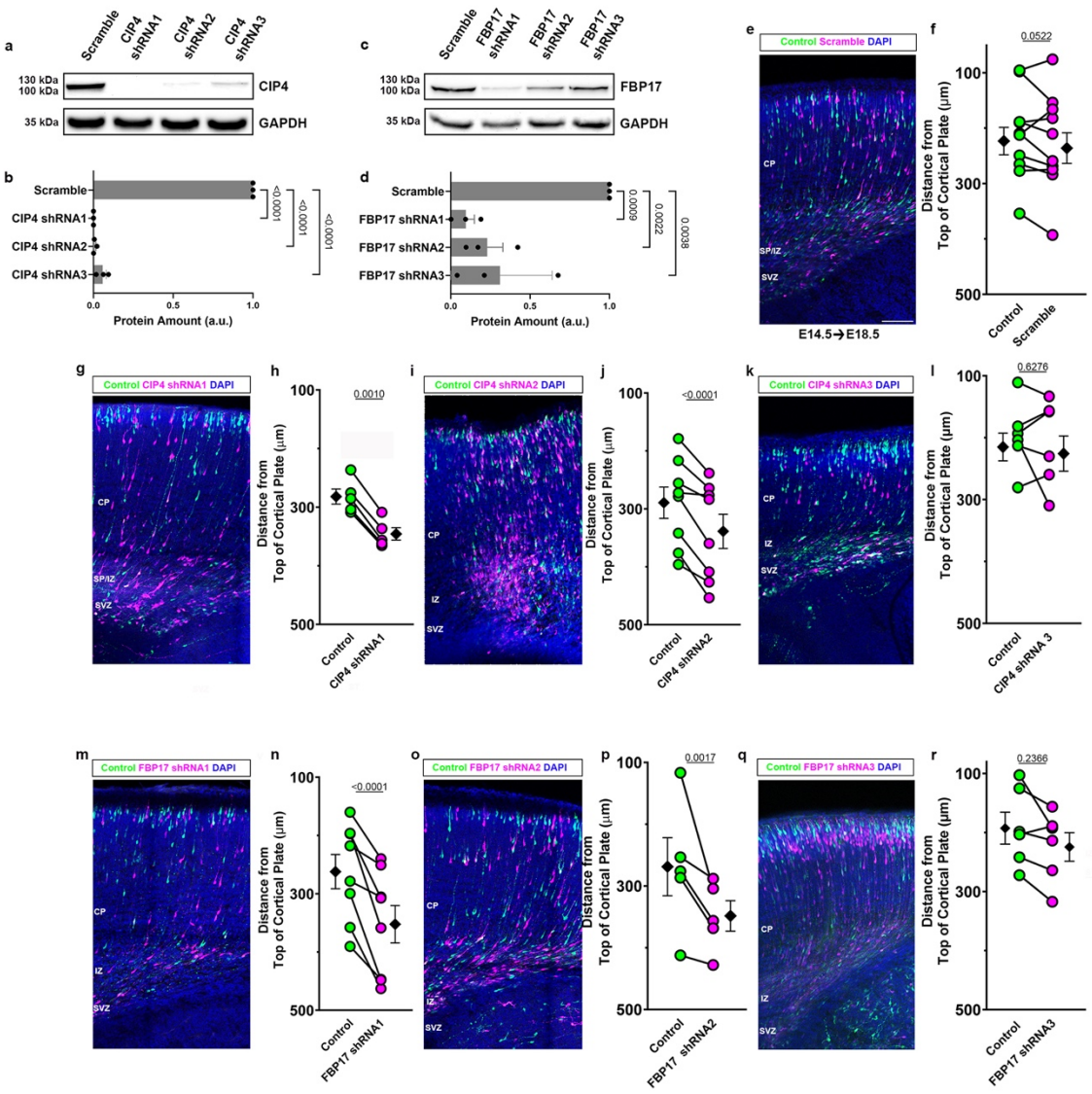

Figure 2. Knockdown of CIP4 or FBP17 decreases migration at E14.5+4 days.

(a) Western blot of HEK293 cells transfected with mouse CIP4 and post-Cre pSico plasmids expressing either scramble or one of three CIP4-targeted shRNAs. (b) Quantification of western blots in (a). (c) Western blot of HEK293 cells transfected with mouse FBP17 and post-Cre pSico plasmids expressing either scramble or one of three FBP17-targeted shRNAs. (d) Quantification of western blots in (c). (e) Representative image of Double UP +

pSico scramble shRNA four days after electroporation at E14.5 (E14.5→E18.5). Scale bar 100μm. (f) Dot plot of migration of green and magenta cells. Each dot represents cumulative mean distance from the top of the cortical plate for all cortical neurons in a coronal brain section. Connected dots indicate measurements were made in the same coronal section (g, i, k) Representative image of Double UP + pSico CIP4 shRNA1 (g), shRNA2 (i), and shRNA3 (k) four days after electroporation at E14.5 (E14.5→E18.5). (h, j, l) Dot plots of migration of green and magenta cells for CIP4 shRNA1 (h), shRNA2 (j), and shRNA3 (l). (m, o, q) Representative image of Double UP + pSico FBP17 shRNA1 (m), shRNA2 (o), and shRNA3 (q) four days after electroporation at E14.5 (E14.5→E18.5). (n, p, r) Dot plots of migration of green and magenta cells for FBP17 shRNA1 (n), shRNA2 (p), and shRNA3 (r). Black diamonds and bars represent cumulative mean ± SEM. All p values are from a weighted paired t-test (two-tailed). (f) 10 brains, Control: 214±25μm, 2453 cells, scramble: 227±28μm, 2142 cells. (h) 5 brains, Control: 293±21μm, 2517 cells, CIP4 shRNA1: 346±16μm, 1369 cells. (j) 8 brains, Control: 290±27μm, 2654 cells, CIP4 shRNA2: 339±30μm, 2176 cells. (l) 6 brains, Control: 197±22μm, 1193 cells, CIP4 shRNA3: 208±28μm, 1155 cells. (n) 8 brains, Control: 262±29μm, 1420 cells, FBP17 shRNA1: 352±32μm, 1231 cells. (p) 5 brains, Control: 269±47μm, 1667 cells, FBP17 shRNA2: 349±25μm, 1011 cells. (r) 6 brains, Control: 191±27μm, 2099 cells, FBP17 shRNA3: 222±24μm, 1446 cells. All values mean±SEM.

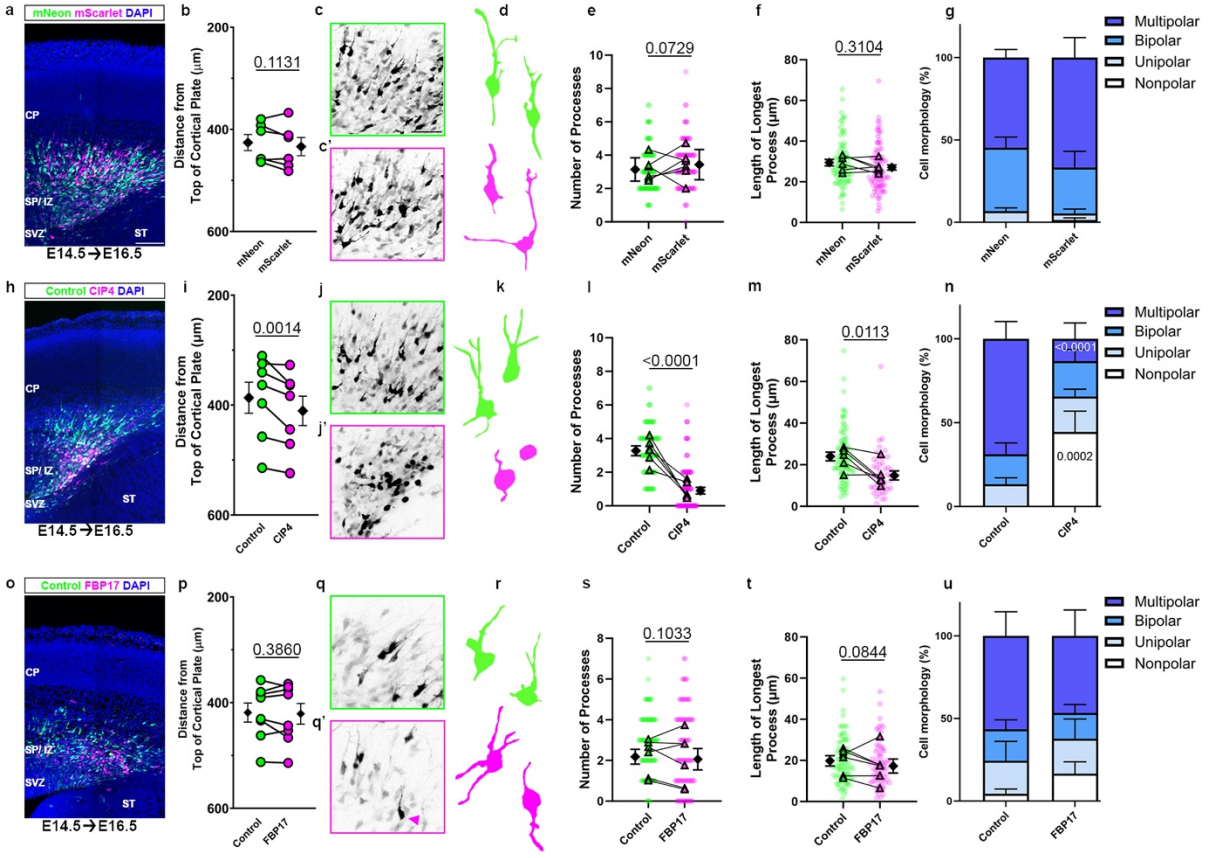

Figure 3. CIP4, but not FBP17, overexpression inhibits migration by decreasing number and length of processes at E14.5+2 days.

(a, h, o) Representative images of migration after electroporation with Double UP (a) Double UP CIP4 (h) and Double UP FBP17 (o) two days after electroporation at E14.5 (E14.5→E16.5). CP= cortical plate, SP/IZ= subplate/ intermediate zone, SVZ= subventricular zone, ST= striatum. Scale bar 100µm. (b, i, p) Dot plots of migration of green and magenta cells. Each dot represents cumulative mean distance from the top of the cortical plate for all cortical neurons in a coronal brain section. Connected dots indicate measurements were made in the same coronal section. Black diamonds and bars represent cumulative mean ± SEM. (c, c', j, j', q, q') Maximum projection of green cells (c, j, q) and magenta cells (c', j', q') from

Double UP, Double UP CIP4, and Double UP FBP17 displayed with inverted contrast to emphasize morphology. Scale bar 50 μm. (d, k, r) Representative traces of electroporated neurons from each condition to emphasize morphology. (e, l, s) SuperPlots showing comparison of the number of processes from individual green and magenta cells. Each dot represents an individual cell. Triangles represent the mean number of cell processes per brain connected with a line to indicate means are from the same brain. (f, m, t) SuperPlots showing comparison of the length of longest processes from individual green and magenta cells. Each dot represents an individual cell. Triangles represent the mean number of cell processes per brain connected with a line to indicate means are from the same brain. Cells without processes are not included in either graph or significance calculations. (g, n, u) Stacked bar graphs of cell polarity percentages, nonpolar= 0 processes, unipolar= 1 process, bipolar= 2 processes, multipolar= 3+ processes. Black error bars show SEM. All p values are from a weighted, paired t-test (two-tailed) (b, e, f, i, l, m, p, s, t) or two-way ANOVA (g, n, u). (b) 6 brains, mNeon: 426±16μm, 824 cells, mScarlet: 434±18μm, 563 cells. (e) 6 brains, mNeon: 3.14±0.29 processes, 90 cells, mScarlet: 3.43±0.37 processes, 90 cells. (f) 6 brains, mNeon: 29.6 ±1.2μm, 87 cells, mScarlet: 27.1±1.2μm, 88 cells. (g) 5 brains, mNeon: nonpolar: 0.0±0.0% of cells, unipolar 7±2% of cells, bipolar 39±9% of cells, multipolar 55±11% of cells, n=75 cells. mScarlet: nonpolar 1±1% of cells, unipolar 4±3% of cells, bipolar 28±10% of cells, multipolar 67±16% of cells, 75 cells. (i) 7 brains, Control: 387±28μm, 933 cells, CIP4: 411±27μm, 880 cells. (l) 6 brains, Control: 3.28±0.29 process, 90 cells, CIP4: 0.90±0.19 process, 90 cells. (m) 6 brains, Control: 24.3±1.3μm, 89 cells, CIP4: 16.0±1.6μm, 46 cells. (n) 6 brains, Control: nonpolar 0.0±0.0% of cells, unipolar 13±4% of

cells, bipolar 18±7% of cells, multipolar 69±10% of cells, 90 cells. CIP4: nonpolar 44±12% of cells, unipolar 21±4% of cells, bipolar 21±7% of cells, multipolar 13±9% of cells, 90 cells. (p) 8 brains, Control: 419±18μm, 1206 cells, FBP17: 421±20μm, 778 cells. (s) 6 brains, Control: 2.73±0.46 processes, 90 cells, FBP17: 2.58±0.66 processes, 90 cells. (t) 6 brains, Control: 19.8±2.6μm, 86 cells, FBP17: 17.3±3.4μm, 72 cells. (u) brain, Control: nonpolar 4±3% of cells, unipolar 20±12% of cells, bipolar 19±6% of cells, multipolar 57±2% of cells, 90 cells. FBP17: nonpolar 17±7% of cells, unipolar 21±12% of cells, bipolar 16±5% of cells, multipolar 47±16% of cells, 90 cells. All values mean±SEM.

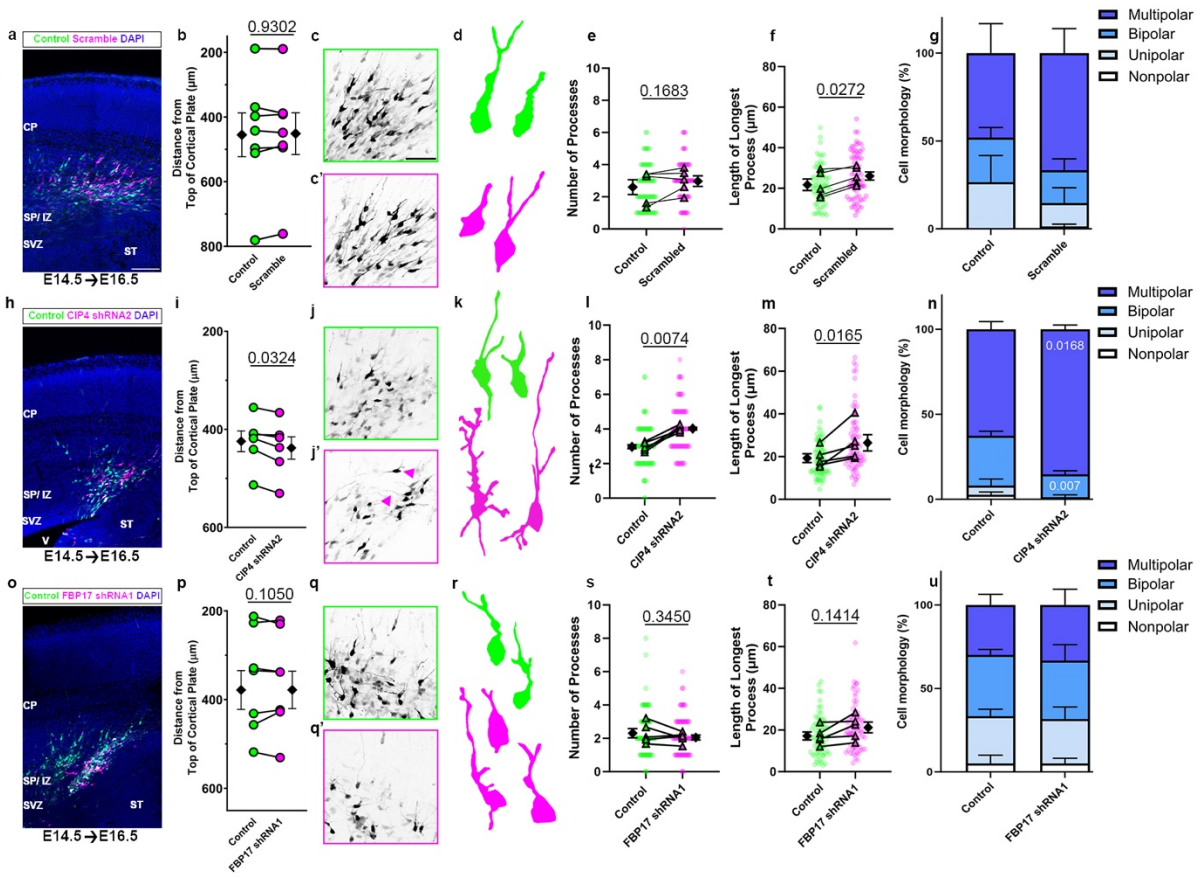

Figure 4. CIP4, but not FBP17, knockdown inhibits migration by increasing number and length of processes at E14.5+2 days.

(a, h, o) Representative image of migration after electroporation with Double UP + pSico scramble (a) Double UP + pSico CIP4 shRNA2 (h) and Double UP + pSico FBP17 shRNA1 (o) at E14.5+2. CP= cortical plate, SP/IZ= subplate/ intermediate zone, SVZ= subventricular zone, ST= striatum, V= lateral ventricle. Scale bar 100µm. (b, i, p) Dot plot of migration of green and magenta cells. Each dot represents mean distance from the top of the cortical plate to the distance of all cortical neurons in a slice. Connected dots indicate measurements were made in the same coronal slice. Black diamonds and bars represent cumulative mean ± SEM. (c, c', j, j', q, q') Max project of green (c, j, q) and magenta (c', j', q')

cells from Double UP + pSico scramble, Double UP + CIP4 shRNA2, and Double UP + pSico FBP17 shRNA1, displayed with inverted black and white to emphasize morphology. Scale bar=50 μm. (d, k, r) Representative traces of electroporated neurons from each condition to emphasize morphology. (e, l, s) SuperPlots of number of processes comparing green and magenta cells. Each dot represents an individual cell. Triangles represent the mean number of processes per condition connected with a line to indicate means come from the same brain. (f, m, t) SuperPlots of length of longest processes of green and magenta cells. Each dot represents an individual cell. Triangles represent the mean length of longest process per condition connected with a line to indicate means come from the same brain. Cells without processes are not included in either graph or significance calculations. (g, n, u) Stacked bar graphs of cell polarity percentages, nonpolar= 0 processes, unipolar= 1 process, bipolar= 2 processes, multipolar= 3+ processes. Black error bars show SEM. All p values are from a weighted, paired t-test (two-tailed) (b, e, f, i, l, m, p, s, t) or two-way ANOVA (g, n, u). (b) 7 brains, Control: 455±68μm, 1450 cells, scramble 451±65μm, 732 cells, (e) 6 brains, Control: 2.62±0.38 processes, 75 cells, scramble: 2.97±0.27 processes, 75 cells, (f) 6 brains, Control: 21.8±2.5μm, 89 cells, scramble: 25.3±1.9μm, 88 cells. (g) 5 brains, control: nonpolar 0.0±0.0 cells, unipolar 27±14% of cells, bipolar 25±7% of cells, multipolar 48±17% of cells, 75 cells. scramble: nonpolar 1±1% of cells, unipolar 13±8% of cells, bipolar 19±7% of cells, multipolar 67±17% of cells, n= 75 cells. (i) 6 brains, Control 424±21μm, 630 cells, CIP4 shRNA2: 438±23μm, 429 cells, (l) 5 brains, Control: 2.97±0.12 processes , 75 cells, CIP4 shRNA2: 4.03±0.08 processes, 75 cells, (m) 5 brains, Control: 19.3±2.1μm, 73 cells, CIP4 shRNA2: 26.5±3.8μm, 74 cells, (n) 5 brains, Control: nonpolar 3±2% of cells, unipolar 5±4%

of cells, bipolar 29±6% of cells, multipolar 63±12% of cells, 73 cells. CIP4 shRNA2: nonpolar 0±0% of cells, unipolar 1±1% of cells, bipolar 13±3% of cells, multipolar 85±16% of cells, 74 cells. (p) 7 brains, Control: 358±44μm, 1439 cells, FBP17 shRNA1: 358±42μm, 720 cells, (s) 5 brains, Control: 2.31±0.28 processes, 74 cells, FBP17 shRNA1: 2.05±0.15 process, 75 cells, (t) 5 brains, Control: 17.2±1.9μm, 71 cells, FBP17 shRNA1: 21.3±2.6μm, 72 cells, (u) 4 brains, Control: nonpolar 5±5% of cells, unipolar 28±7% of cells, bipolar 37±9% of cells, multipolar 30±9% of cells, 56 cells. FBP17 shRNA1: nonpolar 5±3% of cells, unipolar 27±9% of cells, bipolar 35±11% of cells, multipolar 33±11% of cells, 57 cells. All values mean±SEM.

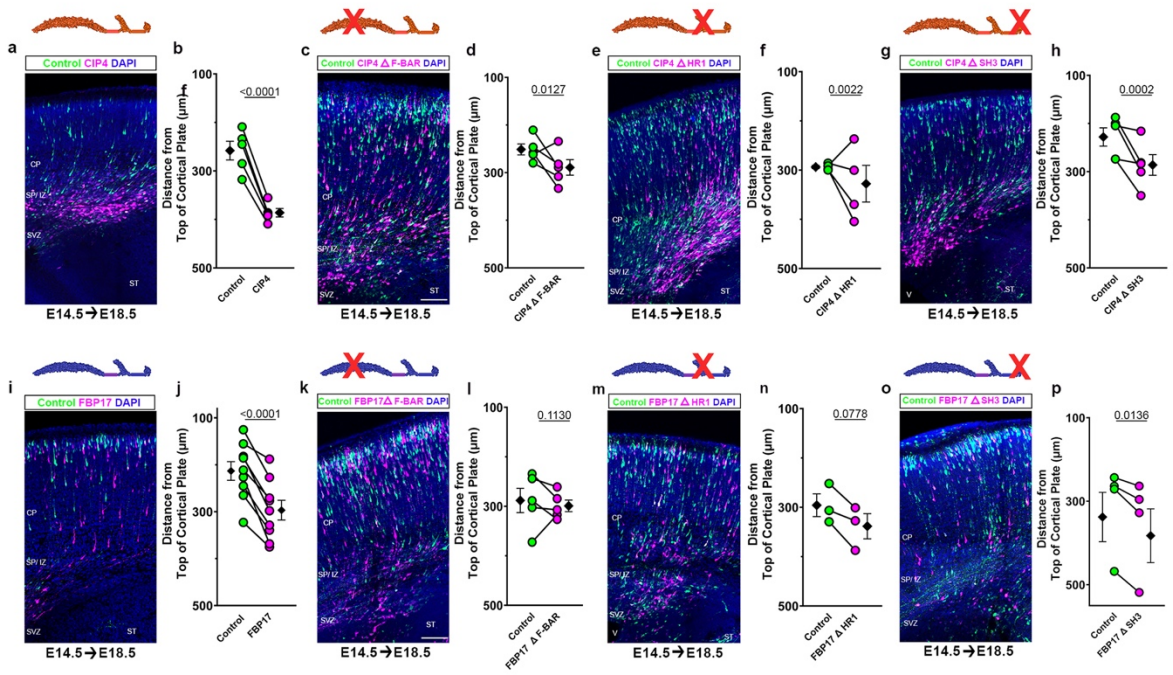

Figure 5. Domain deletions in CIP4 and FBP17 are less effective at inhibiting migration than full-length proteins.

(a, c, e, g, i, k, m, o) Representative image of domain deletions and migration after electroporation with Double UP CIP4 (a), Double UP-CIP4ΔF-BAR (c) Double UP-CIP4ΔHR1 (e), Double UP-CIP4ΔSH3 (g), Double UP FBP17 (i) Double UP-FBP17ΔF-BAR (k) Double UP-FBP17ΔHR1 (m), and Double UP-FBP17ΔSH3 (o) at E14.5+4. Images and quantification of (a, b, i, j) are from Figure 1e-h and shown here for comparison to mutant proteins. CP= cortical plate, SP/IZ= subplate/ intermediate zone, SVZ= subventricular zone, ST= striatum, V= lateral ventricle. Scale bar 100µm. (b, d, f, h, j, l, n, p) Dot plots of migration of green and magenta cells. Each dot represents the mean distance from the top of the cortical plate to all cortical neurons in a slice. Connected dots indicate measurements were made in the same coronal slice. Black diamonds and bars represent cumulative mean ± SEM. All p values are from a

weighted, paired t-test (two-tailed). (b) see figure 1. (d) 5 brains, Control: 251±12μm, 2161 cells, CIP4ΔF-BAR: 289±16μm, 1473 cells. (f) 4 brains, Control: 294±3μm, 2298 cells, CIP4ΔHR1: 328±37μm, 1369 cells. (h) 5 brains, Control: 228±19μm, 2367 cells, CIP4ΔSH3: 286±22μm, 2092 cells. (j) see figure 1. (l) 5 brains, Control: 288±25μm, 2025 cells, FBP17ΔF-BAR: 299±12μm, 1086 cells. (n) 3 brains, Control: 296±23μm, 985 cells, FBP17ΔHR1: 339±26μm, 862 cells. (p) 3 brains, Control: 312±53μm, 1978 cells, FBP17ΔSH3: 351±57μm, 1329 cells. All values mean±SEM.

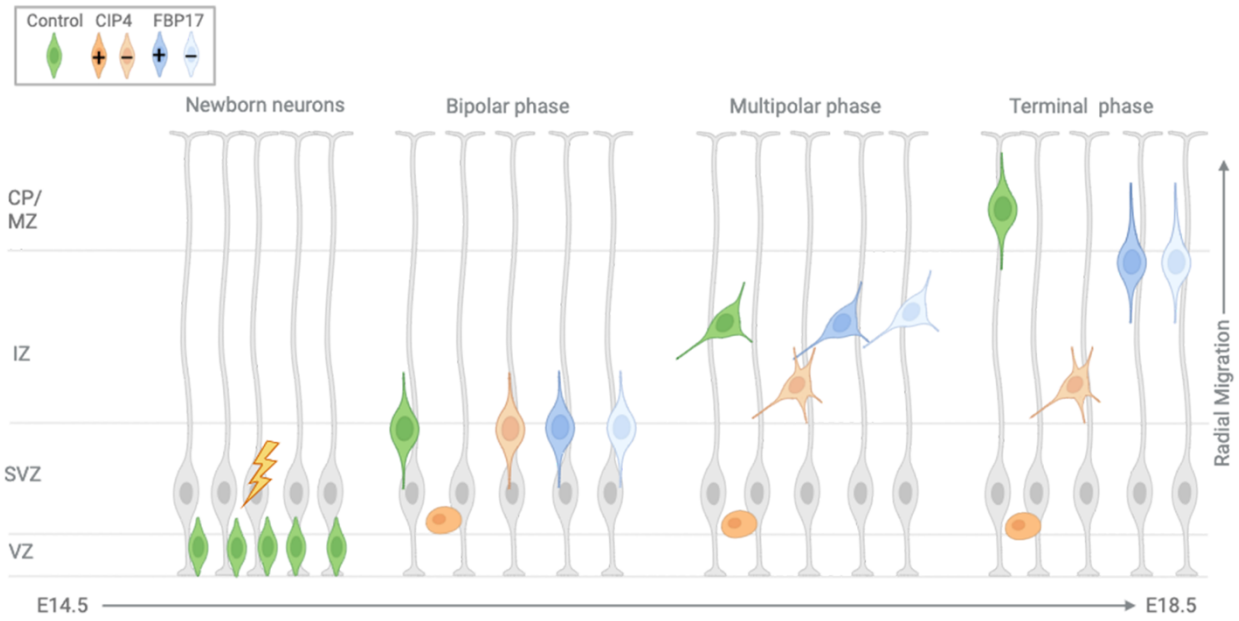

Figure 6. CIP4 and FBP17 have distinct effects on radial migration.

Normally, a newborn neuron (green) assumes a bipolar morphology soon after birth and migrates from the subventricular zone to the intermediate zone (bipolar phase). In this study we electroporated cells in the ventricular zone at E14.5 (lightning bolt). When the wildtype (green) neuron reaches the intermediate zone the neuron transitions to a multipolar morphology. The, the multipolar neuron transitions back into a bipolar morphology as it enters the cortical plate during the terminal stage of migration. High CIP4 expression (+CIP4) leads to a spherical cell, with few if any processes, that is trapped in the subventricular zone (dark orange) throughout embryonic cortical development. Conversely, CIP4 knockdown (-CIP4) leads to highly multipolar cells trapped in the intermediate zone (light orange). Changes to FBP17 expression (+FBP17, -FBP17) slow migration between E17.5 and E18.5. These neurons have longer processes than controls at E18.5 (dark blue and light blue).

CP/MZ= cortical plate/marginal zone, IZ= intermediate zone, SVZ= subventricular zone, VZ= ventricular zone. Created in BioRender. English, L. (2024) BioRender.com/o96j986

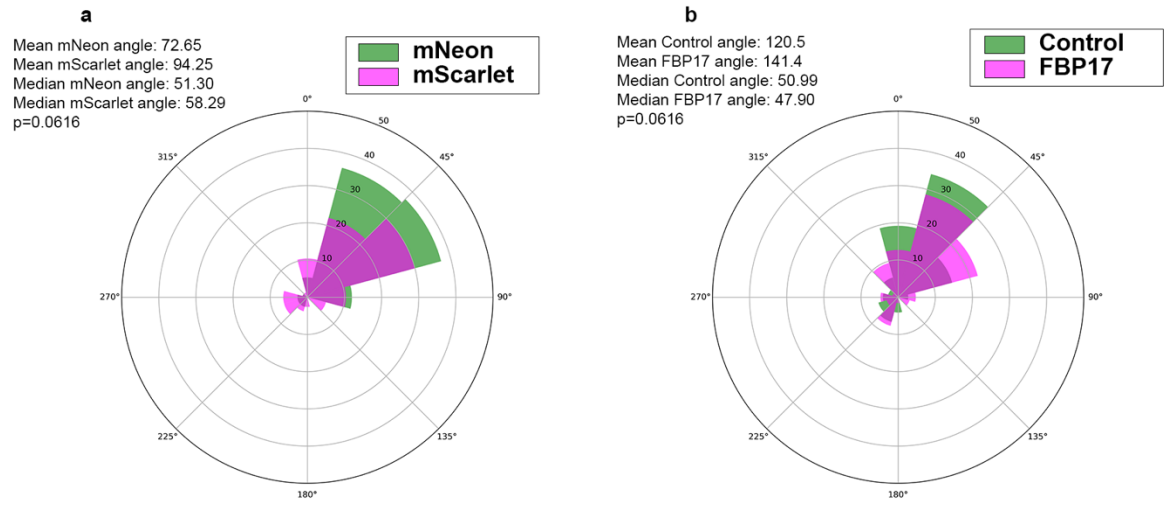

Supplemental Figure 1. FBP17 overexpression does not affect the angle of the longest process.

(a) Rose plot of the angle of the longest process to the cortical plate of green and magenta cells. Degrees represent the angle measurement; numbers represent the number of cells at that angle. (b) Rose plot of the angle of the longest process to the cortical plate of control and FBP17 overexpressing cells. Degrees represent the angle measurement; numbers represent the number of cells at that angle. All p values are from a paired t-test (two-tailed).

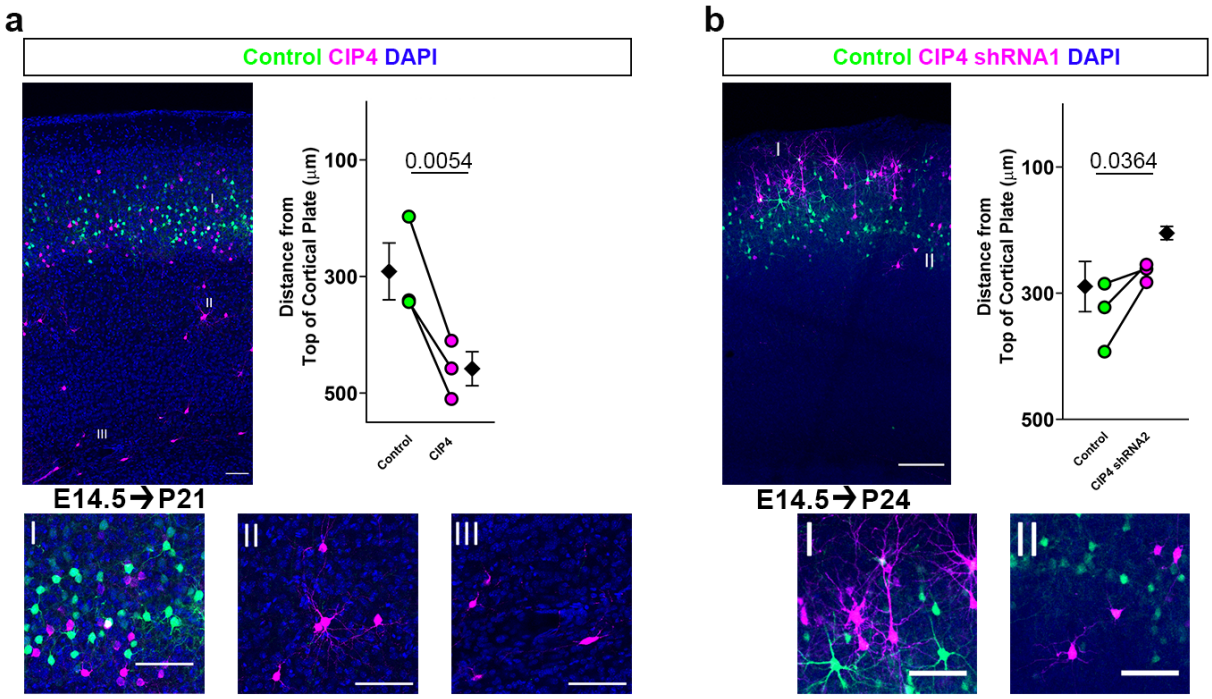

Supplemental Figure 2. Overexpression and knockdown of CIP4 results in opposite phenotypes in postnatal brain.

(a) Representative image and dot plot of migration for Double UP CIP4 at P21. (I) inset image from layer II/III neurons. (II) Inset image from deep cortical layer neurons. (III) inset image from non-migrated neurons. (b) Representative image and dot plot of migration for Double UP + pSico CIP4 shRNA2 at P24. (I) inset image from layer II/III green neurons and over-migrated magenta neurons. (II) Inset image from lower layer II/III neurons. Black diamonds and bars in dot plots represent cumulative mean ± SEM. All p values are from a weighted, paired t-test (two-tailed). (a) 3 brains, Control: 294±48μm, 839 cells, Double UP CIP4: 459±29μm, 746 cells. (b) 3 brains, Control: 333±32μm, 371 cells, CIP4 shRNA2: 266±8μm, 184 cells. Scale bar 200μm for migration images, 100μm for insets.

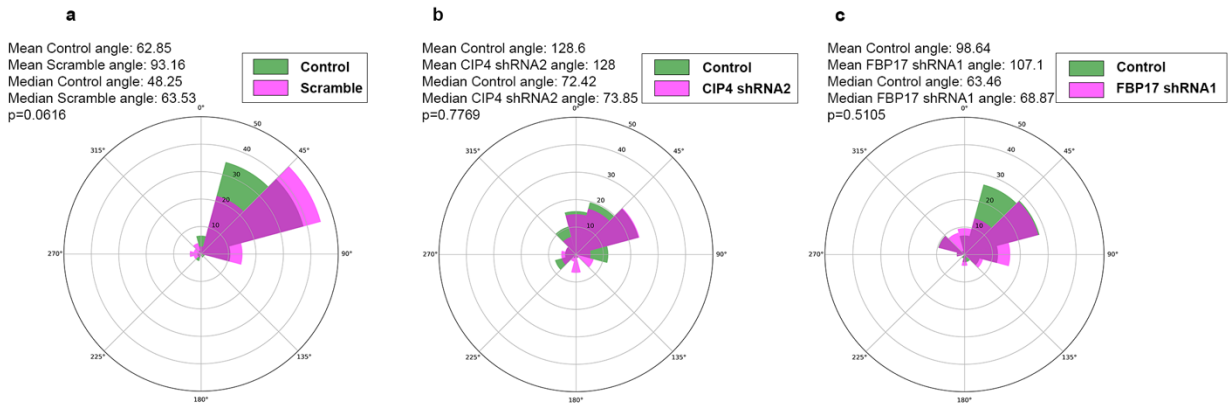

Supplemental Figure 3. Knockdown of CIP4 and FBP17 does not affect the angle of the longest process.

(a-c) Rose plots of the angle of the longest process to the cortical plate of control and scramble cells (a), control and CIP4 shRNA1 treated cells (b) and control and FBP17 shRNA1 treated cells (c). Degrees represent the angle measurement; numbers represent the number of cells at that angle. All p values are from a paired t-test (two-tailed).

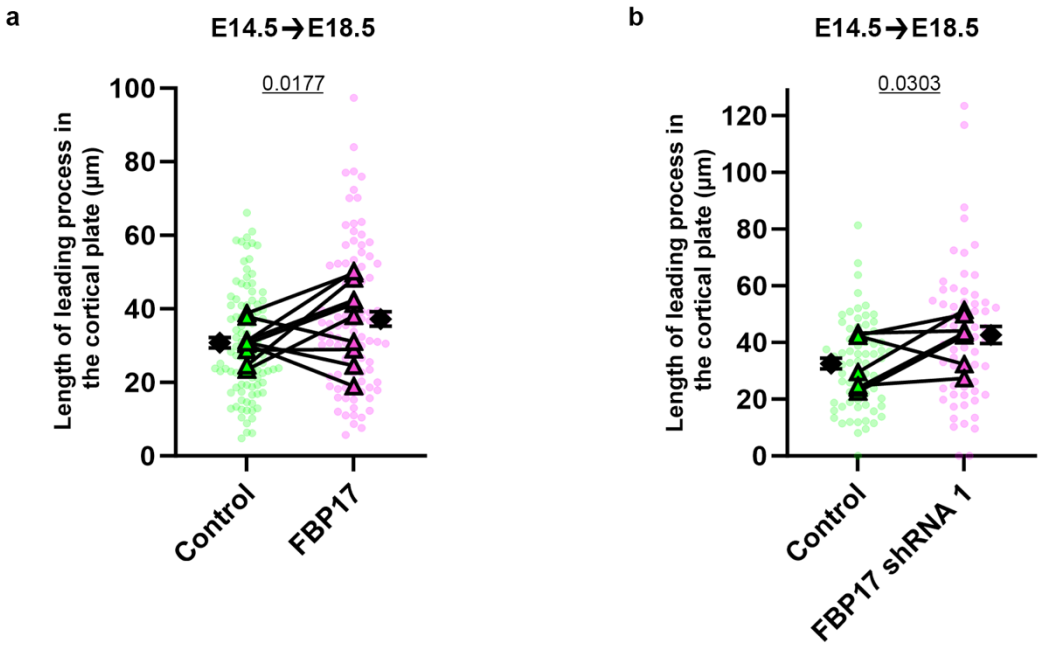

Supplemental Figure 4. FBP17 overexpression or knockdown increases process length of cells in the cortical plate at E14.5+4.

(a) SuperPlot of length of the longest process, comparing control and FBP17 overexpressing cells. Each dot represents an individual cell. Triangles represent the mean length of longest process per condition connected with a line to indicate means come from the same brain. Cells without processes are not included in either graph or significance calculations. Black diamonds and bars in dot plots represent cumulative mean ± SEM. All p values are from a weighted, paired t-test (two-tailed). (b) SuperPlot of length of the longest comparing control and FBP17 shRNA1 treated cells. (a) 10 brains, Control: 30.8±1.4µm, 100 cells, FBP17: 37.3±2.0µm, 96 cells. (b) 7 brains, Control: 32.6±1.9µm, 69 cells, FBP17 shRNA1: 42.6±3.1µm, 63 cells.

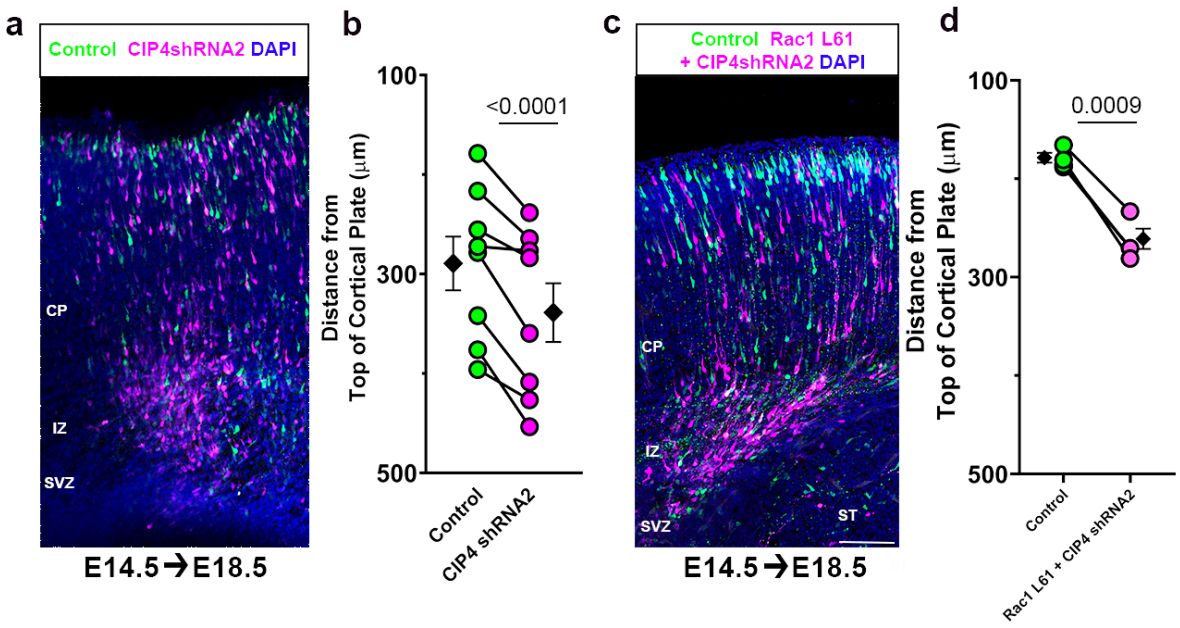

Supplemental Figure 5. Co-electroporation of CIP4 shRNA2 and Rac1 L61 does not rescue migration defect.

(a, c) Representative image of migration after electroporation with Double UP pSico + CIP4 shRNA2 (a), and Double UP Rac1L61 + pSico CIP4 shRNA2. (b, d) Dot plot of migration of green and magenta cells. The image and dot plot in a and b are taken from Fig. 2i and j for comparison. Each dot represents mean distance from the top of the cortical plate to the distance of all cortical neurons in a slice. Connected dots indicate measurements were made in the same coronal slice. Black diamonds and bars in dot plots represent cumulative mean ± SEM. All p values are from a weighted, paired t-test (two-tailed). (b) see figure 2. (d) 3 brains, Control: 180±5μm, 1402 cells, Rac1 L61 + CIP4 shRNA2: 264±11μm, 1433 cells. CP= cortical plate, IZ= intermediate zone, SVZ= subventricular zone, ST= striatum. Scale bar 100μm.

REFERENCES

Aspenstrom, P. (2009). Roles of F-BAR/PCH proteins in the regulation of membrane dynamics and actin reorganization. *Int Rev Cell Mol Biol*, *272*, 1-31. https://doi.org/S1937-6448(08)01601-8

Azzarelli, R., Kerloch, T., & Pacary, E. (2014). Regulation of cerebral cortex development by Rho GTPases: insights from in vivo studies. *Front Cell Neurosci*, *8*, 445. https://doi.org/10.3389/fncel.2014.00445

Bai, J., Ramos, R. L., Ackman, J. B., Thomas, A. M., Lee, R. V., & LoTurco, J. J. (2003). RNAi reveals doublecortin is required for radial migration in rat neocortex. *Nat Neurosci*, *6*(12), 1277-1283. https://doi.org/10.1038/nn1153

Bement, W. M., Goryachev, A. B., Miller, A. L., & von Dassow, G. (2024). Patterning of the cell cortex by Rho GTPases. *Nat Rev Mol Cell Biol*, *25*(4), 290-308. https://doi.org/10.1038/s41580-023-00682-z

Charrier, C., Joshi, K., Coutinho-Budd, J., Kim, J. E., Lambert, N., de Marchena, J., Jin, W. L., Vanderhaeghen, P., Ghosh, A., Sassa, T., & Polleux, F. (2012). Inhibition of SRGAP2 function by its human-specific paralogs induces neoteny during spine maturation [Research Support, N.I.H., Extramural Research Support, Non-U.S. Gov't]. *Cell*, *149*(4), 923-935. https://doi.org/10.1016/j.cell.2012.03.034

Dimidschstein, J., Passante, L., Dufour, A., van den Ameele, J., Tiberi, L., Hrechdakian, T., Adams, R., Klein, R., Lie, D. C., Jossin, Y., & Vanderhaeghen, P. (2013). Ephrin-B1 controls the columnar distribution of cortical pyramidal neurons by restricting their tangential migration. *Neuron*, *79*(6), 1123-1135. https://doi.org/10.1016/j.neuron.2013.07.015

Fan, L., Lu, Y., Shen, X., Shao, H., Suo, L., & Wu, Q. (2018). Alpha protocadherins and Pyk2 kinase regulate cortical neuron migration and cytoskeletal dynamics via Rac1 GTPase and WAVE complex in mice. *Elife*, *7*. https://doi.org/10.7554/eLife.35242

Fricke, R., Gohl, C., Dharmalingam, E., Grevelhorster, A., Zahedi, B., Harden, N., Kessels, M., Qualmann, B., & Bogdan, S. (2009). Drosophila Cip4/Toca-1 integrates membrane trafficking and actin dynamics through WASP and SCAR/WAVE [Research Support, Non-U.S. Gov't]. *Curr Biol*, *19*(17), 1429-1437. https://doi.org/10.1016/j.cub.2009.07.058

Frost, A., Perera, R., Roux, A., Spasov, K., Destaing, O., Egelman, E. H., De Camilli, P., & Unger, V. M. (2008). Structural basis of membrane invagination by F-BAR domains [Research

Support, N.I.H., Extramural Research Support, Non-U.S. Gov't]. *Cell*, *132*(5), 807-817. https://doi.org/10.1016/j.cell.2007.12.041

Fujita, H., Katoh, H., Ishikawa, Y., Mori, K., & Negishi, M. (2002). Rapostlin is a novel effector of Rnd2 GTPase inducing neurite branching [Research Support, Non-U.S. Gov't]. *J Biol Chem*, *277*(47), 45428-45434. https://doi.org/10.1074/jbc.M208090200

Goedhart, J. (2021). SuperPlotsOfData-a web app for the transparent display and quantitative comparison of continuous data from different conditions. *Mol Biol Cell*, *32*(6), 470-474. https://doi.org/10.1091/mbc.E20-09-0583

Govek, E. E., Hatten, M. E., & Van Aelst, L. (2010). The role of Rho GTPase proteins in CNS neuronal migration. *Dev Neurobiol*, *71*, 528-553. https://doi.org/10.1002/dneu.20850

Guerrier, S., Coutinho-Budd, J., Sassa, T., Gresset, A., Jordan, N. V., Chen, K., Jin, W. L., Frost, A., & Polleux, F. (2009). The F-BAR domain of srGAP2 induces membrane protrusions required for neuronal migration and morphogenesis [Research Support, N.I.H., Extramural Research Support, Non-U.S. Gov't]. *Cell*, *138*(5), 990-1004. https://doi.org/10.1016/j.cell.2009.06.047

Hartig, S. M., Ishikura, S., Hicklen, R. S., Feng, Y., Blanchard, E. G., Voelker, K. A., Pichot, C. S., Grange, R. W., Raphael, R. M., Klip, A., & Corey, S. J. (2009). The F-BAR protein CIP4 promotes GLUT4 endocytosis through bidirectional interactions with N-WASp and Dynamin-2 [Research Support, N.I.H., Extramural Research Support, Non-U.S. Gov't Research Support, U.S. Gov't, Non-P.H.S.]. *J Cell Sci*, *122*(Pt 13), 2283-2291. https://doi.org/10.1242/jcs.041343

Hatanaka, Y., & Murakami, F. (2002). In vitro analysis of the origin, migratory behavior, and maturation of cortical pyramidal cells. *J Comp Neurol*, *454*(1), 1-14. https://doi.org/10.1002/cne.10421

Heng, J. I., Nguyen, L., Castro, D. S., Zimmer, C., Wildner, H., Armant, O., Skowronska-Krawczyk, D., Bedogni, F., Matter, J. M., Hevner, R., & Guillemot, F. (2008). Neurogenin 2 controls cortical neuron migration through regulation of Rnd2. *Nature*, *455*(7209), 114-118. https://doi.org/10.1038/nature07198

Henne, W. M., Kent, H. M., Ford, M. G., Hegde, B. G., Daumke, O., Butler, P. J., Mittal, R., Langen, R., Evans, P. R., & McMahon, H. T. (2007). Structure and analysis of FCHo2 F-BAR domain: a dimerizing and membrane recruitment module that effects membrane curvature [Research Support, N.I.H., Extramural Research Support, Non-U.S. Gov't]. *Structure*, *15*(7), 839-852. https://doi.org/10.1016/j.str.2007.05.002

Itoh, T., Erdmann, K. S., Roux, A., Habermann, B., Werner, H., & De Camilli, P. (2005). Dynamin and the actin cytoskeleton cooperatively regulate plasma membrane invagination by BAR and F-BAR proteins. *Dev Cell*, *9*(6), 791-804. http://www.ncbi.nlm.nih.gov/entrez/query.fcgi?cmd=Retrieve&db=PubMed&dopt=Citation&list_uids=16326391

Kawauchi, T., Chihama, K., Nabeshima, Y., & Hoshino, M. (2003). The in vivo roles of STEF/Tiam1, Rac1 and JNK in cortical neuronal migration. *Embo J*, *22*(16), 4190-4201. https://doi.org/10.1093/emboj/cdg413

Konno, D., Yoshimura, S., Hori, K., Maruoka, H., & Sobue, K. (2005). Involvement of the phosphatidylinositol 3-kinase/rac1 and cdc42 pathways in radial migration of cortical neurons. *J Biol Chem*, *280*(6), 5082-5088. https://doi.org/10.1074/jbc.M408251200

Li, Q., Wang, L., Ma, Y., Yue, W., Zhang, D., & Li, J. (2019). P-Rex1 Overexpression Results in Aberrant Neuronal Polarity and Psychosis-Related Behaviors. *Neurosci Bull*, *35*(6), 1011-1023. https://doi.org/10.1007/s12264-019-00408-2

Li, Y., Shelton, B. J., St Clair, W., Weiss, H. L., Villano, J. L., Stromberg, A. J., Wang, C., & Chen, L. (2023). Weighted mean difference statistics for paired data in the presence of missing values. *Stat Methods Med Res*, *32*(10), 2033-2048. https://doi.org/10.1177/09622802231192947

Lord, S. J., Velle, K. B., Mullins, R. D., & Fritz-Laylin, L. K. (2020). SuperPlots: Communicating reproducibility and variability in cell biology. *J Cell Biol*, *219*(6). https://doi.org/10.1083/jcb.202001064

Nagano, T., Morikubo, S., & Sato, M. (2004). Filamin A and FILIP (Filamin A-Interacting Protein) regulate cell polarity and motility in neocortical subventricular and intermediate zones during radial migration. *J Neurosci*, *24*(43), 9648-9657. http://www.ncbi.nlm.nih.gov/entrez/query.fcgi?cmd=Retrieve&db=PubMed&dopt=Citation&list_uids=15509752

Namba, T., Kibe, Y., Funahashi, Y., Nakamuta, S., Takano, T., Ueno, T., Shimada, A., Kozawa, S., Okamoto, M., Shimoda, Y., Oda, K., Wada, Y., Masuda, T., Sakakibara, A., Igarashi, M., Miyata, T., Faivre-Sarrailh, C., Takeuchi, K., & Kaibuchi, K. (2014). Pioneering axons regulate neuronal polarization in the developing cerebral cortex. *Neuron*, *81*(4), 814-829. https://doi.org/10.1016/j.neuron.2013.12.015

Noctor, S. C., Martinez-Cerdeno, V., Ivic, L., & Kriegstein, A. R. (2004). Cortical neurons arise in symmetric and asymmetric division zones and migrate through specific phases. *Nat Neurosci*, *7*(2), 136-144. https://doi.org/10.1038/nn1172

Pacary, E., Heng, J., Azzarelli, R., Riou, P., Castro, D., Lebel-Potter, M., Parras, C., Bell, D. M., Ridley, A. J., Parsons, M., & Guillemot, F. (2011). Proneural transcription factors regulate different steps of cortical neuron migration through Rnd-mediated inhibition of RhoA signaling. *Neuron*, *69*(6), 1069-1084. https://doi.org/10.1016/j.neuron.2011.02.018

Parnavelas, J. G. (2000). The origin and migration of cortical neurones: new vistas. *Trends Neurosci*, *23*(3), 126-131. https://doi.org/10.1016/s0166-2236(00)01553-8

Pinheiro, E. M., Xie, Z., Norovich, A. L., Vidaki, M., Tsai, L. H., & Gertler, F. B. (2011). Lpd depletion reveals that SRF specifies radial versus tangential migration of pyramidal neurons. *Nat Cell Biol*, *13*(8), 989-995. https://doi.org/10.1038/ncb2292

Saengsawang, W., Mitok, K., Viesselmann, C., Pietila, L., Lumbard, D. C., Corey, S. J., & Dent, E. W. (2012). The F-BAR protein CIP4 inhibits neurite formation by producing lamellipodial protrusions [Research Support, N.I.H., Extramural Research Support, Non-U.S. Gov't]. *Curr Biol*, *22*(6), 494-501. https://doi.org/10.1016/j.cub.2012.01.038

Saengsawang, W., Taylor, K. L., Lumbard, D. C., Mitok, K., Price, A., Pietila, L., Gomez, T. M., & Dent, E. W. (2013). CIP4 coordinates with phospholipids and actin-associated proteins to localize to the protruding edge and produce actin ribs and veils. *J Cell Sci*, *126*(Pt 11), 2411-2423. https://doi.org/10.1242/jcs.117473

Saito, T., & Nakatsuji, N. (2001). Efficient gene transfer into the embryonic mouse brain using in vivo electroporation. *Dev Biol*, *240*(1), 237-246. https://doi.org/10.1006/dbio.2001.0439

Shimada, A., Niwa, H., Tsujita, K., Suetsugu, S., Nitta, K., Hanawa-Suetsugu, K., Akasaka, R., Nishino, Y., Toyama, M., Chen, L., Liu, Z. J., Wang, B. C., Yamamoto, M., Terada, T., Miyazawa, A., Tanaka, A., Sugano, S., Shirouzu, M., Nagayama, K., . . . Yokoyama, S. (2007). Curved EFC/F-BAR-domain dimers are joined end to end into a filament for membrane invagination in endocytosis [Research Support, Non-U.S. Gov't Research Support, U.S. Gov't, Non-P.H.S.]. *Cell*, *129*(4), 761-772. https://doi.org/10.1016/j.cell.2007.03.040

Snider, C. E., Wan Mohamad Noor, W. N. I., Nguyen, N. T. H., Gould, K. L., & Suetsugu, S. (2021). The state of F-BAR domains as membrane-bound oligomeric platforms. *Trends Cell Biol*, *31*(8), 644-655. https://doi.org/10.1016/j.tcb.2021.03.013

Stanishneva-Konovalova, T. B., Kelley, C. F., Eskin, T. L., Messelaar, E. M., Wasserman, S. A., Sokolova, O. S., & Rodal, A. A. (2016). Coordinated autoinhibition of F-BAR domain membrane binding and WASp activation by Nervous Wreck. *Proc Natl Acad Sci U S A*, *113*(38), E5552-5561. https://doi.org/10.1073/pnas.1524412113

Stouffer, M. A., Golden, J. A., & Francis, F. (2016). Neuronal migration disorders: Focus on the cytoskeleton and epilepsy. *Neurobiol Dis*, *92*(Pt A), 18-45. https://doi.org/10.1016/j.nbd.2015.08.003

Tabata, H., & Nakajima, K. (2001). Efficient in utero gene transfer system to the developing mouse brain using electroporation: visualization of neuronal migration in the developing cortex. *Neuroscience*, *103*(4), 865-872. https://www.ncbi.nlm.nih.gov/pubmed/11301197

Takano, K., Toyooka, K., & Suetsugu, S. (2008). EFC/F-BAR proteins and the N-WASP-WIP complex induce membrane curvature-dependent actin polymerization [Research Support, Non-U.S. Gov't]. *The EMBO journal*, *27*(21), 2817-2828. https://doi.org/10.1038/emboj.2008.216

Taylor, K. L., Taylor, R. J., Richters, K. E., Huynh, B., Carrington, J., McDermott, M. E., Wilson, R. L., & Dent, E. W. (2019). Opposing functions of F-BAR proteins in neuronal membrane protrusion, tubule formation, and neurite outgrowth. *Life Sci Alliance*, *2*(3), e201800288. https://doi.org/10.26508/lsa.201800288

Taylor, R. J., Carrington, J., Gerlach, L. R., Taylor, K. L., Richters, K. E., & Dent, E. W. (2020). Double UP: A Dual Color, Internally Controlled Platform for in utero Knockdown or Overexpression. *Front Mol Neurosci*, *13*, 82. https://doi.org/10.3389/fnmol.2020.00082

Tsai, J. W., Chen, Y., Kriegstein, A. R., & Vallee, R. B. (2005). LIS1 RNA interference blocks neural stem cell division, morphogenesis, and motility at multiple stages [Comparative Study Research Support, N.I.H., Extramural Research Support, Non-U.S. Gov't Research Support, U.S. Gov't, P.H.S.]. *J Cell Biol*, *170*(6), 935-945. https://doi.org/10.1083/jcb.200505166

Tsujita, K., Suetsugu, S., Sasaki, N., Furutani, M., Oikawa, T., & Takenawa, T. (2006). Coordination between the actin cytoskeleton and membrane deformation by a novel membrane tubulation domain of PCH proteins is involved in endocytosis [Research Support, Non-U.S. Gov't]. *J Cell Biol*, *172*(2), 269-279. https://doi.org/10.1083/jcb.200508091

Ventura, A., Meissner, A., Dillon, C. P., McManus, M., Sharp, P. A., Van Parijs, L., Jaenisch, R., & Jacks, T. (2004). Cre-lox-regulated conditional RNA interference from transgenes. *Proc Natl Acad Sci U S A*, *101*(28), 10380-10385. https://doi.org/10.1073/pnas.0403954101

Wakita, Y., Kakimoto, T., Katoh, H., & Negishi, M. (2011). The F-BAR protein Rapostlin regulates dendritic spine formation in hippocampal neurons [Research Support, Non-U.S. Gov't]. *J Biol Chem*, *286*(37), 32672-32683. https://doi.org/10.1074/jbc.M111.236265

Wang, S., Li, X., Zhang, Q., Chai, X., Wang, Y., Forster, E., Zhu, X., & Zhao, S. (2020). Nyap1 Regulates Multipolar-Bipolar Transition and Morphology of Migrating Neurons by Fyn

Phosphorylation during Corticogenesis. *Cereb Cortex*, *30*(3), 929-941. https://doi.org/10.1093/cercor/bhz137

Xu, Z., Chen, Y., & Chen, Y. (2019). Spatiotemporal Regulation of Rho GTPases in Neuronal Migration. *Cells*, *8*(6). https://doi.org/10.3390/cells8060568

Yang, T., Sun, Y., Zhang, F., Zhu, Y., Shi, L., Li, H., & Xu, Z. (2012). POSH localizes activated Rac1 to control the formation of cytoplasmic dilation of the leading process and neuronal migration. *Cell Rep*, *2*(3), 640-651. https://doi.org/10.1016/j.celrep.2012.08.007

Yoshizawa, M., Kawauchi, T., Sone, M., Nishimura, Y. V., Terao, M., Chihama, K., Nabeshima, Y., & Hoshino, M. (2005). Involvement of a Rac activator,P-Rex1, in neurotrophin-derived signaling and neuronal migration. *J Neurosci*, *25*(17), 4406-4419. https://doi.org/10.1523/JNEUROSCI.4955-04.2005

Yu, Z., Guindani, M., Grieco, S. F., Chen, L., Holmes, T. C., & Xu, X. (2022). Beyond t test and ANOVA: applications of mixed-effects models for more rigorous statistical analysis in neuroscience research. *Neuron*, *110*(1), 21-35. https://doi.org/10.1016/j.neuron.2021.10.030

Zhang, Z., Zheng, F., You, Y., Ma, Y., Lu, T., Yue, W., & Zhang, D. (2016). Growth arrest specific gene 7 is associated with schizophrenia and regulates neuronal migration and morphogenesis. *Mol Brain*, *9*(1), 54. https://doi.org/10.1186/s13041-016-0238-y

Chapter 3

Expression patterns of CIP4 and FBP17 in the developing cortex

The following experiments included data generated from a mouse model designed by R. J. Taylor. L. A. English completed all the experiments with the help of J. Palmos. L. A. English completed the analysis, compiled all the figures, and is the primary author of this chapter.

INTRODUCTION

Although techniques to label transcripts (RNA) and epitopes (protein) in brain sections have been used for decades, it is not always straightforward to determine the expression of RNA and protein over time in the embryonic brain. Furthermore, data from western blots of brain lysates from prenatal brains do not always align with these other methodologies. Previous data from our lab, using western blots of cortical lysates shows that CIP4 expression decreases with development, with little to no detectable expression by postnatal day 3 (P3) (Saengsawang, Mitok et al. 2012). There is limited research on developmental FBP17 expression, but one published western blot suggests FBP17 is expressed at low levels embryonically and increases into adulthood (Wakita, Kakimoto et al. 2011). While a few publicly available datasets confirm early CIP4 and FBP17 expression in the developing cortex, they often are limited to a single developmental timepoint or lack regional specificity (Diez-Roux, Banfi et al. 2011, Yue, Cheng et al. 2014, Speir, Bhaduri et al. 2021).

Nevertheless, three publicly available data sets provide important information regarding the expression of F-BAR proteins in the brain: the Eurexpress dataset, the Allen Institute Brain Atlas, and the ENCODE dataset. All three datasets contain information about RNA expression at various embryonic time points (Lein, Hawrylycz et al. 2007, Diez-Roux, Banfi et al. 2011, Yue, Cheng et al. 2014). The Eurexpress atlas, created by Diez-Roux and colleagues, (Diez-Roux, Banfi et al. 2011) offers whole-mount RNA *in situ* images of E14.5 CIP4 and FBP17 expression. These data show that CIP4 expression is high near the ventricular zone, with lower levels throughout the rest of the brain **(Figure 1a, b)**. The Allen

Institute brain atlas also contains coronal brain sections of CIP4 RNA via in situ hybridization. At E14.5, the Allen dataset shows high CIP4 in the pial surface with moderate CIP4 RNA in the rest of the cortex **(Fig. 1c)**. Lastly, the ENCODE dataset provides RNA-seq data from the embryonic mouse central nervous system and adult cortex in Reads Per Kilobase per Million (RPKM) mapped reads (Yue, Cheng et al. 2014). In the mouse central nervous system (CNS) CIP4 RNA decreases between E11.5 and E18 and is almost non-existent at the adult timepoint **(Fig. 1 d)**. However, compared to Doublecortin (DCX)—a microtubule associated protein expressed in migrating neurons (Francis, Koulakoff et al. 1999, Gleeson, Lin et al. 1999)—CIP4 is expressed at much lower levels in the embryonic CNS at all time points.

FBP17 is also represented in all three online datasets. The Eurexpress and Allen Institute *in situ* data report moderate FBP17 expression only in the ventricular zone at E14.5, and low expression in the rest of the embryonic brain (Lein, Hawrylycz et al. 2007, Diez-Roux, Banfi et al. 2011) **(Fig. 1 e-g)**. The RNA seq data from ENCODE shows increased FBP17 expression over time (Yue, Cheng et al. 2014), agreeing with previously published western blots (Wakita, Kakimoto et al. 2011, Yue, Cheng et al. 2014) **(Fig1 h)**. Like CIP4, FBP17 is also expressed at low levels, compared to DCX, but still shows a consistent trend towards increasing expression throughout embryonic CNS development and into adulthood **(Fig. 1h)**.

The available RNA data from the three datasets agrees with the protein expression data from western blots for CIP4 and FBP17 (Lein, Hawrylycz et al. 2007, Diez-Roux, Banfi et al. 2011, Wakita, Kakimoto et al. 2011, Saengsawang, Mitok et al. 2012, Yue, Cheng et al. 2014). Since western blots cannot provide detailed spatial information, we have long aimed

to expand upon our CIP4 western blot results and the published FBP17 western blot by implementing immunohistochemistry (IHC) at multiple developmental time points. Despite extensive efforts, commercially available antibodies for CIP4 and FBP17 were deemed unsuitable for IHC due to lack of specificity or poor optimization. We previously showed that labeling with several commercial antibodies did not distinguish CIP4 knockout neurons from wild-type neurons, making them unsuitable for IHC(Saengsawang, Taylor et al. 2013).

Instead, we generated an endogenously labeled CIP4 mouse model using CRISPR/Cas9 technology as an alternative. In this model, a hemagglutinin (HA) tag was fused to the C-terminus of endogenous CIP4 via a flexible linker. Although this mouse model successfully enabled CIP4 visualization in fixed specimens with an anti-HA antibody, which does not suffer from labeling knockout tissue, it required a few years of development and was prohibitively expensive. Given these constraints, it was not feasible to create a similarly tagged FBP17 mouse line at this time.

Because of the difficulties and expense of determining the protein expression patterns of CIP4 and FBP17 in cortical development, we explored mRNA expression patterns in embryonic brain tissue via Hybridization Chain Reaction RNA Fluorescent *In Situ* Hybridization (HCR RNA *FISH*), a reportedly highly sensitive and specific method for detecting RNA transcripts in tissue (Dirks and Pierce 2004, Choi, Chang et al. 2010, Choi, Beck et al. 2014, Choi, Schwarzkopf et al. 2018). This approach relies on probe-triggered hairpin polymerization to generate bright, stable fluorescent signals (Dirks and Pierce 2004) **(Fig. 2)**. We selected HCR for its robustness, target specificity, and ease of use for characterizing developmental expression patterns of CIP4 and FBP17 in the cortex. By

combining HCR with IHC in wild-type and CIP4-HA tissue, we aimed to determine the spatial and temporal expression patterns of these two F-BAR proteins during cortical development. These results will aid in our understanding of how CIP4 and FBP17 may function in embryonic cortical development. Interestingly, we discovered that CIP4 and FBP17 may have opposing RNA and protein expression patterns in the embryonic cortex.

METHODS

Animal Models

All mouse procedures were approved by the University of Wisconsin Committee on Animal Care and were in accordance with NIH guidelines. Timed matings of Swiss Webster mice (Inotiv) or CIP4-HA (c57bl/6j background) mice were performed, with the morning of sperm plug visualization considered E0.5. Both male and female embryos were used, but the sex of embryos was not recorded. Pregnant females were housed individually. Prior to becoming pregnant, females were housed with 3-4 other females.

Generation of CIP4-HA Transgenic Mouse

A cassette coding for Linker-LoxP-3xHA-Stop Codon-LoxP-mScarlet was cloned using Gibson Assembly. Genomic DNA was isolated from wild-type mouse liver and used to clone a 1.5kb 5' homology arm and a 2.5kb 3' homology arm located immediately around the stop codon of CIP4. These three components were combined using Gibson Assembly, and the resulting plasmid DNA was used as a template for CRISPR/Cas9 genetic modification. A guide RNA (GAACCCCACCAGAGGGGGACG(AGG)) was validated to cut genomic DNA and then inserted with Cas9 protein and a linearized homology plasmid into fertilized mouse oocytes. Animals were screened for the presence or absence of a transgene via PCR, and a female was found to be mosaic for the insert. The transgene and surrounding 1KB of genomic DNA were sequence verified. The female was used as the founder of the colony. The CIP4-Linker-LoxP-3xHA-STOP-LoxP-mScarlet mouse line is being maintained by the Dent Lab and is available upon request. Genotyping is performed using ACCAGGGGATGTAGCAGTTG (Forward) and CACGTGGGCAGGAATAAAGT (Reverse) primers.

Tissue Collection and Sectioning

For all experiments, embryonic tissue was collected by exposing the embryos via laparotomy after deep anesthesia of the pregnant dam with isoflurane. Embryos were removed from the uterus one by one and perfused by opening the chest cavity, making a small incision in the right atrium, and inserting a 25-gauge needle into the left ventricle. Through this needle, the animal was perfused with approximately 1mL of sterile saline and 3mL of 4% paraformaldehyde in PBS (PFA) at a rate of approximately 1.25mL per minute with a perfusion pump (Instech). Following perfusion, heads were removed and placed in 4% PFA at 4°C overnight. After the last embryo was perfused, the dam was euthanized via live decapitation.

After 16 hours in 4% PFA at 4°C, heads were transferred to PBS and brains were removed from skulls. The brains were placed in 6% low melt agarose and allowed to set on ice. After the agarose hardened, the brains or heads were sectioned on a Leica VT1000S vibratome at 100µm in phosphate-buffered saline (PBS). Sections from endogenous CIP4-HA/WT experiments were incubated in Tris-EDTA buffer for 1 hour at 90°C followed by blocking solution for two hours at RT. Primary antibody anti-HA-Tag (1:500, Cell Signaling), anti-Tbr2 (1:1000, Invitrogen), and anti-MAP2 (1:500, Cell Signaling) were diluted in blocking solution (10% Normal Goat Serum-NGS (Innovative), 0.4% Triton (Sigma), 2% Bovine Serum Albumin (Sigma), 1% Glycine (Sigma) in PBS) for two days at 4°C. On the third day, the primary antibody was washed off with 10% NGS/ PBS three times and a secondary antibody was applied in addition to DAPI overnight at 4°C. Slices were washed in PBS and mounted

onto slides with Aqua-Poly Mount (Polysciences). Slides were allowed to dry for at least one hour and then imaged within two days.

Hybridization Chain Reaction RNA Fluorescent *in situ* Hybridization (HCR RNA *FISH*)

HCR RNA probes and reagents were ordered from Molecular Instruments, and sequences and reagents are reported in **Table 1**. HCR RNA *FISH* was performed as described previously (Choi, Schwarzkopf et al. 2018). Briefly, 100µm sections were pre-hybridized in probe hybridization buffer (Molecular Instruments) for 30 min in a humidified chamber at 37°C. Sections were then incubated with 1.6 pmol of HCR probe in probe hybridization buffer (Molecular Instruments) overnight in a 37°C humidified chamber. After hybridization, sections were washed in 75% probe wash buffer (Molecular Instruments)/ 25% 5X SSCT, 50% probe wash buffer/ 50% 5X SSCT, 25% probe wash buffer/ 75% 5X SSCT, 100% 5X SSCT for 15 minutes at 37°C, followed by a final wash in 5X SSCT for 5 min at room temperature. Sections were incubated in amplification buffer (Molecular Instruments) for 30 min at RT. 12 pmol of each HCR Hairpin (Molecular Instruments) was heated to 95°C for 90 seconds, followed by cooling at RT for 30 min in a dark drawer. Hairpins were mixed with Amplification buffer (Molecular Instruments) and applied to sections overnight at RT in the dark. After hairpin amplification, sections were washed at room temperature in 5X SSCT for 5 minutes, then 2 times for 15 minutes, and a final 5-minute wash before mounting with Aqua-Poly Mount (Polysciences).

Fluorescent Imaging

Imaging was performed on a Zeiss LSM 800 confocal microscope. 50 optical sections were obtained, each 1µm apart. For HCR images, 1x2 tiles were taken and stitched together

in Zen 2.3 (Zeiss). Images were collected with a 10x/0.3NA Plan Apochromat objective, with 4x averaging, and presented as maximum inverted projections (B&W) or maximum overlayed projections (Color).

RESULTS

CIP4 and FBP17 have opposing RNA expression patterns in embryonic brain

We previously showed via western blot that CIP4 protein expression decreases through embryonic development and is barely detectable in the adult brain(Saengsawang, Mitok et al. 2012). We wanted to better understand where and when CIP4 and FBP17 are expressed in the embryonic cortex, so we used HCR RNA FISH to detect CIP4 and FBP17 RNA at various time points during embryonic development.

Surprisingly, the HCR RNA FISH technique showed CIP4 RNA expression appears to be low at E14.5 and E16.5 but increases at E18.5 **(Fig. 3a)**. To make sure our methodology was working properly we used DCX as a control probe, on the same brain sections, since it has a well-established expression pattern in migrating neurons(Francis, Koulakoff et al. 1999, Gleeson, Lin et al. 1999). We show that DCX is present in the cortex from E14.5-E18.5 **(Fig. 3a')**, with especially heavy labeling in the cortical plate, consistent with previous studies(Francis, Koulakoff et al. 1999, Gleeson, Lin et al. 1999, Gdalyahu, Ghosh et al. 2004). However, we observed that CIP4 RNA is barely present at E14.5 and E16.5, but by E18.5, CIP4 and DCX RNA overlap in the cortical plate, suggesting that migrating neurons express CIP4 RNA towards the end of migration **(Fig. 3a-a")**. Because the CIP4 HCR RNA FISH signal at E18.5 may be due to nonspecific labeling of the initiator and hairpins **(see Fig. 2)** we also probed E14.5-E16.5 sections with the initiator and hairpins but did not include the RNA probe as a negative control. Images from these experiments clearly show that there is little background from the initiator and hairpins **(Supp. Fig. 1)**, suggesting the signals present for

CIP4 and FBP17 are not due to nonspecific labeling of the initiator/hairpin incubation. We then used HCR RNA FISH to probe FBP17 RNA localization in the prenatal brain.

A previous study using western blots of brain tissue has shown that FBP17 protein is expressed at low levels in the embryonic brain and increases in the postnatal brain, reaching maximal levels in adulthood(Wakita, Kakimoto et al. 2011), a pattern opposite our western blot data for CIP4(Saengsawang, Mitok et al. 2012). HCR RNA FISH showed that FBP17 RNA expression is opposite to our CIP4 western blots, showing prominent labeling at E14.5 and E16.5 but decreasing at E18.5 **(Fig. 3b)**. At E14.5 and E16.5, FBP17 RNA expression is concentrated around the ventricular and subventricular zones, indicating a potential role in proliferation and early migration **(Fig. 3b)**. Again, we used DCX as a positive control and showed consistent labeling in migrating neurons. Together, these HCR RNA FISH data for both CIP4 and FBP17 suggest that although these two proteins show opposite RNA expression patterns, they demonstrate an inverse pattern when compared to protein expression by western blots in the embryonic mouse brain.

CIP4 protein patterns in the embryonic cortex partially overlaps with CIP4 RNA

To determine if CIP4 RNA and protein expression coincided in the embryonic cortex, we labeled sections of our CIP4-HA CRISPR knock-in mouse with an anti-HA antibody **(Fig. 4)**. At E14.5 CIP4 protein expression is in a concentrated band under the cortical plate **(Fig. 4a, white arrowheads)**. Of note, there is prominent labeling in the skin at E14.5, however this was nonspecific labeling because it was also prominent in wild-type littermate sections **(Fig. 4a')**. Moreover, labeling of E14.5 sections from wild-type littermates confirmed that the CIP4-positive band of cells was absent **(Fig. 4a'),** indicating the signal in the CIP4-HA cortex

was specific. To determine where in the cortex the band of CIP4 expression was observed at E14.5, we also labeled the same section for MAP2, a subplate marker(Fischer, Shea et al. 1986)**(Fig. 4a)**. HA signal is seen directly under the MAP2 signal, indicating CIP4 expression is localized under the subplate, at the top of the intermediate zone at E14.5 **(Fig. 4a, color overlay)**. We also observed that the developing intermediate and subventricular zones appeared to lack CIP4 expression **(Fig. 4a)**. To confirm this, we labeled the same sections of CIP4-HA brains with Tbr2, a marker of intermediate progenitor cells in the subventricular zone(Englund, Fink et al. 2005). The HA (CIP4) and Tbr2 signals do not overlap **(Fig. 4a)**, indicating that CIP4 is not expressed in intermediate progenitor cells in the subventricular zone at E14.5. Matching our HCR data, CIP4 protein expression increased in the lower cortical plate and upper intermediate zone at E18.5 and was distinctly diminished at the very top of the cortical plate **(Fig. 4b, white brackets)**. Thus, as MAP2 expression in post-migratory neurons spreads throughout the cortical plate during development, so does CIP4 expression in an overlapping fashion **(Fig. 4b)**.

Together, these results suggest that CIP4 may have a role in the multipolar to bipolar shift and migration termination. Once neurons reach the top of the cortical plate, they appear to stop expressing CIP4 and finish migration. Conversely, FBP17 RNA is expressed early in cortical development, potentially in progenitor cells. Thus, FBP17 may support the birth and initiation of migration in newborn neurons.

DISCUSSION

Considerations for non-quantitative RNA and protein detection methods

While our HCR and IHC experiments have determined the spatial and temporal expression pattern of CIP4 RNA and protein, there are a few caveats to consider. First, it is essential to note that HCR, IHC and western blot methodologies are inherently qualitative because of the reaction products on tissue sections (HCR and IHC) and membrane (western blots) are not necessarily linear reactions but depend on amplification to detect signals. Moreover, between E14.5 and E18.5, the brain nearly doubles in size (Dehay and Kennedy 2007). Therefore, the apparent increase in CIP4 RNA signal could reflect more cells expressing the same amount of CIP4 rather than increased expression per cell. The increase in cell number would produce a stronger signal that is hard to differentiate from true upregulation at the cellular level. To accurately determine how much CIP4 RNA is expressed over time, a quantitative method such as single-cell RNA sequencing (scRNA-seq) is needed. This approach would allow us to measure transcript levels of CIP4 in individual cells across developmental stages and brain regions.

A second complication arises from the fact that the presence of mRNA does not guarantee protein translation. HCR detects mRNA via a specific probe set targeting mRNA sequences(Choi, Schwarzkopf et al. 2018) **(Fig. 1)**. However, mRNAs can serve roles beyond protein translation, including facilitating protein complex formation, regulating post-translational modifications, or modifying protein conformations (Mayr 2019). Thus, not all transcripts detected by HCR may encode for protein. Given the marked increase in both CIP4 mRNA and protein between E14.5 and E18.5, it is likely that many transcripts are being

translated. Still, a one-to-one ratio is unlikely, and some mRNA may serve noncoding functions (Buccitelli and Selbach 2020).

CIP4 RNA expression increases over time, while FBP17 RNA expression decreases, contradicting previous findings

The CIP4 and FBP17 HCR RNA FISH experiments reveal that these two transcripts exhibit opposing expression patterns in the developing cortex. FBP17 RNA is expressed early in development, with high concentrations near the ventricular zone. In contrast, CIP4 RNA shows low expression initially but increases around E18.5, particularly in the upper intermediate zone and subplate, with a notable absence at the top of the cortical plate **(Figs. 3a, 4a, 4b)**. The strong presence of CIP4 RNA at E18.5 contradicts our earlier findings, where CIP4 protein levels decrease through embryonic development as measured with a western blot (Saengsawang, Mitok et al. 2012). The consistency of this expression pattern across two detection methods, HCR and IHC, suggests the observed increase in CIP4 RNA and protein expression may be real. However, the discrepancy between our older data and new findings suggests further work is necessary.

Thus, multiple lines of experimentation may be needed to determine why the HCR data **(Fig. 3)** and the IHC data from the CIP4-HA knock-in mouse **(Fig. 4)** do not match the previous ISH data from the Eurexpress **(Fig. 2a, b, e, f)** and Allen Brain Atlas **(Fig. 2c, g)** and the RNA seq data from the ENCODE dataset **(Fig. 2d, h)**. One question for further exploration is if the CIP4 and FBP17 probes are specific to CIP4 and FBP17 RNA, respectively. The probes would need to be tested on CIP4 KO embryonic brain sections (we possess a CIP4-KO mouse line) (Feng, Hartig et al. 2010) and brain sections where FBP17 was knocked down

via *in utero* electroporation (IUE) . If the CIP4 probes are specific, there should be no labeling in the KO brain sections and the labeled sections should resemble control HCR experiments without a probe **(Fig. S1)**. Moreover, the FBP17 probe should normally label FBP17 RNA in the CIP4 knockout line. Additionally, an FBP17 knockout mouse that was recently made commercially available could be obtained to check for FBP17 probe specificity (Adams, Barlas et al. 2024). While careful consideration was taken in providing correct RNA sequences to Molecular Instruments for probe design, the discrepancies between our HCR data and publicly available data sets warrant further investigation into the probe design and specificity.

The CIP4 HA mouse reveals a different protein expression pattern than previous data

We were surprised that CIP4 protein expression continues and seemingly increases at E18.5 in CIP4-HA mice. The increase in CIP4 protein contradicted our western blot data and previous studies with this mouse model. The CIP4-HA mouse we generated has an mScarlet after a stop codon and LoxP site. We had previously bred the CIP4-HA-mScarlet mouse with a beta-actin Cre mouse to generate a CIP4-mScarlet line. Staining the CIP4-mScarlet mouse with an anti-mScarlet antibody yielded different results than the HA staining **(Fig. S2)**. The mScarlet mouse shows high CIP4 et E12.5 before the cortical plate has been formed, from the ventricular to the pial surface **(Fig. S2a)**. At E14.5, CIP4 expression is absent from the cortical plate and continues to decrease as the cortical plate expands at E16.5 **(Fig. S2a)**. By E16.5, expression is reduced in both the cortical plate and upper intermediate zone, relative to the ventricular and subventricular zone **(Fig. S2a)**. It

appears that CIP4 is present in neuronal progenitors and newly born neurons but is depleted or otherwise removed prior to or as neurons enter the cortical plate. This pattern continues at E18.5 with progressive reduction of CIP4 in the cortical plate and intermediate zone **(Fig. S2a)**. Lastly, CIP4 expression is essentially undetectable by P10 **(Fig. S2a)**.

These findings differ significantly from our HCR and CIP4-HA mouse data. A possible answer to this discrepancy may in part be due to differences between the HCR and mScarlet antibody specificity. The anti-mScarlet antibody used in **Fig. S2** was produced in rabbits, while the antibody to HA used in **Fig. 4** is of mouse origin. Using an anti-mouse secondary on mouse tissue can result in increases background signal due to possible contamination of fixed slices with endogenous mouse antibodies (the E14.5 heads were drop fixed in PFA). While steps were taken to mitigate off-target binding, the potential increase in signal seen at E18.5 could be due to the anti-mouse secondary antibody. Thus, these experiments should be repeated with a non-mouse host HA antibody to confirm the HA signal.

Moreover, further staining of the HA mice at earlier time points, such as E10.5 and E12.5, and early postnatal and adult time points will help determine when CIP4 protein expression begins and how long it is expressed in cortex. While all published data suggests that CIP4 is mainly expressed embryonically in the brain, one study did identify CIP4 expression in adult human brain samples with Huntington's disease. This study also identified CIP4 as a binding partner of the Huntington protein, suggesting that CIP4 expression in adults may be indicative of Huntington’s pathology (Holbert, Dedeoglu et al.

2003). While this study has not been followed up, examining CIP4 expression in adult mice could provide novel insights for CIP4 in neurodegeneration.

These data highlight the complexity of interpreting the spatial and temporal expression patterns of CIP4 and FBP17 during cortical development. The discrepancy in CIP4 and FBP17 RNA patterns could be because they are both expressed at quite low levels compared to other proteins, such as DCX **(Fig. 1d, h)**. Thus, the differences in expression patterns of RNA may be due to the variability in relatively few transcripts and/or few cells expressing those transcripts. Integrating quantitative techniques such as single-cell RNA sequencing will be essential to resolving these inconsistencies and gaining a more precise understanding of where CIP4 family RNA and protein are expressed during cortical development.

FIGURES & TABLES

Probe Target	Coding Sequence	Probe sequences
mouse CIP4 short	AUggAUUggggUACCgAgUUgUgggAUCAgUUUgAggUgCUggAACgCCACACg CAgUgggggCUggAUUUgUUggACAAAUACgUgAAgUUCgUgAAAgAACgCgCg gAggUggAgCAggCUUAUgCUAAgCAACUCCggAgCCUggUgAAAAAgUAUCU UCCCAAgAgACCUACCAAAgAUgACCCUgAAgUCAAgUUCAgCCAgCAgCAg UCAUUUgUCCAgCUUCUCCAggAggUCAAUgACUUCgCAggCCAgAgAgAgC UggUggCUgAgAgCCUCggUAUCCgAgUgUgUCUggAgCUggCUAAgUAUUCA CAggAgAUgAAgCAggAgAggAAgAUgCACUUCCAggAAggUCgUCgggCCCAg CAgCAgCUggAgAAUggCUUCAAACAgCUggAgAAUAgUAAgCggAAgUUUgAA CgAgAUUgCCgggAggCUgAgAAAgCggCUCACACUgCUgAgCgCCUAgAUCA ggACAUUAAUgCCACCAAggCggAUgUggAgAAggCCAAgCAgCAAgCUCACC UUCggAACCACAUggCAgAAgAgAgCAAgAAUgAAUAUgCggCCCAgCUgCAg CgCUUCAACCgAgACCAggCUCACUUCUACUUCUCACAgAUgCCCCAgAU AUUCgAUAAgCUgCAggACAUggACgAACgCCgggCCACCCgCCUgggggCCgg gUAUgggCUCUUAUCAgAggCUgAACUgCAggUggUUCCCAUUAUUggCAAA UgCUUggAgggCAUgAAggUggCCgCCgAgUCUgUggAUgCUAAgAACgACUCA CAggUCCUCAUCgAAUUACACAAgUCCgggUUUgCCCgCCCAggggACUUgg AAUUUgAAgACUUUAgCCAAgUUAUCAACCgAgUgCCUUCggACAgCAgCC UgggCACCCCggAUggCAggCCUgAgCUCCgAgCAgCCUCCAgCCgUAgCCg CgCCAAgCgUUggCCUUUCgggAAAAAgAACAAgACCgUggCUACCgAAgAUU UCAgUCACUUgCCCCCggAgCAgCAgAgAAAgCgACUUCAgCAACAgCUggA AgAgCggAACCgAgAgUUgCAgAAggAggAggACCAgAgggAggCCCUgAAgAAgA UgAAAgAUgUAUAUgAgAAAACACCACAAAUgggggACCCUgCCAgCUUAgAg CCCCgCAUUgCAgAgACCCUgggCAACAUUgAgAggCUgAAgUUggAAgUgCA gAAgUAUgAggCUUggUUggCAgAAgCUgAAAgCCgggUCCUCAgUAACCgAgg ggACAgCCUAAgCCgUCACgCUAggCCCCCUgAUCCCCCAACUACUgCCCC ACCUgAUAgCAgCAgUAgCAgCACCAACAgUggAUCCCAggACAAUAAggAgA gCUCAgAAgAgCCCCCUUCAgAAggCCAggACACCCCCAUCUAUACUgAgU UCgAUgAggACUUUgAggAgCCUgCAUCCCCUAUCggCCAgUgUgUggCUAU CUACCAUUUUgAAggAUCCAgCgAgggAACCgUCUCCAUgUCCgAgggggAAg ACCUCAgCCUgAUggAggAAgACAAgggUgAUggAUggACgCgggUCAggAggAA ACAgggAgCUgAgggCUACgUgCCCACCUCUUACCUCCgAgUCACACUCAA CUgA	CAgTgggggCTggATTTgTTggACAAATACgTgAAgTTCgTgAAAgAACgCg TCCATgTCCgAgggggAAgACCTCAgCCTgATggAggAAgACAAgggTgATg TggACgCgggTCAggAggAAACAgggAgCTgAgggCTACgTgCCCACCTCTT gCTgAgAgCCTCggTATCCgAgTgTgTCTggAgCTggCTAAgTATTCACAgg CTggAgAATggCTTCAAACAgCTggAgAATAgTAAgCggAAgTTTgAACgAg TgCCgggAggCTgAgAAAgCggCTCACACTgCTgAgCgCCTAgATCAggACA TCAgAggCTgAACTgCAggTggTTCCCATTATTggCAAATgCTTggAgggCA AAggTggCCgCCgAgTCTgTggATgCTAAgAACgACTCACAggTCCTCATCg CCACAAATgggggACCCTgCCAgCTTAgAgCCCCgCATTgCAgAgACCCTgg gCTgAAAgCCgggTCCTCAgTAACCgAggggACAgCCTAAgCCgTCACgCTA ATCggCCAgTgTgTggCTATCTACCATTTTgAAggATCCAgCgAgggAACCg TTTgTCCAgCTTCTCCAggAggTCAATgACTTCgCAggCCAgAgAgAgCTgg CgAgACCAggCTCACTTCTACTTCTCACAgATgCCCCAgATATTCgATAAgC CAggACATggACgAACgCCgggCCACCCgCCTgggggCCgggTATgggCTCT CAAgTTATCAACCgAgTgCCTTCggACAgCAgCCTgggCACCCCggATggCA CCTgAgCTCCgAgCAgCCTCCAgCCgTAgCCgCgCCAAgCgTTggCCTTTCg CAgAgAAAgCgACTTCAgCAACAgCTggAAgAgCggAACCgAgAgTTgCAgA AACATTgAgAggCTgAAgTTggAAgTgCAgAAgTATgAggCTTggTTggCAg CCCCCTgATCCCCCAACTACTgCCCCACCTgATAgCAgCAgTAgCAgCACCA gACACCCCCATCTATACTgAgTTCgATgAggACTTTgAggAgCCTgCATCCC
mouse FBP17 short	AUgAgCUggggCACUgAgCUCUgggAUCAgUUUgACAACUUggAAAAACAUAC ACAgUggggAAUCgAUAUUCUUgAgAAAUACAUCAAgUUUgUCAAggAgAggA CggAgAUUgAgCUCAgCUAUgCCAAgCAACUCAggAAUCUUUCAAAgAAAUA CCAACCUAAgAAgAACUCgAAggAAgAggAggAgUACAAgUACACggCUUgCAA AgCCUUUCUUUCCACCCUgAAUgAgAUgAAUgACUACgCCgggCAgCACgAg gUCAUCUCUgAgAACAUgACgUCACAgAUCACggUggACCUgAUgCgCUACg UUCAggAgCUgAAgCAggAgAggAAAUCgAACUUCCAUgAUggACggAAggCUC AgCAgCACAUAgAAACgUgUUggAAgCAACUggAgUCAAgUAAgAggAggUUUg AgCgggACUgUAAggAAgCCgACCgggCACAgCAgUACUUCgAgAAAAUggACg CUgACAUCAACgUgACCAAggCggAUgUggAAAAggCACgACAACAAgCUCAg AUACgCCAgCAAAUggCAgAggACAgCAAAgCAgAUUACUCCUUAAUCCUgC AgAgAUUCAACCAggAgCAAUgggAAUACUACCAUACCCACAUCCCCAACAU CUUCCAgAAAAUACAAgAgAUggAggAgAggCggAUUgUgCgUAUUggggAgUC CAUgAAgACgUACgCAgAggUggACCggCAggUgAUACCCAUCAUCgggAAgUg CCUggACgggAUAgUgAAggCggCCgAgUCUAUCgACCAgAAAAACgACUCCC AgCUggUCgUAgAAgCCUAUAAgUCAggAUUCgAgCCUCCUggAgACAUUgAA UUCgAAgAUUACACACAgCCAAUgAAACgCACAgUgUCAgACAACAgCCUUU CCAgCUCCAAAgAAggCAAgCCUgAgCUCAgAUUUggCggCAAgUCCAgAggC AAgCUCUggCCAUUCAUCAAgAAAAACAAgggUgUCACACCAgAAgACUUCA gCAACUUCCCACCUgAgCAgAgAAggAAAAAACUACAACAgAAAgUUgACgAU CUCAAUAgAgAgAUACAgAAggAgACggACCAgAgAgAUgCCAUCACCAAAAU gAAAgAUgUgUACCUAAAgAACCCUCAgAUgggAgACCCAgCCAgCCUggACC AgAAgCUCACCgAAgUCACCCAgAACAUAgAgAAACUgCggCUggAggCUCAg AAgUUUgAggCCUggCUggCUgAggUAgAAggCAgACUCCCAgCUCggAgUgAg CAggCACgCCggCAgAgUggACUgUAUgAUggCCAgACACACCAgACggUCAC UAACUgUgCCCAggACCgggAgAgCCCAgAUggUAgUUACACAgAggAgCAAAg CCAggAgAgCgAgCACAAggUCCUggCCCCggAUUUCgACgAUgAAUUUgAUg AUgAggAgCCgCUUCCAgCCAUAgggACCUgCAAggCCCUCUACACAUUUgA AggUCAgAACgAAggCACCAUUUCCgUAgUUgAAggAgAgACgCUgAgCgUgAU UgAAgAggACAAAggCgAUgggUggACUCgCAUCCgCAgAAAUgAAgACgAggAg ggUUACgUCCCCACUUCCUACgUCgAAgUCUAUUUAgACAAAAACgCCAAA ggUUCCUAA	CAgTggggAATCgATATTCTTgAgAAATACATCAAgTTTgTCAAggAgAggA AAgCCTgAgCTCAgATTTggCggCAAgTCCAgAggCAAgCTCTggCCATTCA TATgATggCCAgACACACCAgACggTCACTAACTgTgCCCAggACCgggAgA CCAgATggTAgTTACACAgAggAgCAAAgCCAggAgAgCgAgCACAAggTCC TTTCTTTCCACCCTgAATgAgATgAATgACTACgCCgggCAgCACgAggTCA TCTgAgAACATgACgTCACAgATCACggTggACCTgATgCgCTACgTTCAgg ATAgAAACgTgTTggAAgCAACTggAgTCAAgTAAgAggAggTTTgAgCggg TgTAAggAAgCCgACCgggCACAgCAgTACTTCgAgAAAATggACgCTgACA CAAATggCAgAggACAgCAAAgCAgATTACTCCTTAATCCTgCAgAgATTCA gTgAAggCggCCgAgTCTATCgACCAgAAAAACgACTCCCAgCTggTCgTAg gCCTATAAgTCAggATTCgAgCCTCCTggAgACATTgAATTCgAAgATTACA CAgCCAATgAAACgCACAgTgTCAgACAACAgCCTTTCCAgCTCCAAAgAAg ACCTgCAAggCCCTCTACACATTTgAAggTCAgAACgAAggCACCATTTCCg CgCATCCgCAgAAATgAAgACgAggAgggTTACgTCCCCACTTCCTACgTCg CCTAAgAAgAACTCgAAggAAgAggAggAgTACAAgTACACggCTTgCAAAg CAAgAgATggAggAgAggCggATTgTgCgTATTggggAgTCCATgAAgACgT

		gCAgAggTggACCggCAggTgATACCCATCATCgggAAgTgCCTggACgggA AgAAggAAAAAACTACAACAgAAAgTTgACgATCTCAATAgAgAgATACAgA CCTCAgATgggAgACCCAgCCAgCCTggACCAgAAgCTCACCgAAgTCACCC gCCCCggATTTCgACgATgAATTTgATgATgAggAgCCgCTTCCAgCCATAg
mouse TOCA1 short	AUgAgCUggggCACCgAgCUgUgggAUCAgUUCgACAgCUUAgAUAAgCAUAC CCAAUggggAAUUgACUUCUUggAAAgAUAUgCCAAgUUUgUUAAAgAgAgAA UUgAAAUUgAACAgAACUAUgCgAAACAAUUgAgAAAUCUggUUAAgAAgUAC UgUCCCAAACgCUCCUCCAAAgAUgAAgAgCCAAggUUUACUUCAUgUAUC gCCUUUUUUAACAUCCUUAAUgAgUUAAACgACUAUgCAggACAgCgAgAgg UAgUAgCAgAAgAAAUggCgCACAgAgUAUAUggUgAAUUAAUgAgAUAUgCC CAUgAUCUgAAAACggAAAgAAAAAUgCAUCUCCAAgAAggACgAAAAgCUCA ACAAUACCUUgACAUgUgUUggAAACAgAUggAUAAUAgUAAAAAgAAgUUUg AAAgAgAAUgUAgAgAAgCggAgAAAgCACAgCAgAgUUAUgAgAggUUggAUAA UgACACCAAUgCCACCAAggCAgAUgUUgAAAAggCCAAACAgCAgUUgAAC CUUCgUACgCAUAUggCUgAUgAgAAUAAAAAUgAAUAUgCUgCACAgCUgC AAAAUUUUAAUggAgAACAgCACAAACAUUUUUAUgUggUAAUUCCUCAgAU UUACAAgCAACUACAAgAAAUggAUgAACgAAggACAAUUAAACUCAgUgAAU gUUACAgAgggUUUgCAgACUCAgAACgCAAAgUUAUUCCUAUCAUCUCAAA AUgUUUAgAAggAAUgAUUCUUgCAgCAAAAUCAgUUgAUgAAAgAAgAgAUU CUCAAAUggUAgUAgACUCCUUCAAgUCUggCUUUgAACCUCCAggAgACU UUCCAUUUgAAgAUUACAgUCAgCACAUUUACAgAACCAUUUCUgACgggA CCAUCAgUgCAgCCAAACAggAgAgUggCAAgAUggAUUCCAAgUCCACAgUg gggAAggCCAAgggCAAgCUgUggCUCUUUggAAAgAAgCCAAAgggCCCAgCA CUAgAAgAUUUCAgUCAUUUgCCACCAgAgCAgAggCggAAgAAgUUACAgCA gCgCAUUgACgAgCUUAACCgAgggCUgCAgAAggAAgCAgACCAAAAAgAAgC ACUCAACAAAAUgAAggAUgUgUAUgAgAAAAAUCCACAgAUgggggAUCCAgg AAgUCUgCAgCCUAAAUUAgCAgAgACCAUgAAUAACAUUgACCgCUUACgA AUggAAAUCCACAAgAAUgAggCAUggCUCUCUgAAgUUgAAggCAAAACAgg UAUAAgAggUgACAgAAgACACAgCAgUgACAUAAAUCAUCUUgUgACACAgg gACgAgAAAgCCCUgAgggAAgUUACACUgAUgAUgCAAACCAAgAAgUUCgU gggCCACCCCAACAACAUggCCACCACAgUgAgUUUgAUgAUgAgUUCgAAgA UgAUgAUCCCCUgCCUgCUAUUggACACUgCAAAgCAAUCUACCCUUUUgA UgggCAUAAUgAAggUACUCUggCAAUgAAAgAAggUgAAgUUCUgUACAUUA UUgAggAggACAAAggUgAUggAUggACAAgAgCUCggAgACAgAACggUgAAgA AggCUACgUUCCCACAACAUACAUAgAUgUUACUCUAgAgAAAAgCAgUAAA ggUgCAgUAACUUAUAUCUAA	CAATggggAATTgACTTCTTggAAAgATATgCCAAgTTTgTTAAAgAgAgAA gAgCAgAggCggAAgAAgTTACAgCAgCgCATTgACgAgCTTAACCgAgggC AAAAATCCACAgATgggggATCCAggAAgTCTgCAgCCTAAATTAgCAgAgA ATAAATCATCTTgTgACACAgggACgAgAAAgCCCTgAgggAAgTTACACTg gAAATTgAACAgAACTATgCgAAACAATTgAgAAATCTggTTAAgAAgTACT CCCAAACgCTCCTCCAAAgATgAAgAgCCAAggTTTACTTCATgTATCgCCT gAAgAAATggCgCACAgAgTATATggTgAATTAATgAgATATgCCCATgATC gAAATggATgAACgAAggACAATTAAACTCAgTgAATgTTACAgAgggTTTg CTTgCAgCAAAATCAgTTgATgAAAgAAgAgATTCTCAAATggTAgTAgACT TTCAAgTCTggCTTTgAACCTCCAggAgACTTTCCATTTgAAgATTACAgTC CACATTTACAgAACCATTTCTgACgggACCATCAgTgCAgCCAAACAggAgA ggCAAgATggATTCCAAgTCCACAgTggggAAggCCAAgggCAAgCTgTggC gATgCAAACCAAgAAgTTCgTgggCCACCCCAACAACATggCCACCACAgTg gCAATCTACCCTTTTgATgggCATAATgAAggTACTCTggCAATgAAAgAAg AgACAgAACggTgAAgAAggCTACgTTCCCACAACATACATAgATgTTACTC TTTAACATCCTTAATgAgTTAAACgACTATgCAggACAgCgAgAggTAgTAg AAAACggAAAgAAAAATgCATCTCCAAgAAggACgAAAAgCTCAACAATACC gACATgTgTTggAAACAgATggATAATAgTAAAAAgAAgTTTgAAAgAgAAT gAACAgCACAAACATTTTTATgTggTAATTCCTCAgATTTACAAgCAACTAC TTTgATgATgAgTTCgAAgATgATgATCCCCTgCCTgCTATTggACACTgCA
mouse DCX	AUAgAgAgAUUggUUUUCUUUCUCUCAgCAUCUCCACCCAACCAgCAgAAA ACCggUgAgUggggCUUUCgAgUgAUUUUCAAgCAgAAUgUAACAgAUgUCAA CCgggAAAgCACAAggCACACggCUUUCUUUCUCUgUgUgUUCgCCUCUUU CUUCUCUUUUAUUUgCCUUAUUCUAUAggAUUUUUgUCCUCUAAgAUUC UACCUgggAUUUUCCUUUggAAAAgUUgCUgUggUUCCACCAAAAUAUggAA CUUgAUUUUggACAUUUUgACgAACgAgACAAAgCAUCUAgAAAUAUgAgAgg gUCACggAUgAAUggACUUCCAAgUCCCACUCAUAgUgCCCACUgUAgCUU CUACAgAACCAgAACCUUgCAggCAUUAAgUAAUgAgAAgAAggCCAAgAAgg UACgUUUCUACCgCAAUggggACCgUUACUUCAAggggAUUgUgUACgCUgU UUCUUCUgACCgUUUUCgUAgUUUUgAUgCgUUgCUggCUgACCUgACCCg AUCCUUgUCUgACAACAUUAACCUgCCUCAgggAgUgCgCUACAUUUAUAC CAUUgACggAUCCAggAAgAUUggAAgCAUggAUgAACUggAAgAAggggAAAgC UAUgUCUgCUCCUCAgACAACUUCUUUAAAAAggUUgAgUACACCAAgAAU gUCAACCCCAACUggUCUgUCAACgUAAAgACAUCUgCCAACAUgAAAgCC CCCCAgUCCUUggCUAgCAgCAACAgUgCUCAAgCCAgAgAgAACAAggACU UUgUgCgCCCCAAACUUgUgACCAUCAUUCgCAgCggggUgAAgCCACggAAg gCUgUgCgCgUgCUUCUCAACAAgAAAACAgCCCACUCUUUCgAgCAggUC CUgACUgACAUCACAgAAgCgAUCAAACUggAAACCggAgUUgUCAAAAAAC UCUACACCCUUgAUggAAAgCAggUCACCUgUCUCCAUgAUUUCUUUggUg AUgAUgAUgUgUUCAUUgCUUgUggUCCUgAAAAAUUCCgCUAUgCUCAAgA UgAUUUCUCCUUggAUgAgAAUgAAUgCAgAgUCAUgAAAgggAAUCCAUCUg CCgCAgCUggCCCAAAggCUUCCCCAACACCUCAAAAgACAUCUgCUAAAA gCCCAggCCCAAUgCgCCgCAgCAAgUCUCCAgCUgACUCAggUAACgACCA AgACgCAAAUggAACUUCCAgCAgUCAgCUCUCAACACCUAAgUCAAAgCAg UCUCCUAUCUCUACACCCACAAgCCCUggAAgUCUgCggAAgCACAAggUA gACCUgUACCUgCCgCUgUCAUUggAUgACUCUgAUUCACUUggCgAUUCC AUgUgAAAgAUgAUAggCUAAAUCAAAgCCUAUUAUUgUAgCAgAAUACUUU CgCUCAAgUgACCAACAAggCUAUUggUgCUUAAACAUUUUUgUUAUUgUU	

	gCUUUUCAAAACACUCUgUAgUAUgUAgggUUUAUUUUCUUgUgACUUCU CUUCUgggCCACUAAUUCACAUUUACCAAUAAgAgAUAgAUUgAUAACCAU CCUUUUgAgUgACUUUUCCAgAACUUCAAAgUgUgCUACUCCAUgACCUU UCUACUgAAUgCUUAggggCCUUUgUAUUUUCCCCACUCAAUUUgUUCAg AAACUAgUCUUCCUUCUCUggAAggCUgUUUACAUACACAUCACUUAAAA UgUUUAUgUgUggggAAAACUUUCAUAUgCAgAUCUAAAAgCgAAAAACCUA AgUgUCCCUUgCCUCUgUAUCUUCAgAAUgCUggAggAUCUCAggAgAgUgg CAAgUCAgAUCCUUggUCUCACUCUUUgCUCUUAAUUgAgCCCCCAgUgU AUUgUCUAgCAUUCAUCCUggCUgUUgAgAUggAgAAACACCAgCgACUUUU gAUgUgACACCAUgUgCUUAgggCUgUggUAUAgggCUgUCUgAAAgAUAUgAg gUAgAAUAUAgggggAAAACUgCCCAAAUUUCAgUAggAUUUgUAUAAAgCAC AgUggAUUCCUggUUAACCCCUCUACUggggAAAUUUggAAUCAAUCAAUUg AUUAgUUUggggUACAUgAUgUCACAUACAUgAUCCUUCCAggAggCUUUCU AAUgUACAAgUUAgUACAUgAACggUAUggUAUCCAUCUAgCUCUgUUCUAU UgAAUgCCUUgUAAACAACCAACACUACAAACACUgUgAgAAUUUgUUUUC AggUCUgACACCUUUUggUCgCUUUUUAUAgCAAgAAACCAUAUCCUUUU UUAUAAAAAACUCAACUCUgUAUUUCAggAgCAAAACUCUUCAggCUCCU UUUUUAUAAgCUggUgAUUUUUUUCCUUUgUCUAAAAAACACAAgUAgAAA AUUgACCAAAAAAAUgCAgAAgAAUACUgUAgUUUAgAAAUCAUgCUCUCAC UgCCAAACAgAAAgCUCCgggAgAAAACACAAUgACUAgAggCCAAUUCAAUA gAAUCAggUUUUUgAUACCUUUUUAACAgUUACACUUACAgUAAUAAUUUC AAUgUggACCAgACAUUCUAgUUAUAUUUUAAAUgAAAUgUUAUggCAUAUU UUAAgUAACUCUUUUUUAUCUAUAAUCCUAAUAUUUCAUACUUAAgAUgC AgAAACCUUUCACUUgACUUUAACAUUAggAAggACUUCUCUUUAUUACgg AUUgAUCACUUgAAAUAACUCUgUCUUUgAggUACAggUUUAUAACAUUgC UUUUUCUCUgUAUUCAUAgCCCAUAAUAgCCAAgACAACgAAAgUUAggUg AAAgCCAUgCAUgCCAAUUCUgUgUUUgAUUUgACgAgAUAggAAgAUUUCC UUCACUUCUUUgUAAUUgUUCAgAUAgUUUgAAAgAUgCAgCAUUCAAAgU UUggCUgCUgAAUgACAUgCAgUUgUCCCUCCAUUCUAAgUAgAAUgAgUgU ggggUUCAUUUgUgUgUgUgUgUgUgUgUgUgUgUgUgUgUgUgUgCUCg CgCgCgCAUgCgCAAgCACgCCUAggCUgCUUCAUACUUAgCAAAUACUgCA CAAgACAACUCAACAUgAAUUgAUgACAACUUggUggCAUUgCUgAUgUgCAg ggggAAgUAggAUggCAggggUACCUAgAgCCCCCUUgAUAAAUUUCAgAUgU CCUUAAUUAUgAgAUUCCAAgAAACAUUUUUgCUUUUggUUCAgCAgAAgggg ggAUgAUgAgAgCUCUggUUUCUgCUUACACUgCUCAUUgAAgAgCCCAAAA UCAUgAggUUUUgCUCCCCCCCCCUUUAUUgCUAUgCCCACAUgAAAUgA UUAAgAAACCCAUUUUAAUCggCCCCUAUUUUUUUUUCUACAAgCUCAgU gAUUUCUUAgUgCCUCCCAgAACAUUUgAgUUAAUUAgggAAAAUUggUUAU UUgggAUggAUAgAAAUUgUggUAggAgAUCUAUUUUUAACCUCUgggCCAgA UCCUCCAgCACACUCUAUgUUgUUCUUUgAgCAAAUCCCAUgUUgUCCCA AgUAUUCAUUUAAgAUgAgACAUggAgAUUCUACUgAAAgAgUgggAgCAAAgA AAUUUCAACAgUCCCUAUgCCCAggCUUCUUggUAgUUCUCUgAgCAUUU UUCUACUUgUAgUAUAAUAUAgCACUAgAAAAUACUAUggACAUAUCUUUU UUAgAAUAUUCUUAgAACAgACAUUCUUgUAUAACAACAgUgUCCUUUCUg UUUUUCUUUgUgCUAACUACAAgUAAACCUUUAACAAAUACUUUUCCUU UAUAUACAggCACAgAUACAUACAUAUAAgAAAACUUUUUUUUUACUgCUAC UUCgUgUggCAAgggUUggUAAAAUUgAAAACUCAAgUCUCCAAUAAUUUAg UUUUAAAUUggCUCAAAUUCAAgUAAUUUUUUUCAgAACUAAgCUCUUAC AUCCCCCgUAUUCUUUCUCAgUUUUUCCUAAUCCACUUUUACCACUUU AgUCCCAUCAAgUUCAgCgUgCAUggUCAgCAAgCAUUUgCCACUAUUUUC CAUAAACACCCCCUCUCUCUUUUUCCCUCCUCCUCCCCUCCUUCUCUCU CUCUCUCUCUCUCUCUCUCUCUCUCUCUCUCACACACACACACACACA CACACACAAAgAAUAUgUUgCUUgUUCCUACCUCCUgACUgUUCUUCCCCC ACAgAAAUAgAAAUAggggCAAAAAAAAAAAAgggAAAUgUAUAUAUAggggCUg ggUUgAACAACUAACUUCgUAAgUAgUgCUAAgUAUAAUUAAAgUgAgAgAAA AgCUCCUUUUCUCAUAAUUgUUUUggAAAggAUAgCCAUUAgCAUgACUgC UUUgUgUCCUUgUggACUUUAgUAUUAgCCUAgACUgAAUUAUAgCAUUUU CUAgCUggAAAgAggAUUAAgAUCUCAUCAUCUgCUCCCAAUUUUUCAUUU UCUUAAggCCAggAAACAgACAAAgACAUAAAgUgAUUUCCCCCUAAggUCA CACAgCUgCCCAUUggCAgUgCUgggAUUAgAACCUACACCUCUUggCUCU UAUUCCAAUUUUUUUCCCCCAACUAgUgAgUAUUgUCCUUUgUgAggCUC CUgCAAAUUCUUUCCCAgggUCAUgUUgCACCCUggAUCCAUAUgCUACU UUgUUggUCUCAgCAAgAAAUCCACACAgCAAUAUAAUCUggCCCUUCCUC CUCACUUUCACAUUACUUCAUCCACAUggCCUgCAgACAgUUCCAAggAgA gggAggCAUUgAgACgUUgAgCACCAgAgggUUgCUgCCCUACCUUgAggAAU CUUCCAAAUAgCUCgCUgAACUCCACUCUAUUCAUggAgAAUggAAAAUgA CUACUUUgUCCCUUAUCAgCUUCCUUCAAggUCAUgUCACACgUgUUCCU CCCAggAUAggggAgUgAUUUCCAgAgCACAgAAAAUUAgAAgUgAAUAACAgA gUAAUAgCUUUgUUUAUUCUgACUUUCUAAAgAUgACUUUUUUUUAgCCA UUUAAAAAAUUAgUCUggCUAUCUUUACUACUAAUAACAAUUUCCUUUAA AAUAUggCAgUgAgCCAAgCCAgAgAAAgAUAAUCAAgUCUUgUgUUUAUCC UCAAUCUCUACgCCCUUgUAgCCAUgCUCCCUggUACAAACAAUUUUCAg gUAUAAACAAgUgUCUUUUgUCACUAAAUUgUgCCCUggCUgACACUgAAU AUUUgUAUCUAUACCAAAAAUAgCAUACAgUgACCUUACACAUUAUAUUCU CUCUCUCUCUCUCUCUCUCUCUCUCUCUCUCUCUCUCUCUCUCUgUg UAgCCUgUUUCUgUgCUUUCCAUgACAgAAgUUAgggCAACAUgAUCUgUAU gUgUAggUUUCUUUgCAgCAAggCUUUCCUggAACUAAUgAAUAUUCACUgA AUUCUAgAAgAUCUCUUACUAAAUUUACCCAAgUUCAggAACUUCUCUAU CUUUUCUUCCCUCCAUCUgggAgUgACCAAggAAUUgUAAAgUgggUAggUA gCUUCCAUgUCCUAgAAUCAUCAAgCCUAAgUUgAAggCAAAUgACUCAAUg CUUgAUUUgCAUAAACUUgUgUCCCCAUgCCCAgUCUCUCCAAUAgUCUA CAUAgAgAUUUCCCCAUUUCCUCUCACAUUUgACUCCAAAUggAUUUUUC CUUUAgAAAACAgggAAggAAAUAAgCCCUAUCUCCUUAgAAUgggAgCgAUC ACACACCCAUgggUCCCCAAUgAgCUUCUgUgAUggUgAgAAUgUUgCAAgAg AUgAgACUgCCUUgggAACAgUUgUAUCAAgAgACUUCUCUAgCAgAAACCC AAUgACAgCAUAgCUUUACggACUUCCUUCAUggUCUAgUUUgCUAUggAAA UAgAAAACAUAggAUCUUUCUCUUUUCUUUCUUUUUUUUUCUUCUUUU UgAAACAAUgCUUggAUCCUgUUCUUgggCACAUggggCCAUUUggACCCAU	

	ACCUAggCCUCAgUUAUAUAUUgCCUUCAUUAUAUUAAgACgUUUAggCUU CUAggCUCAAAUUAgUUUUCUAAACAgAgCAAgggUACUUUggAgCUCAUAU gggUgCACAggAAggCCUAUgUCCUAUgAUUUAgAUCUggAACCAUgggAUgg UAAAggCUgUAUAgUgACCUAgUCAUUUAgAgUAUgUCAggUAUAAUgUgUU AgAAgCUCAUgCUUCUgCCUCUgCCCUUCUAAAACCACgUgUgUCgUgCCA CUCACUgUUACgUgAAUCCUgAAggAUUUCCUCUUCUUUCAAACAUgACC ACCUggAgCAAgAAUAggUCACUgACUUUUUgUgCUUUCUUUUUgAUUAgA gAgACCUCUAUCUCCCUUggAUgCAUAAAUgAAgUUUCAUUAgCCAUCACA CCAAgggCUUCUUAgUgUUgAUUAAUgUggAgCUCAUgUUUUggCCAAACUg gUgUgAgAUUggCUAUCAUUgggAAgUgAAgUAUUUCUUAACUUUACUggAgU CAAAAAUCUUCUgAAAUUAgAAgUgAUUUUUUUUUCUAUCUggCAUACCUg gggCUAgggAAgUAgAgAAUUCUCAgUUgAAAgUAAggCACUUUCCUACUUgg AUUACAAgAgCAgUUgAgUUgAAAAAggUCAAAgAgAACAgAgAAgUCAgAAgA CCAAgUCUUgUAAACUAAAACAAAgACCCgAAgCUUCAgAAUgUCUCgAUU UUgggCAAUAACUCAAggAAAUAAAUggCUUUUUgUCAUUCCAUUUCCUgU UUUCUUUCUCUAUUUAgAUgCCUAUAUUUgUUCUCAgUUAUCAgUCUCU CAUUCggUAgCAAAAACAUCCAUUCUUUgACUUgUgAggUACUUCCUCCU CUUUUggAAUCCgUUgCUUCUUCCCACCUCACUACUgggUAUAAgCUUCU UCAUAgUCUgUAAgUUUUACCUUgggAUUgAAgAgAAAUUAUUUUCUgUUU CAAAAAUUCCUggUUCUACCCCUgUUCAgUCACAAgUAggUUggUAgAAAA CAACCUgAUUCUgACCCUUUCUUUUUUUUUUUCCUgUUUUAgUCUCAgU AgAUCUUUUCAAgCACUgUCCUUACAgCUCAUgAAUgUUUAggUCUUUAU CUUCUAAgCAAgCAUUgUACAgAACACgUUgUgCUUCUUCUUUUUgUCUg CCAUUUUgUgAACggUgUAAUgUgCUCAgAUAAAUAAUCAgCUgAgCAggAAA AgAgUCUACUCAUCUAUUCAAAUUggCAAACCAUUgUUUAgUUUgUAUCAU UAAAUUUgCUCAUAgCUUCgAAAAgCUgCAAUAUAAUgUCAUgAgAgACCAC AggUAAUUgUUCCUgUCAUUUggUUgggCUUAgUggAgAUgggggUgggCAggA ACAAUUUgUUUAAACUUUUAACgCUAUUCAUUAAgCUCUCUgUUAUAAACA UUAUgAUCUgUgAUCUUggCCACCUgUCgAACUgUUUAAgCUAAACUAgUgg gCAAUUAAAgUUAAUUUAAgUAAAAAAUUAUCUAACAAAUCCAggCUACAgA AAAAAAAAAAAACUUAgUUAAAUgUAUUUgUCCUUACgAUACUAgAUUUAC CUAAACAUUUUCCUUUUAACACCAACUgUUCACgAUCCAggACUgCCUgU CCAUgUAUCAAUAAUgAgCAgUCUUAAgUCUgCUAAUUAAUUCAgAAACCU UggggAUgUCAAUgUCACUgCUUggCAgUACCAUAUgCAUUgCCCAUUUUU CCAgUAACUUUUCUUUCUAAgUUCUCUUAAAgACUUUUgAgAAAgUAAgAA gCUAAgUgAACAUAUAUCCAAUgUUUUgUAAUgUAUUAUAUUgCAgCAUUA AgUCAACAACCCCUUAUgACgUgUACCCAgCUAAUgCAUggUUUCAgAgUgg AUUUUgCAUUUUUCAUgUgCAgUAAAUgAUUUAAAAAUgUUUUUggUCACC UUUUUgUgCCAUUAAACUUgUACAgAAAAUgCUUUUAUggCCAUUUUCAA UgggAgAAAgUUAAAAAAUggAAACAgCCCACCCUUUCUgCCCUAUAgCUgU AgUUAgAAUUgAgUACAUgUAgAAAUACggCUgUAAUUggUggUUgUAgUgUU AUAgUUgUUAgCUUgCUAgUgACUgCCUUUggAgAgUAAAUgCAUggUCUUg UACAUCACAUUUCUUAAAUAACUCAUUUUAACCUCUgAAAAggAUAUAUU AUUCCAUgUggCCCUCUUCCCUCCCUCCAUUCCCUgCUCCCAgAUAUCU UACCAUUAACUgUAAAUACCUgAUUUAggggCCAAgAgUUUCUgCCAAgUAA AgUUAgCAAggAgCAAAUAACCCAAAAggggUgAAgAgAAUUUCACAACAAUU UCUCAgAAgUUAUUgACCCUUUCUCAAggAAUggCAUggUUAUCAAAgACU CAgCUgUCUUUUACAUAAAAAUCAgAggCAAAUUgggAgUgUCUUUggCUgC CAgAUUACAgAAUUgAAAAAUUCUUAgAAUCAUACAACCCAAggAUgUCCC UgAUCCCUgCAUUACUUgUgAggCAUUUggAgACAUCAgAgAUUUgCUgACU AAUAUUUAUUggggAUAAAAAgAAAAgCAAAACAgAgAUgUgCgACAgAUACU CAggggUUUCAgCUAggCUCCAgUCAgCAAAggUAAggAUgUgggUUUAgAUg CAUUgUUAUCUgUUUCCCAggCAAUgCUUAACACACUCUUAgUgCUUUgAg UgAUACAAAggCAgUgUUUCAACAAgACACUCUCUUCUUUggUUUgCUgUU CUCUCUUggACUggAAUgUUUggCAAggCCCAUgUAAACUggUUAgAgCAggC CCUUUAUAUCUCCUgUgACCgUUAAUCUCCCCCACCAUAAUUUgAUgAgg gCUgUUUggUUUgAggACUUCAAggAUgUCUAgAgAAgUUCCCCCAUgUgUg UgAggUgUUgUgAACUgUgAACACUgUACAUCUUCAgUgUUCAAUACUgggC AgCCAAAgAgCUgCUCUUgCAAUCUUUUUUUggCUCUCAAgCUCUgUUCU CCAUCgAAUUCUCAUUUCUgUgUACAUUUg	

Table 1. RNA sequences used for HCR RNA *FISH* probe design. Target Sequences from NCBI gene database, probe sequences from Molecular Instruments Inc.

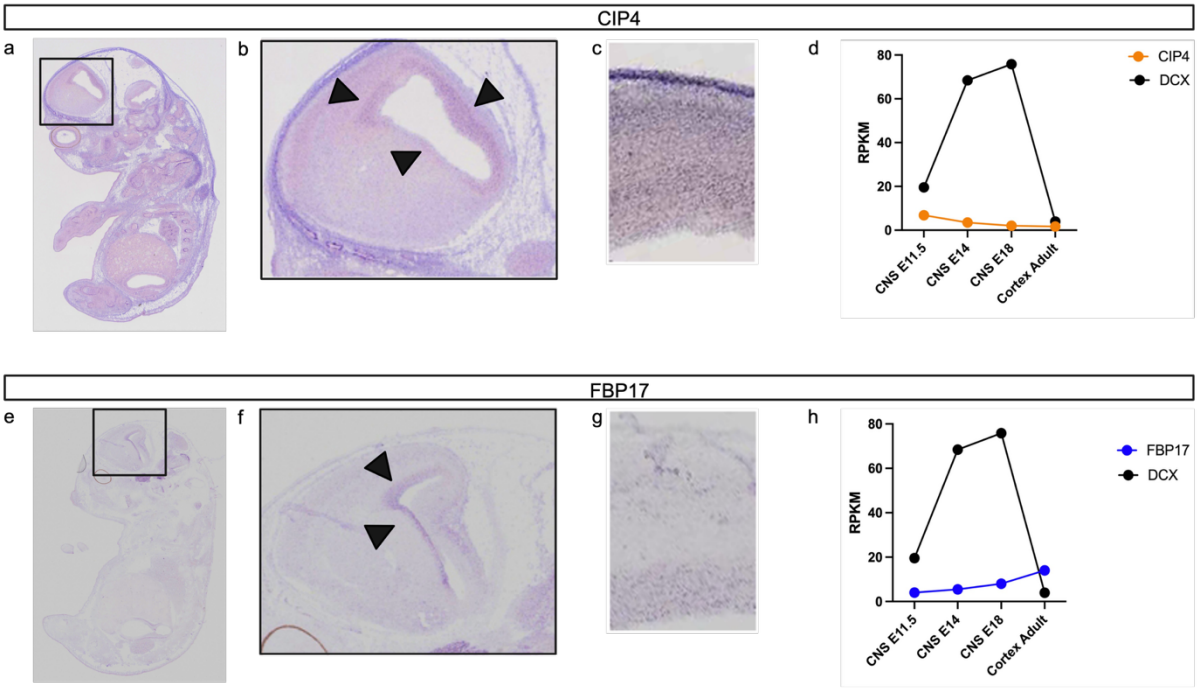

Figure 1. RNA expression data from the online datasets for CIP4 and FBP17

(a) Sagittal section of CIP4 RNA expression in an E14.5 mouse from the Eurexpress dataset. **(b)** Inset of (a) showing a close-up image of the boxed region. Black triangles indicate areas of higher signal. **(c)** Coronal section of E14.5 CIP4 RNA in the cortex from the Allen Brain Atlas dataset. **(d)** Graph based on data from the ENCODE dataset of CIP4 RNA expression in the embryonic central nervous system and adult cortex. Doublecortin (DCX) is also plotted for comparison. **(e)** Sagittal section of FBP17 RNA expression in an E14.5 mouse from the Eurexpress dataset. **(f)** Inset shows a close-up image of the boxed region. Black triangles indicate areas of high signal. **(g)** Coronal section of FBP17 RNA in the cortex from the Allen Brain Atlas dataset. **(h)** Graph based on data from the ENCODE data set of FBP17 RNA expression in the embryonic central nervous system and adult cortex. Doublecortin (DCX) is also plotted for comparison. Adapted from(Lein, Hawrylycz et al. 2007, Diez-Roux, Banfi et al. 2011, Yue, Cheng et al. 2014).

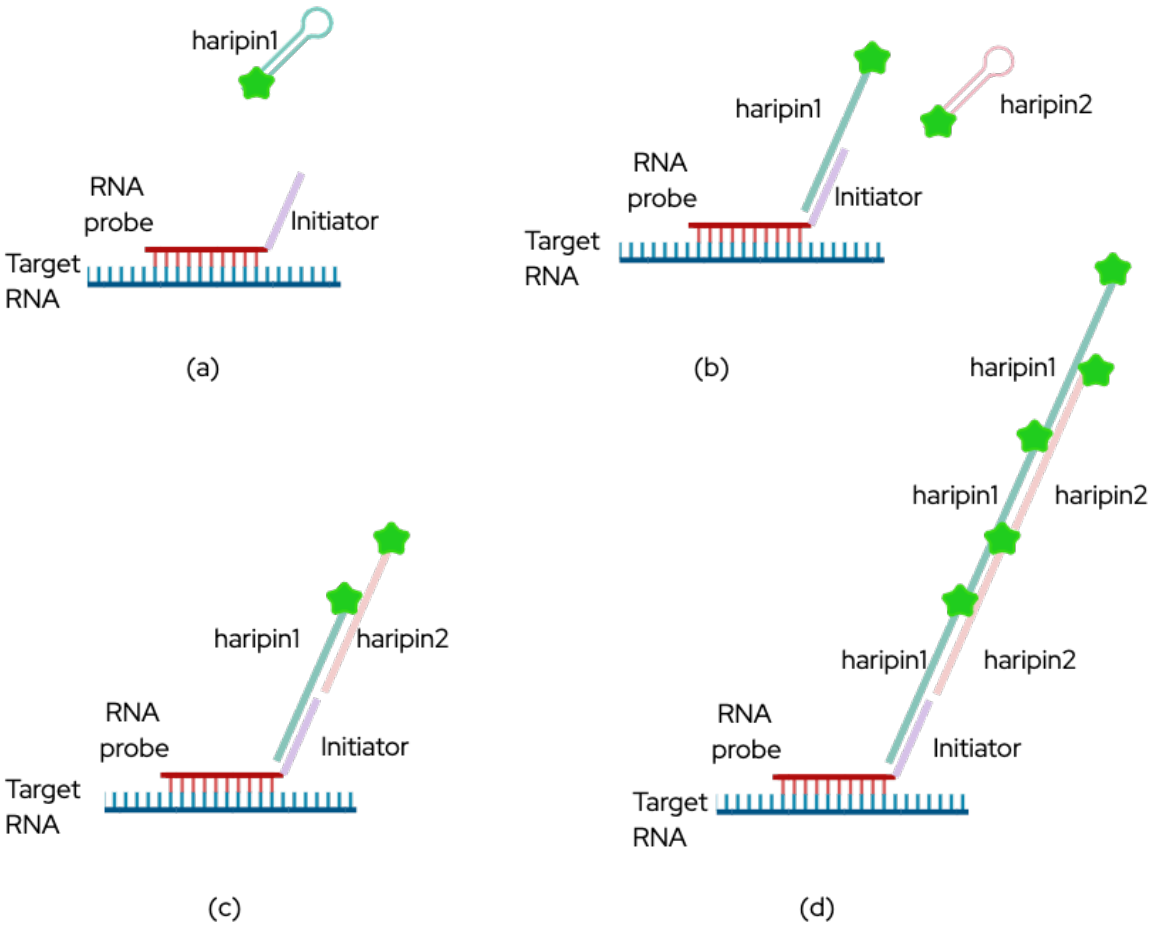

Figure 2. Schematic of HCR RNA FISH probe binding and hairpin chain reaction

(a) An RNA probe (red) containing an initiator (purple) bind to a target RNA sequence (blue). The hairpins (teal) contain a fluorophore (neon green star) and bind to the complementary sequence on the initiator. **(b)** Hairpin 1 unfolds and binds to the initiator. **(c)** Hairpin 2 (pink) recognizes hairpin 1. Hairpin 2 unfolds and binds to the complementary sequence of hairpin 1. **(d)** Another hairpin one then binds to the complementary region of hairpin 2, leading to a chain reaction polymerization(Dirks and Pierce 2004, Choi, Schwarzkopf et al. 2018). Created in BioRender. English, L. (2025) https://BioRender.com/80tqper

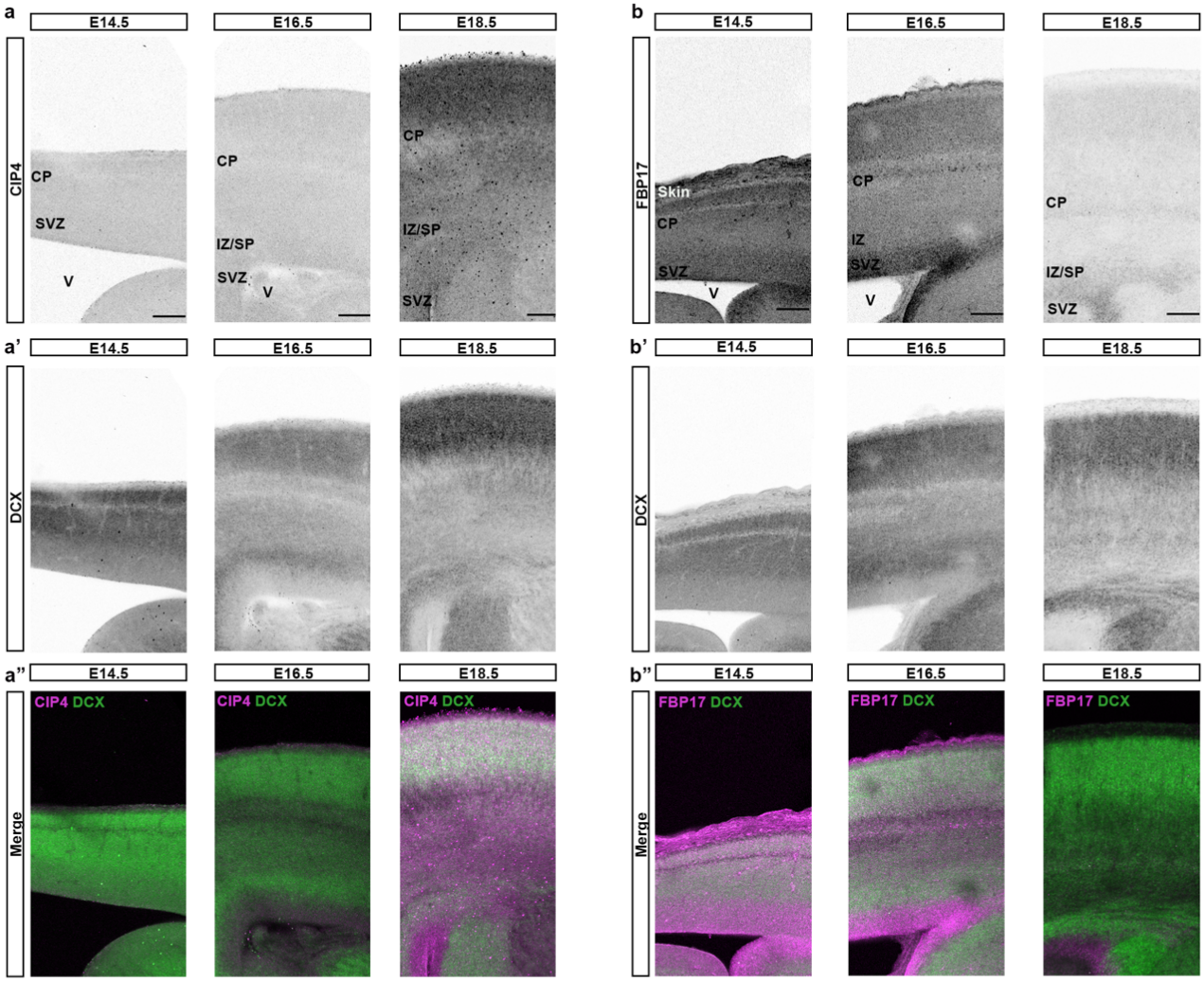

Figure 3. CIP4 and FBP17 have opposing RNA expression patterns in the embryonic cortex

(a) Representative images of CIP4 HCR RNA *FISH* in the cortex at E14.5, E16.4 and E18.5. **(a')** Representative images of Doublecortin (DCX) HCR RNA *FISH* in the cortex at E14.5, E16.4 and E18.5. **(a")** Representative merged images of CIP4 and DCX HCR RNA *FISH* in the cortex at E14.5, E16.4 and E18.5. **(b)** Representative images of FBP17 HCR RNA *FISH* in the cortex at E14.5, E16.4 and E18.5. **(b')** Representative images of Doublecortin (DCX) HCR RNA *FISH* in the cortex at E14.5, E16.4 and E18.5. **(b")** Representative merged images of FBP17 and DCX HCR RNA *FISH* in the cortex at E14.5, E16.4 and E18.5. CP= cortical plate, SP/IZ= subplate/intermediate zone, SVZ= subventricular zone, V= lateral ventricle Scale bar 100µm.

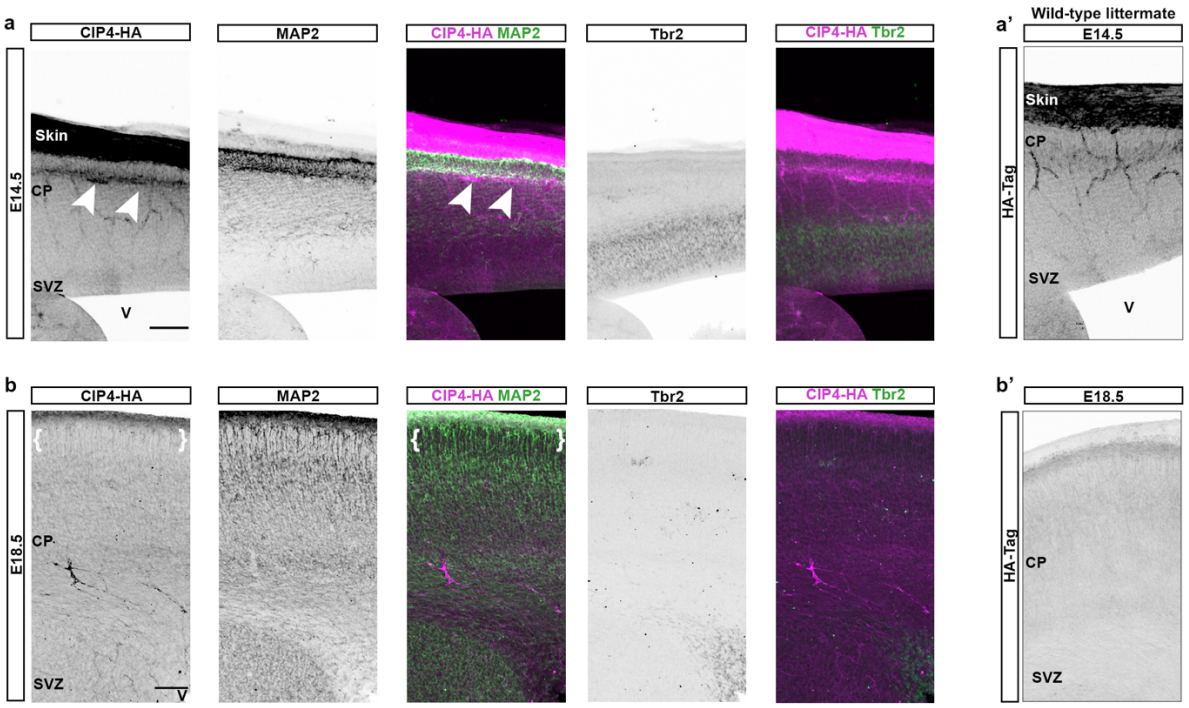

Figure 4. Cortical expression of CIP4 decreases during embryonic development.

(a) Endogenous expression of CIP4-mScarlet in the mouse cortex at E14.5 stained for HA-tag MAP2, and Tbr2. White arrows indicate regions of high signal. **(a')** WT littermate of E14.5 CIP4-HA mouse stained for HA-tag. **(b)** Endogenous expression of CIP4-mScarlet in the mouse cortex at E18.5 stained for HA-tag, MAP2, and Tbr2. White brackets indicate the region of low signal. **(b')** WT littermate of E14.5 CIP4-HA mouse stained for HA-tag. Scale bar 100μm.

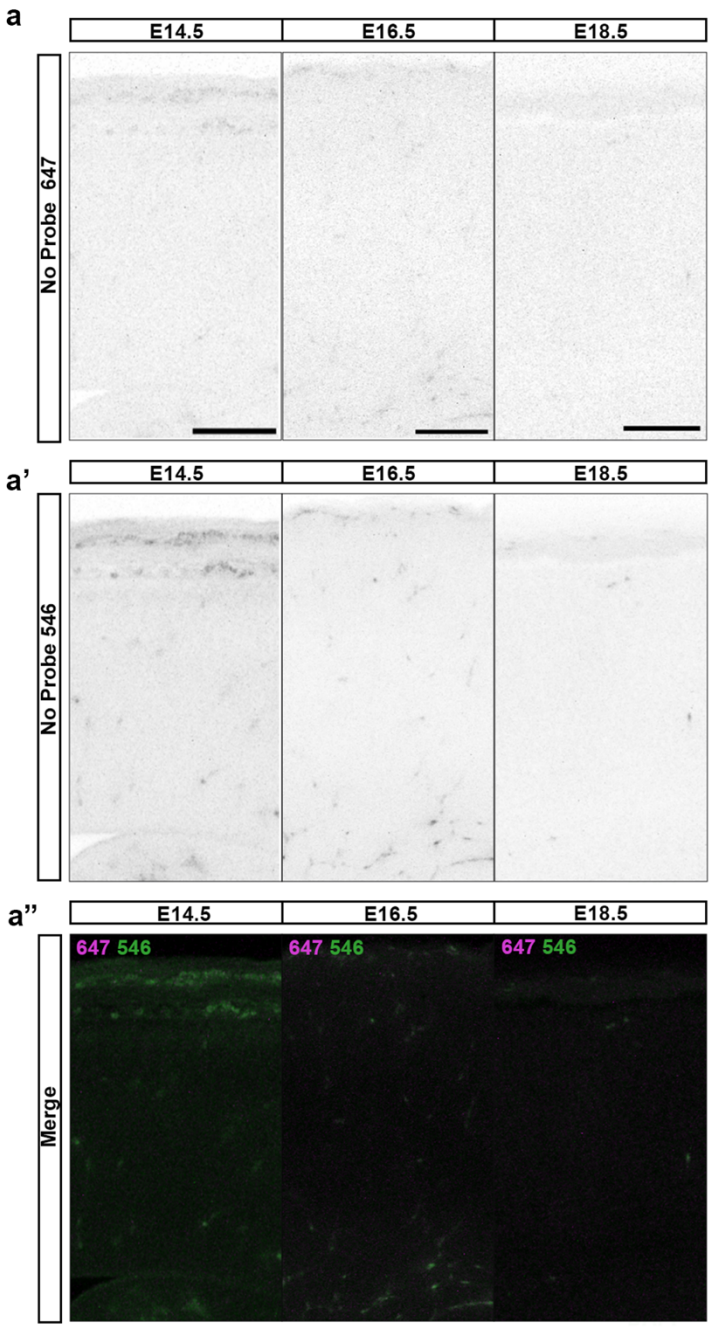

Supplemental Figure 1: HCR hairpins do not bind to non-probe targets.

HCR RNA FISH of wild-type brains at E14.5, E16.5 and E18.5 with no probe and **(a)** 647 hairpins. **(a')** 546 hairpins. **(a")** merged image Scale bar is 100µm.

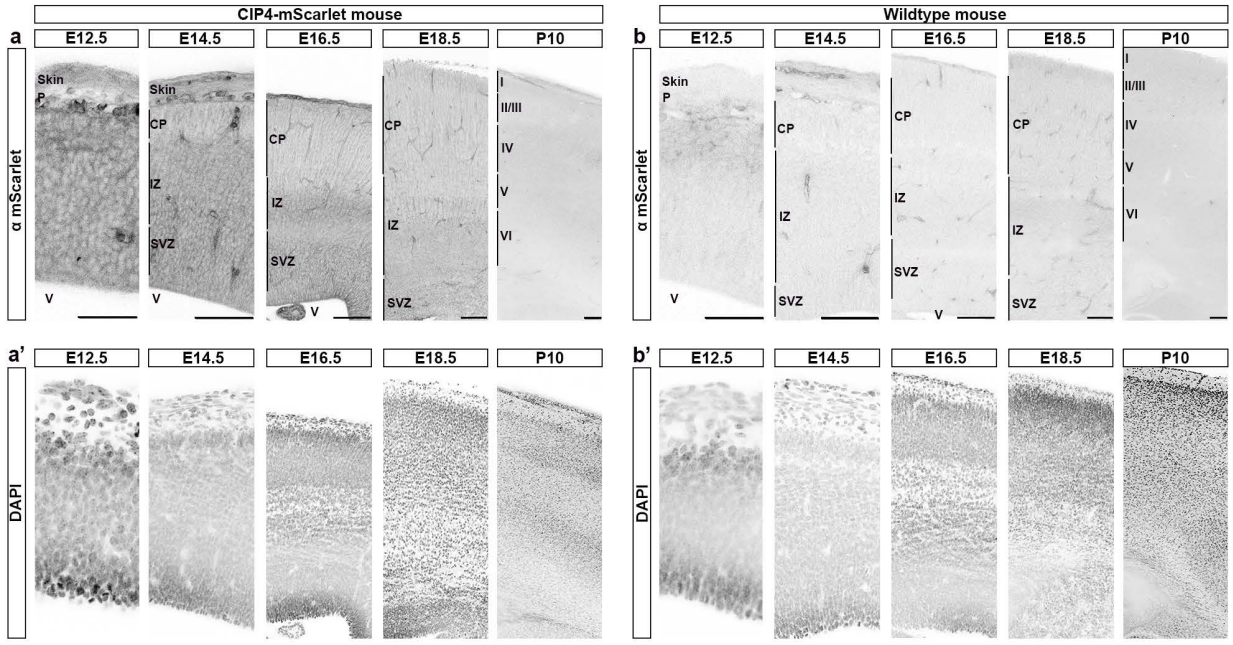

Supplemental Figure 2: Expression of endogenous CIP4 tagged to mScarlet in the developing cortex.

(a) Endogenous expression of CIP4-mScarlet in the mouse cortex from E12.5 though P10, stained for mScarlet. **(a')** DAPI staining of corresponding sections from a. **(b)** WT littermates of mice in a, stained for mScarlet expression. **(b')** DAPI staining of corresponding sections from a'. P= pial surface CP= cortical plate, IZ= intermediate zone, SVZ= subventricular zone, V= lateral ventricle, I= cortical layer 1, II/III= cortical layers 2 and 3, IV= cortical layer 4, V= cortical layer 5, and VI= cortical layer 6. Scale bar 50μm for E12.5 and 100μm for all other time points. E12.5-E16.5 time points were collected by R. J. Taylor, and E18.5 and P10 time points were collected by L. A. English.

REFERENCES

Adams, D. J., Barlas, B., McIntyre, R. E., Salguero, I., van der Weyden, L., Barros, A., Vicente, J. R., Karimpour, N., Haider, A., Ranzani, M., Turner, G., Thompson, N. A., Harle, V., Olvera-Leon, R., Robles-Espinoza, C. D., Speak, A. O., Geisler, N., Weninger, W. J., Geyer, S. H., . . . Balmus, G. (2024). Genetic determinants of micronucleus formation in vivo. *Nature*, *627*(8002), 130-136. https://doi.org/10.1038/s41586-023-07009-0

Buccitelli, C., & Selbach, M. (2020). mRNAs, proteins and the emerging principles of gene expression control. *Nat Rev Genet*, *21*(10), 630-644. https://doi.org/10.1038/s41576-020-0258-4

Choi, H. M., Beck, V. A., & Pierce, N. A. (2014). Next-generation in situ hybridization chain reaction: higher gain, lower cost, greater durability. *ACS Nano*, *8*(5), 4284-4294. https://doi.org/10.1021/nn405717p

Choi, H. M., Chang, J. Y., Trinh le, A., Padilla, J. E., Fraser, S. E., & Pierce, N. A. (2010). Programmable in situ amplification for multiplexed imaging of mRNA expression. *Nat Biotechnol*, *28*(11), 1208-1212. https://doi.org/10.1038/nbt.1692

Choi, H. M. T., Schwarzkopf, M., Fornace, M. E., Acharya, A., Artavanis, G., Stegmaier, J., Cunha, A., & Pierce, N. A. (2018). Third-generation in situ hybridization chain reaction: multiplexed, quantitative, sensitive, versatile, robust. *Development*, *145*(12). https://doi.org/10.1242/dev.165753

Dehay, C., & Kennedy, H. (2007). Cell-cycle control and cortical development. *Nat Rev Neurosci*, *8*(6), 438-450. https://doi.org/10.1038/nrn2097

Diez-Roux, G., Banfi, S., Sultan, M., Geffers, L., Anand, S., Rozado, D., Magen, A., Canidio, E., Pagani, M., Peluso, I., Lin-Marq, N., Koch, M., Bilio, M., Cantiello, I., Verde, R., De Masi, C., Bianchi, S. A., Cicchini, J., Perroud, E., . . . Ballabio, A. (2011). A high-resolution anatomical atlas of the transcriptome in the mouse embryo. *PLoS Biol*, *9*(1), e1000582. https://doi.org/10.1371/journal.pbio.1000582

Dirks, R. M., & Pierce, N. A. (2004). Triggered amplification by hybridization chain reaction. *Proc Natl Acad Sci U S A*, *101*(43), 15275-15278. https://doi.org/10.1073/pnas.0407024101

Englund, C., Fink, A., Lau, C., Pham, D., Daza, R. A., Bulfone, A., Kowalczyk, T., & Hevner, R. F. (2005). Pax6, Tbr2, and Tbr1 are expressed sequentially by radial glia, intermediate progenitor cells, and postmitotic neurons in developing neocortex. *J Neurosci*, *25*(1), 247-251. https://doi.org/10.1523/JNEUROSCI.2899-04.2005

Feng, Y., Hartig, S. M., Bechill, J. E., Blanchard, E. G., Caudell, E., & Corey, S. J. (2010). The Cdc42-interacting protein-4 (CIP4) gene knock-out mouse reveals delayed and decreased endocytosis [Research Support, N.I.H., Extramural Research Support, Non-U.S. Gov't]. *J Biol Chem*, *285*(7), 4348-4354. https://doi.org/10.1074/jbc.M109.041038

Fischer, I., Shea, T. B., Sapirstein, V. S., & Kosik, K. S. (1986). Expression and distribution of microtubule-associated protein 2 (MAP2) in neuroblastoma and primary neuronal cells. *Brain Res*, *390*(1), 99-109. http://www.ncbi.nlm.nih.gov/entrez/query.fcgi?cmd=Retrieve&db=PubMed&dopt=Citation&list_uids=3512042

Francis, F., Koulakoff, A., Boucher, D., Chafey, P., Schaar, B., Vinet, M. C., Friocourt, G., McDonnell, N., Reiner, O., Kahn, A., McConnell, S. K., Berwald-Netter, Y., Denoulet, P., & Chelly, J. (1999). Doublecortin is a developmentally regulated, microtubule-associated protein expressed in migrating and differentiating neurons. *Neuron*, *23*(2), 247-256. https://doi.org/10.1016/s0896-6273(00)80777-1

Gdalyahu, A., Ghosh, I., Levy, T., Sapir, T., Sapoznik, S., Fishler, Y., Azoulai, D., & Reiner, O. (2004). DCX, a new mediator of the JNK pathway. *EMBO J*, *23*(4), 823-832. https://doi.org/10.1038/sj.emboj.7600079

Gleeson, J. G., Lin, P. T., Flanagan, L. A., & Walsh, C. A. (1999). Doublecortin is a microtubule-associated protein and is expressed widely by migrating neurons. *Neuron*, *23*(2), 257-271. https://doi.org/10.1016/s0896-6273(00)80778-3

Holbert, S., Dedeoglu, A., Humbert, S., Saudou, F., Ferrante, R. J., & Neri, C. (2003). Cdc42-interacting protein 4 binds to huntingtin: neuropathologic and biological evidence for a role in Huntington's disease. *Proc Natl Acad Sci U S A*, *100*(5), 2712-2717. http://www.ncbi.nlm.nih.gov/entrez/query.fcgi?cmd=Retrieve&db=PubMed&dopt=Citation&list_uids=12604778

Lein, E. S., Hawrylycz, M. J., Ao, N., Ayres, M., Bensinger, A., Bernard, A., Boe, A. F., Boguski, M. S., Brockway, K. S., Byrnes, E. J., Chen, L., Chen, L., Chen, T. M., Chin, M. C., Chong, J., Crook, B. E., Czaplinska, A., Dang, C. N., Datta, S., . . . Jones, A. R. (2007). Genome-wide atlas of gene expression in the adult mouse brain. *Nature*, *445*(7124), 168-176. https://doi.org/10.1038/nature05453

Mayr, C. (2019). 3' UTRs Regulate Protein Functions by Providing a Nurturing Niche during Protein Synthesis. *Cold Spring Harb Symp Quant Biol*, *84*, 95-104. https://doi.org/10.1101/sqb.2019.84.039206

Saengsawang, W., Mitok, K., Viesselmann, C., Pietila, L., Lumbard, D. C., Corey, S. J., & Dent, E. W. (2012). The F-BAR protein CIP4 inhibits neurite formation by producing lamellipodial protrusions [Research Support, N.I.H., Extramural Research Support, Non-U.S. Gov't]. *Curr Biol*, *22*(6), 494-501. https://doi.org/10.1016/j.cub.2012.01.038

Saengsawang, W., Taylor, K. L., Lumbard, D. C., Mitok, K., Price, A., Pietila, L., Gomez, T. M., & Dent, E. W. (2013). CIP4 coordinates with phospholipids and actin-associated proteins to localize to the protruding edge and produce actin ribs and veils. *J Cell Sci*, *126*(Pt 11), 2411-2423. https://doi.org/10.1242/jcs.117473

Speir, M. L., Bhaduri, A., Markov, N. S., Moreno, P., Nowakowski, T. J., Papatheodorou, I., Pollen, A. A., Raney, B. J., Seninge, L., Kent, W. J., & Haeussler, M. (2021). UCSC Cell Browser: visualize your single-cell data. *Bioinformatics*, *37*(23), 4578-4580. https://doi.org/10.1093/bioinformatics/btab503

Wakita, Y., Kakimoto, T., Katoh, H., & Negishi, M. (2011). The F-BAR protein Rapostlin regulates dendritic spine formation in hippocampal neurons [Research Support, Non-U.S. Gov't]. *J Biol Chem*, *286*(37), 32672-32683. https://doi.org/10.1074/jbc.M111.236265

Yue, F., Cheng, Y., Breschi, A., Vierstra, J., Wu, W., Ryba, T., Sandstrom, R., Ma, Z., Davis, C., Pope, B. D., Shen, Y., Pervouchine, D. D., Djebali, S., Thurman, R. E., Kaul, R., Rynes, E., Kirilusha, A., Marinov, G. K., Williams, B. A., . . . Mouse, E. C. (2014). A comparative encyclopedia of DNA elements in the mouse genome. *Nature*, *515*(7527), 355-364. https://doi.org/10.1038/nature13992

Chapter 4

Final Conclusions and Future Directions

CIP4 expression may regulate the termination of migration

In chapter 2, we demonstrated that CIP4 and FBP17 function in distinct and opposing ways during neuronal migration. Chapter 3 further supports this view by showing that CIP4 and FBP17 exhibit inverse spatial and temporal mRNA expression patterns. These findings highlight the need to investigate the precise localization of each protein during cortical development. Based on current data, we hypothesize that CIP4 regulates the process retraction required for neurons to transition from the multipolar to bipolar state in the intermediate zone. Supporting this idea, CIP4 protein is highly expressed in the intermediate zone but notably absent from the top of the cortical plate **(Ch3 Fig. 2)**, even though CIP4 mRNA remains detectable in that region **(Ch3 Fig. 1)**. This spatial mismatch suggests that once neurons complete the multipolar to bipolar transition, CIP4 protein expression is rapidly downregulated, potentially by miRNA.

Our published western blot data show that CIP4 protein levels decrease sharply after E18.5 (Saengsawang, Mitok et al. 2012), suggesting that tight temporal regulation is critical for proper migration. Once neurons reach the cortical plate, they begin extending stable processes required for maturation, and thus downregulation of CIP4, and its signaling in neurite retraction, is essential (Nadarajah, Brunstrom et al. 2001, Sawada, Ohno et al. 2018). Our HCR probes detect any RNA sequence matching CIP4, including untranslated or repressed transcripts, and therefore likely captures mRNA not actively being translated (Choi, Schwarzkopf et al. 2018, Zhuang, Zhang et al. 2020). This raises the possibility that miRNAs or RNA-binding proteins may repress CIP4 translation or promote degradation of

CIP4 transcripts during late-stage migration. Despite the sharp decline in protein, our knockdown data show that CIP4 expression must be carefully titrated. Excessive production or exogenous downregulation disrupts migration and process retraction, suggesting that precise modulation of CIP4 levels is necessary for coordinated cortical development.

Additional support for the role of CIP4 in migration termination comes from postnatal studies. At postnatal day 21 (P21) CIP4 overexpressing neurons fall into three distinct categories: some reach their correct layer II/III position and appear morphologically similar to controls **(Ch2 Fig. S2a, inset I)**, others stall in deep cortical layers (layers V/VI) **(Ch2 Fig. S2a inset II)**, and a third group remains near the ventricular zone with oblong cell bodies **(Ch2 Fig. S2a inset III)**. Notably these overexpressing neurons fail to project their axons across the corpus callosum (data not shown). These data indicate that excessive CIP4 impairs both migration and axon extension, reinforcing its role as a negative regulator of neuronal motility and polarity.

In contrast, CIP4 knockdown produces an over-migration phenotype by P24 **(Ch. 2, Fig. S2b)**. As shown earlier, CIP4 knockdown increases process number in migrating neurons, which persists postnatally and suggests a prolonged multipolar state. Although these neurons eventually exit the intermediate zone, they are delayed, causing them to overshoot their intended destination. Two possible mechanisms could explain this phenotype: (1) delayed arrival at the cortical plate leads to migration alongside later-born neurons, causing overshooting due to the inside-out nature of cortical migration; or (2) the

absence of CIP4 disrupts the reception of termination signals, such as expression of receptors for Reelin signaling (Sekine, Kubo et al. 2014, Hirota and Nakajima 2017).

Interestingly, some CIP4 knockdown neurons at P24 display large apical arbors that invade layer I, resembling layer II marginal neurons (L2MNs) (Peters and Kara 1985, Cho, Segawa et al. 2004, Staiger, Bojak et al. 2015, Luo, Hasegawa et al. 2017). These L2MNs reside between layers I and II and are distinct from typical layer II/III neurons. To test whether CIP4 knockdown induces an L2MN-like identity, future experiments should examine expression of markers such as SMI-32 and N-52 (layer III), and RELN (layer I) (Martinez-Cerdeno, Galazo et al. 2002, Hevner 2007). CIP4 knockdown-induced L2MNs would be expected to be negative for all three.

The over-migration phenotype caused by CIP4 knockdown was unexpected. While rare, it resembles phenotypes seen after overexpression or knockdown of other genes. For example, overexpression of the tubulin-binding protein Mllt11 causes over-migration at E15.5 (Stanton-Turcotte, Hsu et al. 2022). In contrast, Mllt11 knockout leads to decreased migration and reduced callosal axons. These parallels raise the possibility that dual knockdown of Mllt11 and CIP4 might result in phenotypic rescue. Knockdown of Mllt11 could aid CIP4 knockdown neurons in migrating further, while the reduced corpus callosal crossing in Mllt11 knockdown may mitigate extra processes caused by loss of CIP4. This double knockdown could result in phenotypically normal neurons that are able to migrate.

To further investigate CIP4's role in positioning, it will be important to determine whether CIP4-overexpressing or knockdown neurons maintain their original layer identity

despite their altered locations. Neurons born at E14.5 populate layer II/III and express Cux2. Earlier-born neurons express Tbr1 (layer VI) or Ctip2 (layer V/VI) (Hevner, Shi et al. 2001, Hevner 2007). Immunostaining for Cux2, Tbr1, Ctip2, NeuN (neuronal marker), and GFAP (astrocyte marker) (Eng, Vanderhaeghen et al. 1971, Gusel'nikova and Korzhevskiy 2015, Yang and Wang 2015) will clarify whether mispositioned neurons retain their original identity or adopt one appropriate to their ectopic layer. Because cortical layer identity is largely determined by birthdate and transcription factor expression (Greig, Woodworth et al. 2013), and CIP4 is not a transcription factor, it is unlikely that CIP4 directly alters layer identity. Nonetheless, confirming that CIP4-manipulated neurons maintain a layer II/III signature would clarify the distinction between migratory defects and fate specification.

Potential roles of CIP4 and FBP17 in other modes of neuronal migration

This dissertation has focused on the migration of excitatory neurons in the cortex. However, inhibitory neurons also migrate into the cortex coincident with the radial migration of excitatory neurons (Kriegstein and Noctor 2004). Inhibitory neurons are born on the ventral sides of the lateral ventricle in the medial and lateral ganglionic eminences (Toudji, Toumi et al. 2023). While interneurons migrate, they maintain a bipolar morphology with a slightly branched leading process and a trailing process (Valiente and Martini 2009). CIP4 knockdown in interneurons would likely push these cells to a multipolar morphology, likely inhibiting their migration, like we have shown here for excitatory neurons.

Modulating FBP17 expression in tangentially migrating inhibitory neurons could also have an interesting effect on migration. Increases or decreases of FBP17 expression showed

an increase in leading process length. Thus, overexpression or knockdown of FBP17 in migrating interneurons may cause longer leading processes, which may disrupt nucleokinesis (Tsai and Gleeson 2005; Yanagida et al., 2012) during migration. However, while FBP17 neurons did have longer leading processes, they were otherwise morphologically akin to controls in both overexpression and knockdown conditions. Therefore, it would be interesting to see if the longer leading process persists in interneurons, and if their trailing processes are affected as well. Our data suggest that trailing processes were not affected by FBP17 expression (data not shown), but interneurons do not dramatically change their morphology, as excitatory neurons do and may be more sensitive to the effects of FBP17 on process length (Valiente and Martini 2009).

In addition to interneurons, it is also worth considering the roles of FBP17 and CIP4 in neuronal proliferation. Data from Kendra Taylor's thesis suggests that CIP4 may have a role in cortical neuron proliferation, but these data were inconclusive (Taylor 2018). Since these two proteins are expressed in the ventricular and subventricular zone **(Ch3 Fig. 2, 3)**, it is likely they are also present in radial glial cells. Discovering a role for CIP4 or FBP17 in proliferation would be novel for these F-BAR proteins.

Connecting CIP4 and FBP17 to migration disorders

The hallmark of periventricular heterotopia (PH) is the nodes of unmigrated neurons lining the ventricle (Buchsbaum and Cappello 2019). CIP4 overexpression at P21, did suggest a potential phenotype resembling PH. The third population of unmigrated CIP4 neurons residing closer to the ventricle could be reminiscent of a PH node on a smaller scale

(Ch2 Fig. S2). Furthermore, knockdown of FLNA, a gene associated with PH, causes migrating neurons to get stuck in the intermediate zone, resembling the CIP4 knockdown phenotype (Nagano, Morikubo et al. 2004).

To determine if CIP4 overexpression could lead to PH, or PH-like nodes, a whole animal or large-scale conditional expression model would be needed. *In utero* electroporation is a great tool for studying neuronal migration, but it only targets a small population of cells (Hatanaka and Murakami 2002). As seen in our postnatal data, the number of CIP4 cells remaining near the ventricle was small, not enough to cause a disruption like PH. There are groups perform double electroporations hours to days apart to target more cells or different population of cells (Zhang, Getz, and Bordey 2021). Electroporating a large enough population of cells could recapitulate nodule formation resembling those seen in PH.

In contrast, CIP4 knockdown neurons potentially mimic other developmental disorders. If CIP4 knockdown neurons are not L2MNs, they may be forming a band similar to those in subcortical band heterotopia (SBH). While this band would be between layers I and II/III it could still cause epilepsy, intellectual disability, or developmental delays seen in SBH (Romero, Bahi-Buisson et al. 2018, Buchsbaum and Cappello 2019).

It is harder to predict a role for FBP17 in developmental disorders as its effect on migration is more subtle. We have preliminary data suggesting the FBP17 overexpression phenotype continues to decrease migration at P21 (data not shown). If FBP17 overexpressing neurons group together below the cortex, a band comparable to SBH could

develop, but more postnatal studies are needed to determine if this theory is correct. While currently not directly linked to a developmental disorder, the requirement of a precise amount of CIP4 or FBP17 for proper radial migration suggests that mutations affecting protein levels could be disruptive to development.

TOCA1, the third CIP4 F-BAR family member

TOCA1 is the third member of the CIP4 subfamily. The Eurexpress and Allen Institute online data sets show high TOCA1 expression in the cortex and very high expression in the cortical plate (Lein, Hawrylycz et al. 2007, Diez-Roux, Banfi et al. 2011). Moreover, the ENCODE online dataset suggested that TOCA1 was highly expressed in the embryonic CNS, even higher than DCX (Yue, Cheng et al. 2014). Based on these data, it is possible that TOCA1 has an important role in the termination of migration. The high endogenous expression of TOCA1 also may explain why we have previously struggled to study TOCA 1 overexpression. When we have previously expressed TOCA1 the cells died very quickly, which was probably due to exceptionally high levels of endogenous TOCA1 expression (data not shown).

Considering the high expression of TOCA 1 in the cortical plate, experiments focused on TOCA1's role in the termination of migration, as well as the multipolar-bipolar switch, should be carried out in the future. Examining the effect of TOCA1 knockdown on migration would also be interesting. If TOCA1 is involved in the termination of migration, the loss of TOCA1 would cause an over migration phenotype like CIP4 knockdown. Furthermore, it would be interesting to know if slight overexpression of TOCA1 could rescue CIP4 knockdown induced over-migration,

In summary, this dissertation reveals that the F-BAR proteins CIP4 and FBP17 are essential regulators of process dynamics during radial neuronal migration in the developing cerebral cortex. Through a combination of *in vivo* manipulation, domain-specific analyses, and expression profiling, we demonstrate that these proteins function in distinct but complementary ways to guide neuronal morphology and positioning. CIP4 appears to play a pivotal role in process retraction and the transition from multipolar to bipolar morphology, with tightly regulated expression critical for proper migration and termination. The unexpected over-migration phenotype observed with CIP4 knockdown highlights the complexity of temporal regulation in cortical development. These findings also underscore the potential for additional roles for CIP4, FBP17, and the related protein TOCA1 in postnatal development and brain function. Altogether, these studies provide new insight into the cellular and molecular mechanisms that shape cortical architecture and lay the foundation for future investigations into F-BAR protein function in both development and disease.

REFERENCES

Buchsbaum, I. Y., & Cappello, S. (2019). Neuronal migration in the CNS during development and disease: insights from in vivo and in vitro models. *Development*, *146*(1). https://doi.org/10.1242/dev.163766

Cho, R. H., Segawa, S., Okamoto, K., Mizuno, A., & Kaneko, T. (2004). Intracellularly labeled pyramidal neurons in the cortical areas projecting to the spinal cord. II. Intra- and juxta-columnar projection of pyramidal neurons to corticospinal neurons. *Neurosci Res*, *50*(4), 395-410. https://doi.org/10.1016/j.neures.2004.08.007

Choi, H. M. T., Schwarzkopf, M., Fornace, M. E., Acharya, A., Artavanis, G., Stegmaier, J., Cunha, A., & Pierce, N. A. (2018). Third-generation in situ hybridization chain reaction: multiplexed, quantitative, sensitive, versatile, robust. *Development*, *145*(12). https://doi.org/10.1242/dev.165753

Diez-Roux, G., Banfi, S., Sultan, M., Geffers, L., Anand, S., Rozado, D., Magen, A., Canidio, E., Pagani, M., Peluso, I., Lin-Marq, N., Koch, M., Bilio, M., Cantiello, I., Verde, R., De Masi, C., Bianchi, S. A., Cicchini, J., Perroud, E., . . . Ballabio, A. (2011). A high-resolution anatomical atlas of the transcriptome in the mouse embryo. *PLoS Biol*, *9*(1), e1000582. https://doi.org/10.1371/journal.pbio.1000582

Eng, L. F., Vanderhaeghen, J. J., Bignami, A., & Gerstl, B. (1971). An acidic protein isolated from fibrous astrocytes. *Brain Res*, *28*(2), 351-354. https://doi.org/10.1016/0006-8993(71)90668-8

Greig, L. C., Woodworth, M. B., Galazo, M. J., Padmanabhan, H., & Macklis, J. D. (2013). Molecular logic of neocortical projection neuron specification, development and diversity. *Nat Rev Neurosci*, *14*(11), 755-769. https://doi.org/10.1038/nrn3586

Gusel'nikova, V. V., & Korzhevskiy, D. E. (2015). NeuN As a Neuronal Nuclear Antigen and Neuron Differentiation Marker. *Acta Naturae*, *7*(2), 42-47. https://www.ncbi.nlm.nih.gov/pubmed/26085943

Hatanaka, Y., & Murakami, F. (2002). In vitro analysis of the origin, migratory behavior, and maturation of cortical pyramidal cells. *J Comp Neurol*, *454*(1), 1-14. https://doi.org/10.1002/cne.10421

Hevner, R. F. (2007). Layer-specific markers as probes for neuron type identity in human neocortex and malformations of cortical development. *J Neuropathol Exp Neurol*, *66*(2), 101-109. https://doi.org/10.1097/nen.0b013e3180301c06

Hevner, R. F., Shi, L., Justice, N., Hsueh, Y., Sheng, M., Smiga, S., Bulfone, A., Goffinet, A. M., Campagnoni, A. T., & Rubenstein, J. L. (2001). Tbr1 regulates differentiation of the preplate and layer 6. *Neuron*, *29*(2), 353-366. https://doi.org/10.1016/s0896-6273(01)00211-2

Hirota, Y., & Nakajima, K. (2017). Control of Neuronal Migration and Aggregation by Reelin Signaling in the Developing Cerebral Cortex. *Front Cell Dev Biol*, *5*, 40. https://doi.org/10.3389/fcell.2017.00040

Kriegstein, A. R., & Noctor, S. C. (2004). Patterns of neuronal migration in the embryonic cortex. *Trends Neurosci*, *27*(7), 392-399. https://doi.org/10.1016/j.tins.2004.05.001

Lein, E. S., Hawrylycz, M. J., Ao, N., Ayres, M., Bensinger, A., Bernard, A., Boe, A. F., Boguski, M. S., Brockway, K. S., Byrnes, E. J., Chen, L., Chen, L., Chen, T. M., Chin, M. C., Chong, J., Crook, B. E., Czaplinska, A., Dang, C. N., Datta, S., . . . Jones, A. R. (2007). Genome-wide atlas of gene expression in the adult mouse brain. *Nature*, *445*(7124), 168-176. https://doi.org/10.1038/nature05453

Luo, H., Hasegawa, K., Liu, M., & Song, W. J. (2017). Comparison of the Upper Marginal Neurons of Cortical Layer 2 with Layer 2/3 Pyramidal Neurons in Mouse Temporal Cortex. *Front Neuroanat*, *11*, 115. https://doi.org/10.3389/fnana.2017.00115

Martinez-Cerdeno, V., Galazo, M. J., Cavada, C., & Clasca, F. (2002). Reelin immunoreactivity in the adult primate brain: intracellular localization in projecting and local circuit neurons of the cerebral cortex, hippocampus and subcortical regions. *Cereb Cortex*, *12*(12), 1298-1311. https://doi.org/10.1093/cercor/12.12.1298

Nadarajah, B., Brunstrom, J. E., Grutzendler, J., Wong, R. O., & Pearlman, A. L. (2001). Two modes of radial migration in early development of the cerebral cortex. *Nat Neurosci*, *4*(2), 143-150. https://doi.org/10.1038/83967

Nagano, T., Morikubo, S., & Sato, M. (2004). Filamin A and FILIP (Filamin A-Interacting Protein) regulate cell polarity and motility in neocortical subventricular and intermediate zones during radial migration. *J Neurosci*, *24*(43), 9648-9657. http://www.ncbi.nlm.nih.gov/entrez/query.fcgi?cmd=Retrieve&db=PubMed&dopt=Citation&list_uids=15509752

Peters, A., & Kara, D. A. (1985). The neuronal composition of area 17 of rat visual cortex. II. The nonpyramidal cells. *J Comp Neurol*, *234*(2), 242-263. https://doi.org/10.1002/cne.902340209

Romero, D. M., Bahi-Buisson, N., & Francis, F. (2018). Genetics and mechanisms leading to human cortical malformations. *Semin Cell Dev Biol*, *76*, 33-75. https://doi.org/10.1016/j.semcdb.2017.09.031

Saengsawang, W., Mitok, K., Viesselmann, C., Pietila, L., Lumbard, D. C., Corey, S. J., & Dent, E. W. (2012). The F-BAR protein CIP4 inhibits neurite formation by producing lamellipodial protrusions [Research Support, N.I.H., Extramural
Research Support, Non-U.S. Gov't]. *Curr Biol*, *22*(6), 494-501. https://doi.org/10.1016/j.cub.2012.01.038

Sawada, M., Ohno, N., Kawaguchi, M., Huang, S. H., Hikita, T., Sakurai, Y., Bang Nguyen, H., Quynh Thai, T., Ishido, Y., Yoshida, Y., Nakagawa, H., Uemura, A., & Sawamoto, K. (2018). PlexinD1 signaling controls morphological changes and migration termination in newborn neurons. *EMBO J*, *37*(4). https://doi.org/10.15252/embj.201797404

Sekine, K., Kubo, K., & Nakajima, K. (2014). How does Reelin control neuronal migration and layer formation in the developing mammalian neocortex? *Neurosci Res*, *86*, 50-58. https://doi.org/10.1016/j.neures.2014.06.004

Staiger, J. F., Bojak, I., Miceli, S., & Schubert, D. (2015). A gradual depth-dependent change in connectivity features of supragranular pyramidal cells in rat barrel cortex. *Brain Struct Funct*, *220*(3), 1317-1337. https://doi.org/10.1007/s00429-014-0726-8

Stanton-Turcotte, D., Hsu, K., Moore, S. A., Yamada, M., Fawcett, J. P., & Iulianella, A. (2022). Mllt11 Regulates Migration and Neurite Outgrowth of Cortical Projection Neurons during Development. *J Neurosci*, *42*(19), 3931-3948. https://doi.org/10.1523/JNEUROSCI.0124-22.2022

taylor, K. L. (2018). *Opposing Functions of F-BAR Proteins CIP4 and FBP17 in Neuronal Membrane Protrusion, Tubule Formation and Cortical Neuronal Developmen* (Publication Number 10932881) [, The University of Wisconsin - Madison]. ProQuest.

Toudji, I., Toumi, A., Chamberland, E., & Rossignol, E. (2023). Interneuron odyssey: molecular mechanisms of tangential migration. *Front Neural Circuits*, *17*, 1256455. https://doi.org/10.3389/fncir.2023.1256455

Valiente, M., & Martini, F. J. (2009). Migration of cortical interneurons relies on branched leading process dynamics. *Cell Adh Migr*, *3*(3), 278-280. https://doi.org/10.4161/cam.3.3.8832

Yang, Z., & Wang, K. K. (2015). Glial fibrillary acidic protein: from intermediate filament assembly and gliosis to neurobiomarker. *Trends Neurosci*, *38*(6), 364-374. https://doi.org/10.1016/j.tins.2015.04.003

Yue, F., Cheng, Y., Breschi, A., Vierstra, J., Wu, W., Ryba, T., Sandstrom, R., Ma, Z., Davis, C., Pope, B. D., Shen, Y., Pervouchine, D. D., Djebali, S., Thurman, R. E., Kaul, R., Rynes, E., Kirilusha, A., Marinov, G. K., Williams, B. A., . . . Mouse, E. C. (2014). A comparative encyclopedia of DNA elements in the mouse genome. *Nature*, *515*(7527), 355-364. https://doi.org/10.1038/nature13992

Zhuang, P., Zhang, H., Welchko, R. M., Thompson, R. C., Xu, S., & Turner, D. L. (2020). Combined microRNA and mRNA detection in mammalian retinas by in situ hybridization chain reaction. *Sci Rep*, *10*(1), 351. https://doi.org/10.1038/s41598-019-57194-0